

Beam Instrumentation & Diagnostics Part 2

CAS Introduction to Accelerator Physics

Santa Susanna, 30th of September 2022

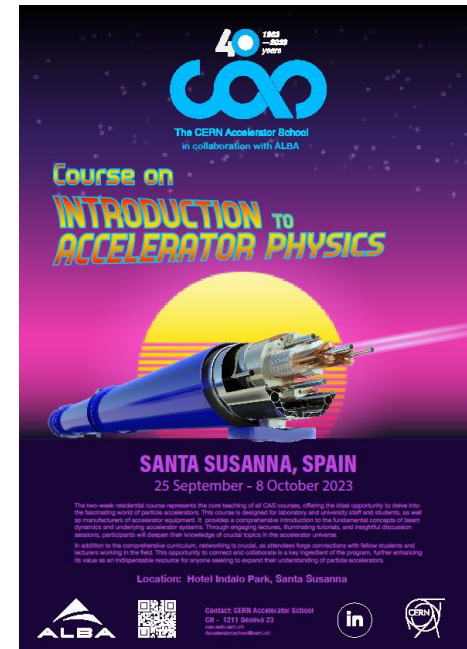
Peter Forck

Gesellschaft für Schwerionenforschung (GSI)

p.forck@gsi.de

2nd part of this lecture covers:

- Transverse profile techniques
- Emittance determination at transfer lines
- Diagnostics for bunch shape determination



Copyright statement and speaker's release for video publishing

The author consents to the photographic, audio and video recording of this lecture at the CERN Accelerator School. The term “lecture” includes any material incorporated therein including but not limited to text, images and references.

The author hereby grants CERN a royalty-free license to use his image and name as well as the recordings mentioned above, in order to post them on the CAS website.

The material is used for the sole purpose of illustration for teaching or scientific research. The author hereby confirms that to his best knowledge the content of the lecture does not infringe the copyright, intellectual property or privacy rights of any third party. The author has cited and credited any third-party contribution in accordance with applicable professional standards and legislation in matters of attribution.

Measurement of Beam Profile

The beam width can be changed by focusing via quadruples.

Transverse matching between ascending accelerators is done by focusing.

→ Profiles have to be controlled at many locations.

Synchrotrons: Lattice functions $\beta(s)$ and $D(s)$ are fixed \Rightarrow width σ and emittance ε are:

$$\sigma_x^2(s) = \varepsilon_x \beta_x(s) + \left(D(s) \frac{\Delta p}{p} \right)^2 \quad \text{and} \quad \sigma_y^2(s) = \varepsilon_y \beta_y(s) \quad (\text{no vertical bend})$$

Transfer lines: Lattice functions are ‘smoothly’ defined due to variable input emittance.

Typical beam sizes:

e⁻-beam: typically \varnothing 0.01 to 3 mm, **protons:** typically \varnothing 1 to 30 mm

A great variety of devices are used:

- **Optical techniques:** Scintillating screens (all beams),
synchrotron light monitors (e⁻), optical transition radiation (e⁻, high-energetic p),
ionization profile monitors (protons)
- **Electronics techniques:** Secondary electron emission SEM grids, wire scanners (all)

Measurement of Beam Profile

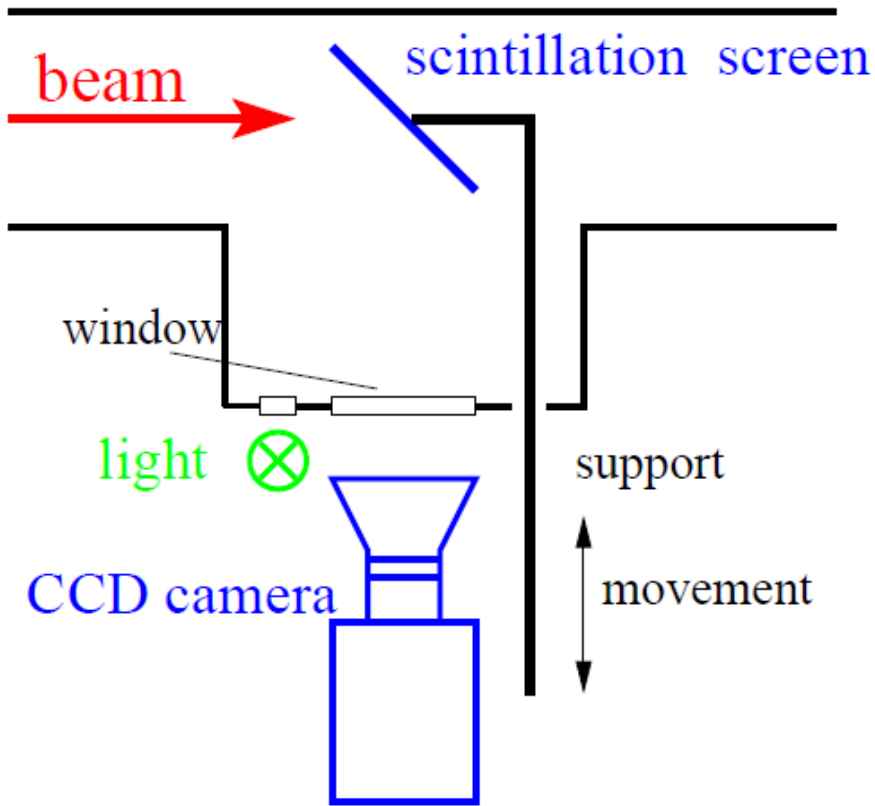
Outline:

- **Scintillation screens:**
 emission of light, universal usage, limited dynamic range
- **Optical Transition Radiation**
- **SEM-Grid**
- **Wire scanner**
- **Ionization Profile Monitor**
- **Synchrotron Light Monitors**
- **Summary**

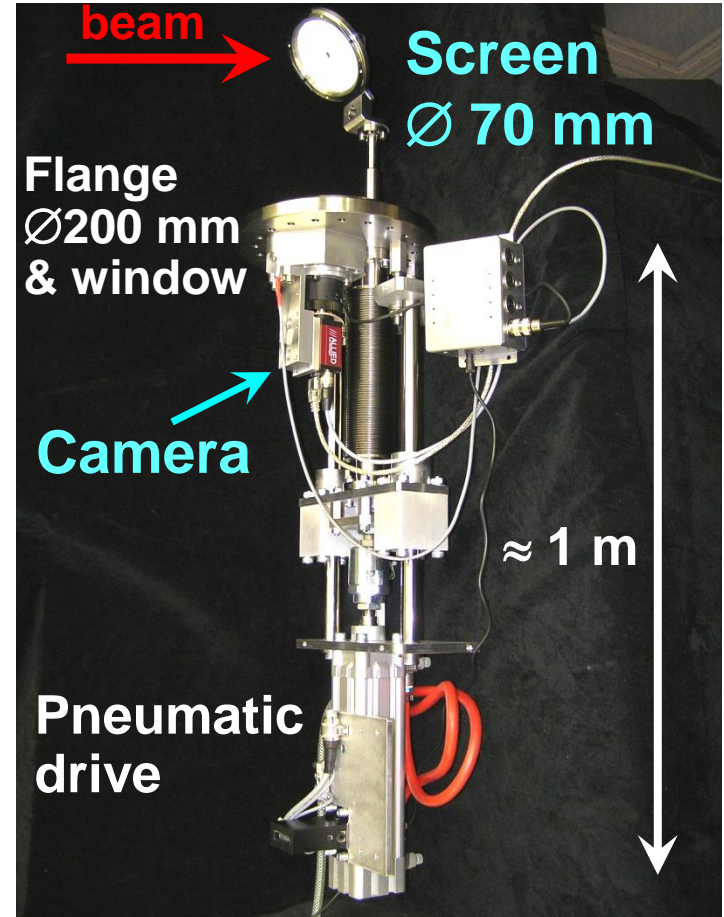
Scintillation Screen

Scintillation: Particle's energy loss in matter causes emission of light

→ the most direct way of profile observation as used from the early days on!



Pneumatic drive with $\varnothing 70$ mm screen:



In beam dynamics and by Volker Ziemann: Profile measurement is called 'Screens'

Example of Screen based Beam Profile Measurement

Example: GSI LINAC, 4 MeV/u, low current, YAG:Ce screen

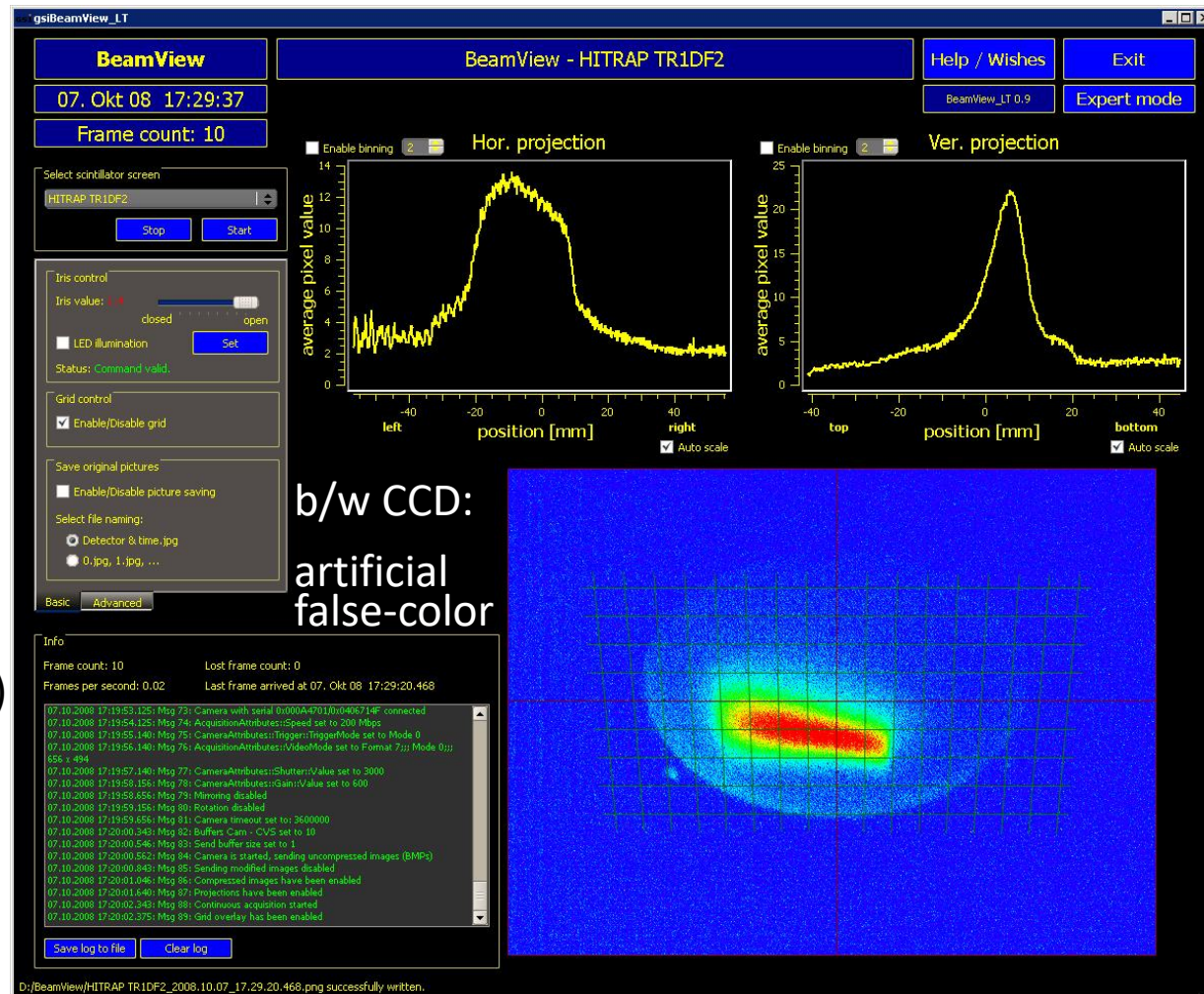
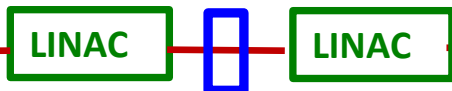
Advantage of screens:

- Direct 2-dim measurement
 - High spatial resolution
 - Cheap realization
- ⇒ widely used at transfer lines

Disadvantage of screens:

- Intercepting device
- Some material might be brittle
- Possible low dynamic range
- Might be destroyed by the beam (radiation damage)

Observation with CMOS camera
Scintillation Screen (beam stopped)

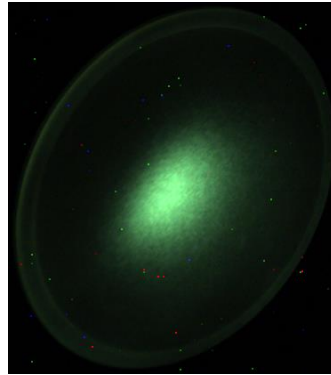


Light output from various Scintillating Screens

Example: Color CCD camera: Images at different particle intensities determined for U at 300 MeV/u



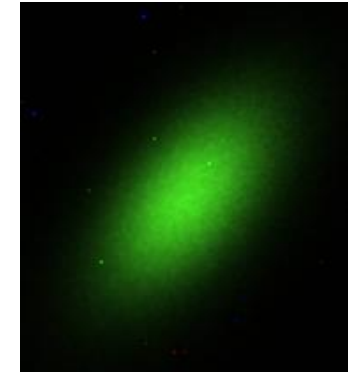
Alumina: Al_2O_3



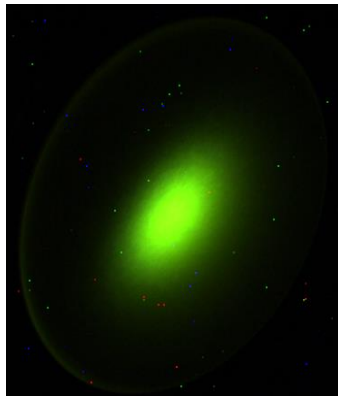
CsI:Tl



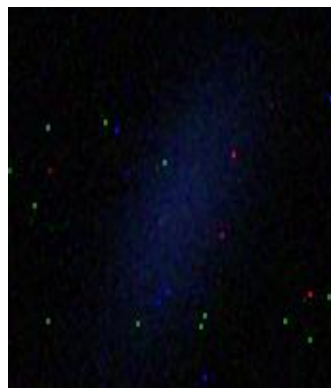
Chromox: Al_2O_3 :Cr



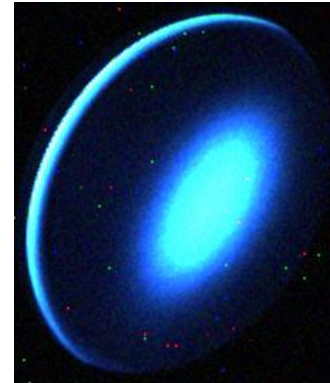
P43



YAG:Ce



Quartz



Quartz:Ce



ZrO₂:Mg

- Very different light yield i.e. photons per ion's energy loss
- Different wavelength of emitted light

Material Properties for Scintillating Screens

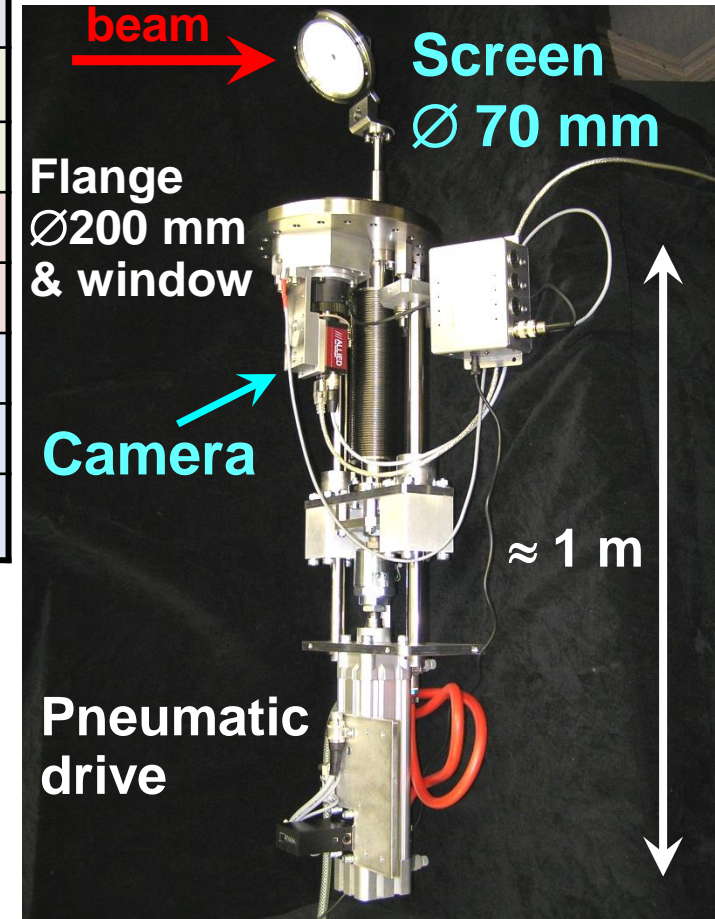
Some materials and their basic properties:

Type	Name	Material	Activ.	Max. λ	Decay
Cera- mics	Chromox	Al_2O_3	Cr	700nm	$\approx 10\text{ms}$
	Alumina	Al_2O_3	Non	380nm	$\approx 10\text{ns}$
Crystal	YAG:Ce	$\text{Y}_3\text{Al}_5\text{O}_{12}$	Ce	550nm	200ns
	LYSO	$\text{Lu}_{1.8}\text{Y}_{0.2}\text{SiO}_5$	Ce	420nm	40ns
Powder of gains $\varnothing \approx 10\mu\text{m}$ on glass	P43	$\text{Gd}_2\text{O}_3\text{S}$	Tb	545nm	1ms
	P46	$\text{Y}_3\text{Al}_5\text{O}_{12}$	Ce	530nm	300ns
	P47	Y_2SiO_5	Ce&Tb	400nm	100ns

Properties of a good scintillator:

- Large light output at optical wavelength
→ standard camera can be used
- Large dynamic range → usable for different currents
- Short decay time → observation of variations
- Radiation hardness → long lifetime
- Good mechanical properties → typ. size up to $\varnothing 10\text{ cm}$
(Phosphor Pxx grains of $\varnothing \approx 10\ \mu\text{m}$ on glass or metal).

Standard drive with P43 screen



Measurement of Beam Profile

Outline:

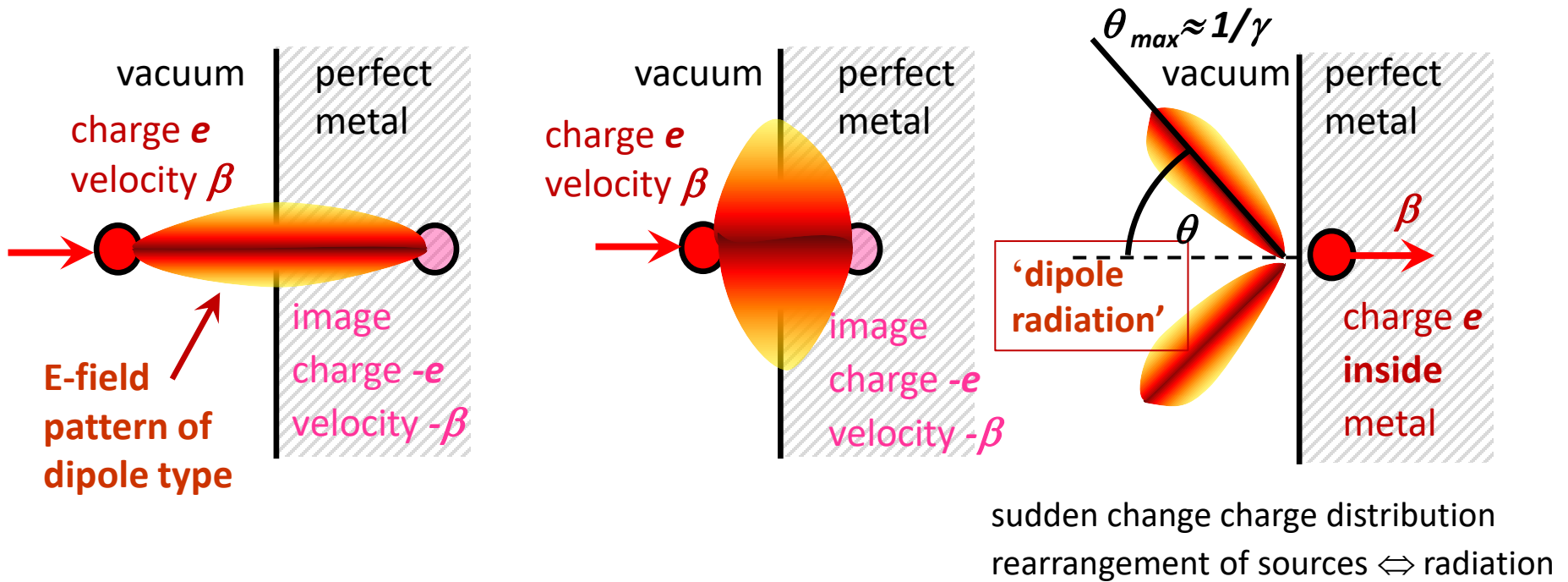
- Scintillation screens:
 - emission of light, universal usage, limited dynamic range
- **Optical Transition Radiation:**
 - light emission due to crossing material boundary, mainly for relativistic beams**
- **SEM-Grid**
- **Wire scanner**
- **Ionization Profile Monitor**
- **Synchrotron Light Monitors**
- **Summary**

Optical Transition Radiation: Depictive Description

Optical Transition Radiation OTR for a single charge e :

Assuming a charge e approaches an ideal conducting boundary e.g. metal foil:

- Image charge is created by electric field
- Dipole type field pattern
- Field distribution depends on velocity β and Lorentz factor γ due to relativistic trans. field increase
- Penetration of charge through surface within $t < 10$ fs: sudden change of source distribution
- Emission of radiation with dipole characteristic



Other physical interpretation: Impedance mismatch at boundary leads to radiation

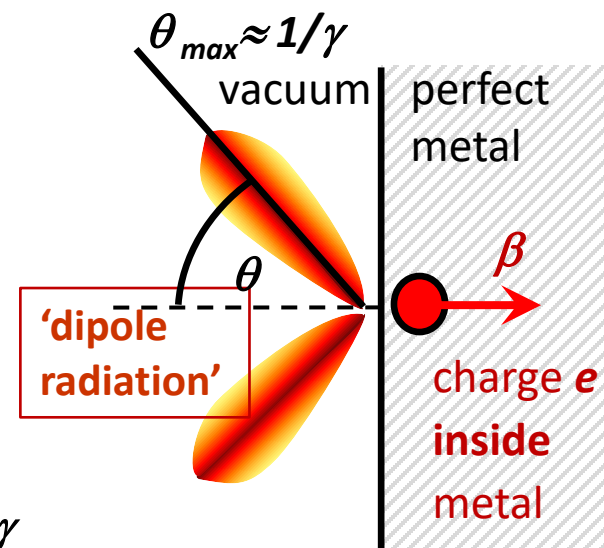
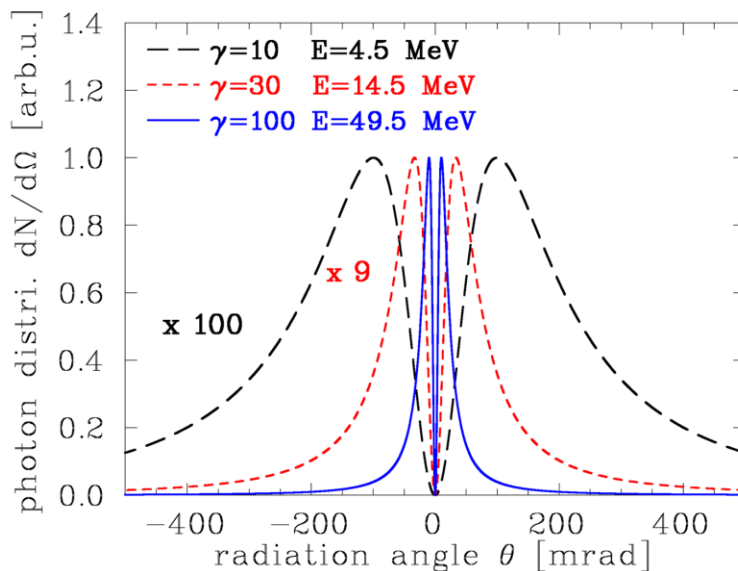
Optical Transition Radiation: Depictive Description

Optical Transition Radiation OTR can be described in classical physics:

Approximated formula
for normal incidence
& in-plane polarization:

$$\frac{d^2W}{d\theta d\omega} \approx \frac{2e^2 \beta^2}{\pi c} \cdot \frac{\sin^2 \theta \cdot \cos^2 \theta}{(1 - \beta^2 \cos^2 \theta)^2}$$

W : radiated energy
 ω : frequency of wave



Angular distribution of radiation in optical spectrum:

- Lobe emission pattern depends on velocity or Lorentz factor γ
 - Peak at angle $\theta \approx 1/\gamma$
 - Emitted energy i.e. amount of photons scales with $W \propto \beta^2$
 - Broad wave length spectrum (i.e. no dependence on ω)
- Suited for high energy electrons

sudden change charge distribution
rearrangement of sources \leftrightarrow radiation

OTR is emitted by charged particle passage through a material boundary.

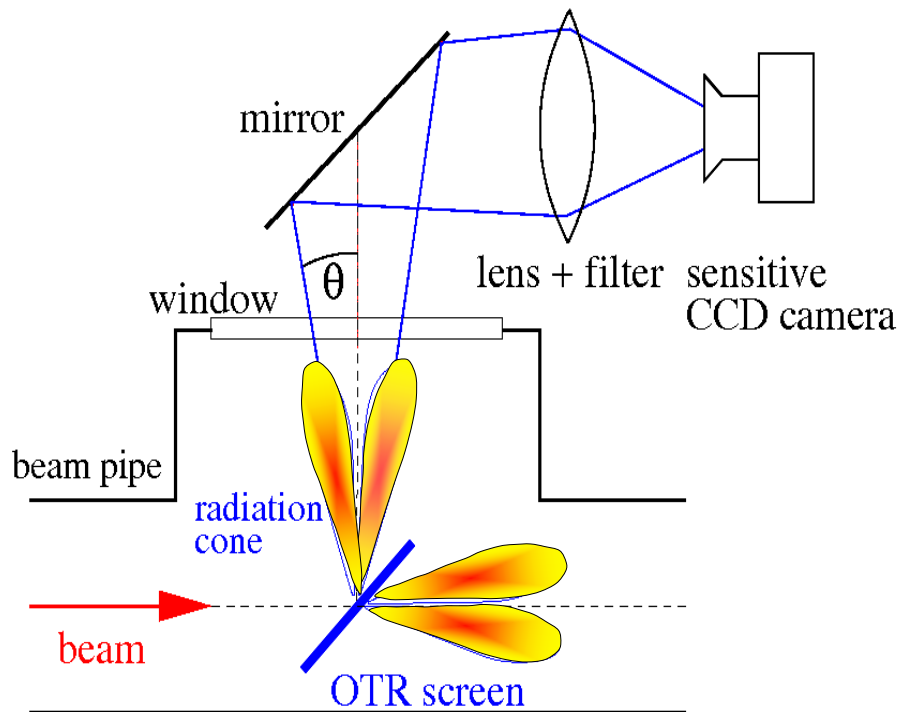
Photon distribution:

within a solid angle $d\Omega$ and

$$\frac{dN_{photon}}{d\Omega} = N_{beam} \cdot \frac{2e^2 \beta^2}{\pi c} \cdot \log\left(\frac{\lambda_{begin}}{\lambda_{end}}\right) \cdot \frac{\theta^2}{(\gamma^{-2} + \theta^2)^2}$$

Wavelength interval λ_{begin} to λ_{end}

- Detection: Optical $400 \text{ nm} < \lambda < 800 \text{ nm}$
- Larger signal for relativistic beam $\gamma \gg 1$
- Low divergence for $\gamma \gg 1 \Rightarrow$ large signal
- \Rightarrow **Well suited for e^- beams**
- \Rightarrow **p-beam used for $E_{kin} \gtrsim 10 \text{ GeV} \Leftrightarrow \gamma \gtrsim 10$**

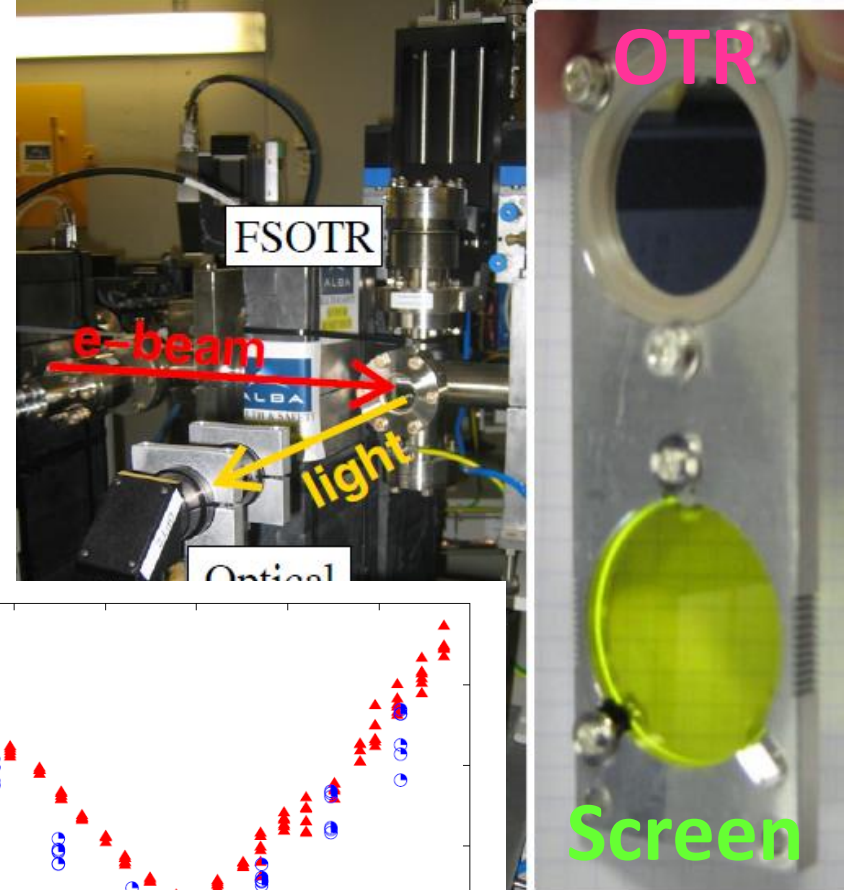
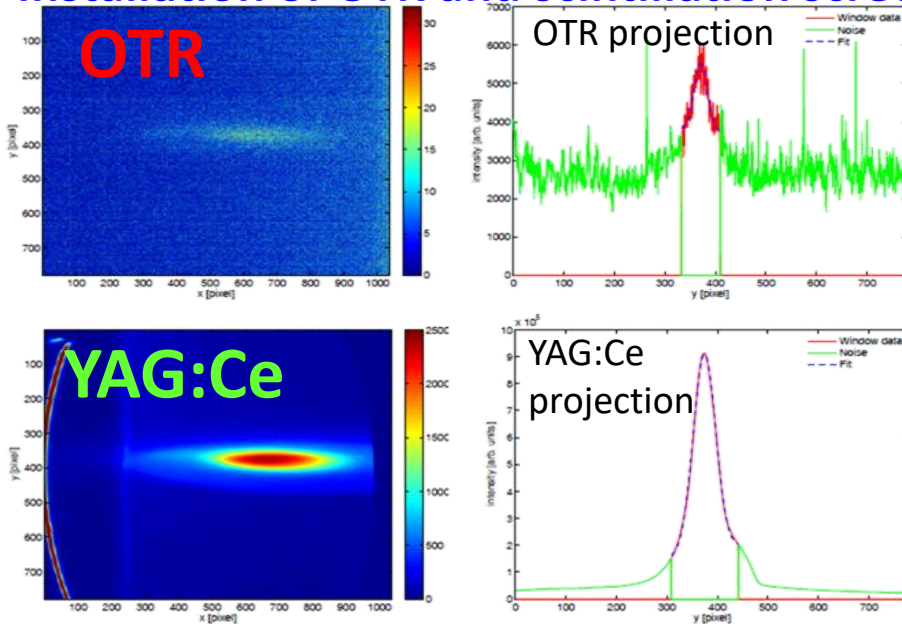


- Insertion of thin Al-foil under 45°
- Observation of low light by CCD.

Optical Transition Radiation compared to Scintillation Screen

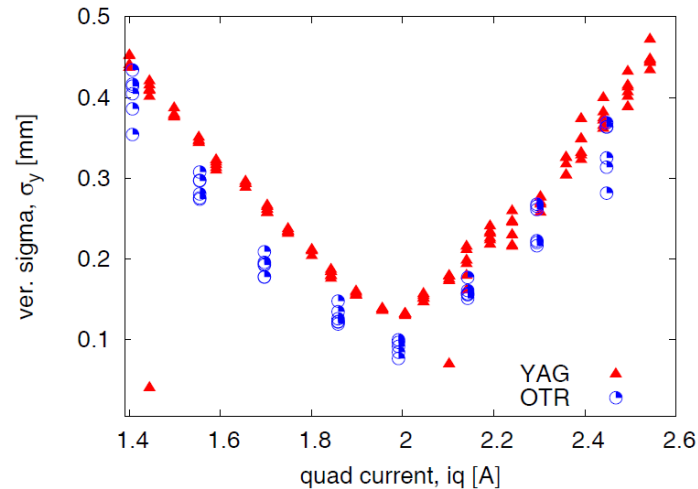
Installation of OTR and scintillation screens on same drive:

Example: ALBA LINAC 100 MeV



Results:

- Much more light from YAG:Ce for 100 MeV ($\gamma \approx 200$) electrons light output $I_{YAG} \approx 10^5 I_{OTR}$
- Broader image from YAG:Ce due to finite YAG:Ce thickness



Courtesy of U. Iriso et al., DIPAC'09

Comparison between Scintillation Screens and OTR

OTR: electrodynamic process → beam intensity linear to # photons, high radiation hardness

Scint. Screen: complex atomic process → saturation possible, for some low radiation hardness

OTR: thin foil Al or Al on Mylar, down to 0.25 μm thickness

→ minimization of beam scattering (Al is low Z-material e.g. plastics like Mylar)

Scint. Screen: thickness ≈ 1 mm inorganic, fragile material, not always radiation hard

OTR: low number of photons → sensitive & expensive camera required

Scint. Screen: large number of photons → simple camera is sufficient

OTR: large γ needed → e^- -beam with $E_{kin} > 100$ MeV, proton-beam with $E_{kin} > 100$ GeV

Scint. Screen: for all beams

OTR: complex angular photon distribution → resolution limited

Scint. Screen: isotropic photon distribution → simple interpretation

Remark:

1. **OTR:** beam angular distribution measurable → beam emittance

2. **OTR not** suited for LINAC-FEL due to **coherent** light emission (not covered here)
but scintillation screens can be used.

Outline:

- Scintillation screens:
emission of light, universal usage, limited dynamic range
- Optical Transition Radiation:
light emission due to crossing material boundary, mainly for relativistic beams
- **SEM-Grid:**
emission of electrons, workhorse, limited resolution
- **Wire scanner**
- **Ionization Profile Monitor**
- **Synchrotron Light Monitors**
- **Summary**

Secondary Electron Emission by Ion Impact

Energy loss of ions in metals close to a surface:

Closed collision with large energy transfer: \rightarrow fast e^- with $E_{kin} \gg 100$ eV

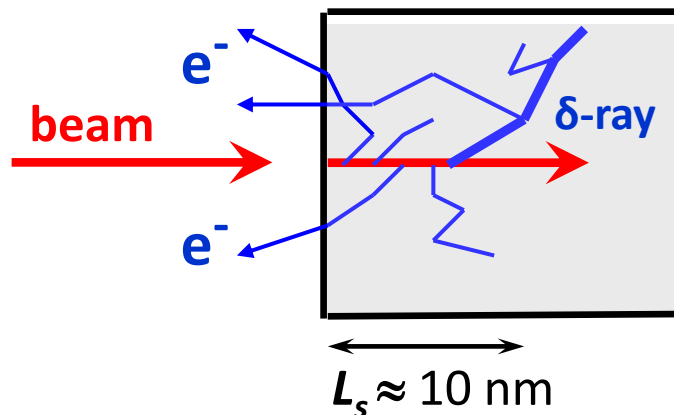
Distant collision with low energy transfer: \rightarrow slow e^- with $E_{kin} \leq 10$ eV

\rightarrow 'diffusion' & scattering with other e^- : scattering length $L_s \approx 1 - 10$ nm

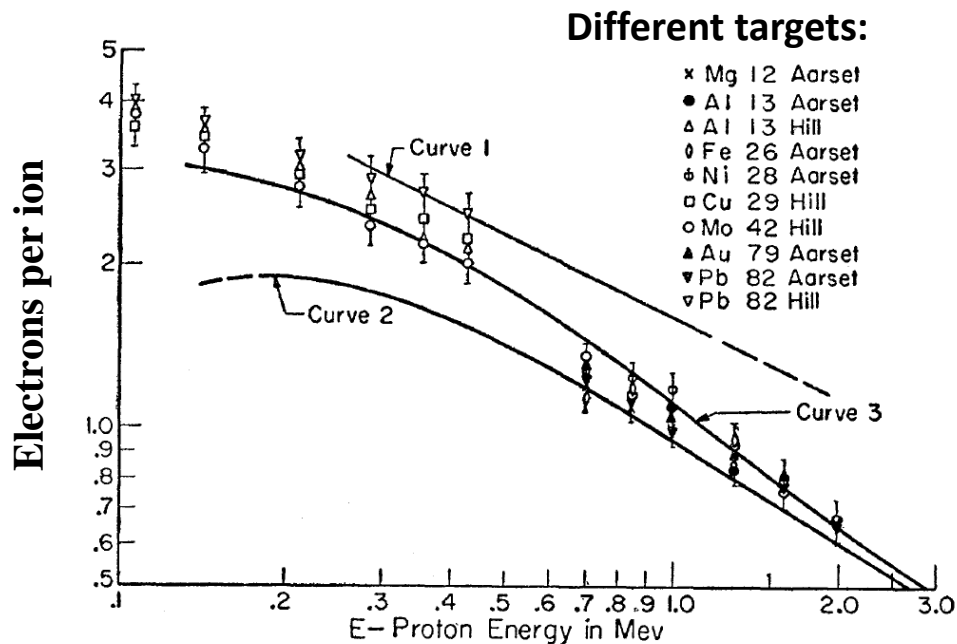
\rightarrow at surface $\approx 90\%$ probability for escape

Secondary **electron yield** and energy distribution comparable for all metals!

$$\Rightarrow Y = \text{const.} * dE/dx \quad (\text{Sternglass formula})$$



From E.J. Sternglass, Phys. Rev. 108, 1 (1957)

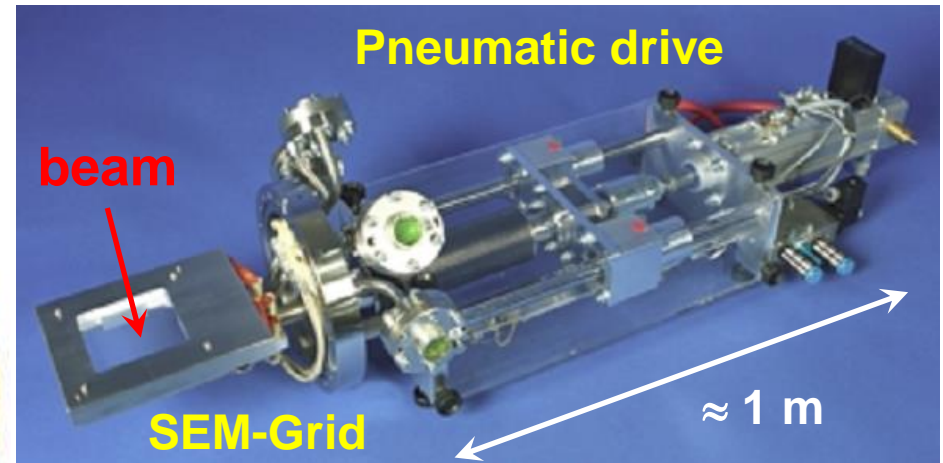
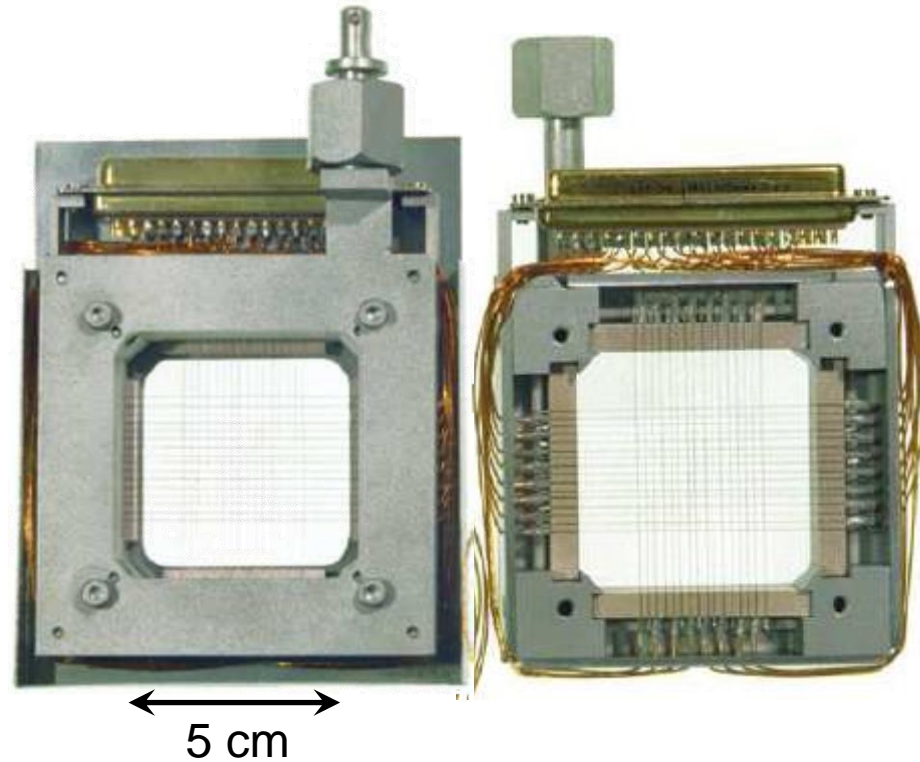


Secondary Electron Emission Grids = SEM-Grid

Beam surface interaction: e^- emission \rightarrow measurement of current.

Example: 15 wire spaced by 1.5 mm:

SEM-Grid drive on $\varnothing 200$ mm flange:

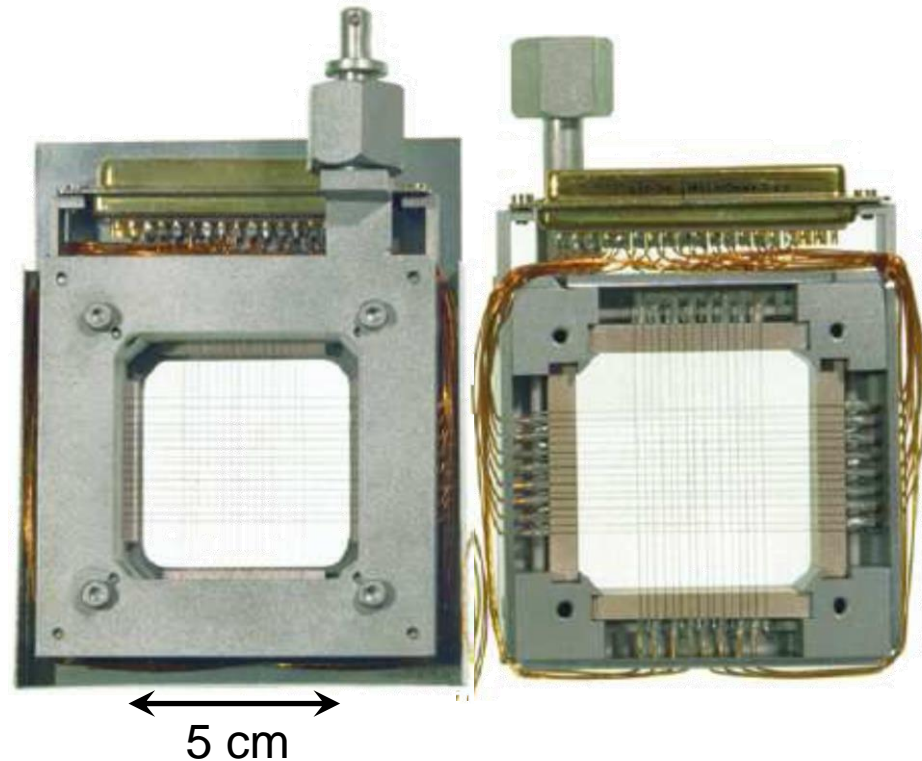


Parameter	Typ. value
# wires per plane	10 ...100
Active area	(5...20 cm) ²
Wire \varnothing	25...100 μ m
Spacing	0.3...2 mm
Material	e.g. W or Carbon
Max. beam power	1 W/mm

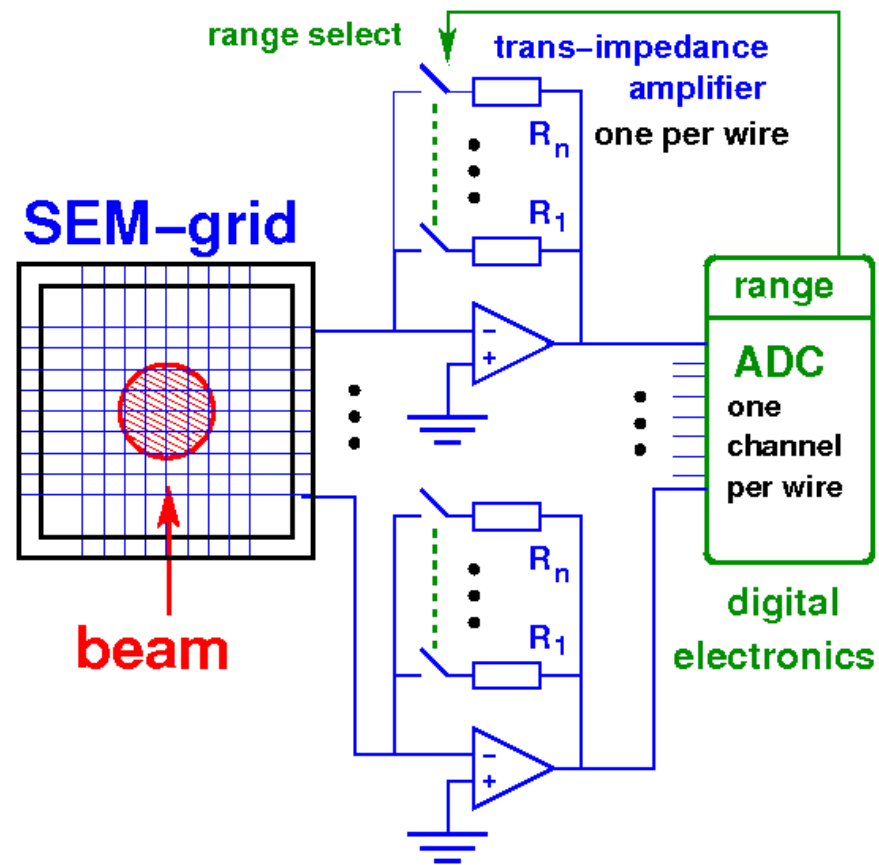
Secondary Electron Emission Grids = SEM-Grid

Beam surface interaction: e^- emission \rightarrow measurement of current.

Example: 15 wire spaced by 1.5 mm:



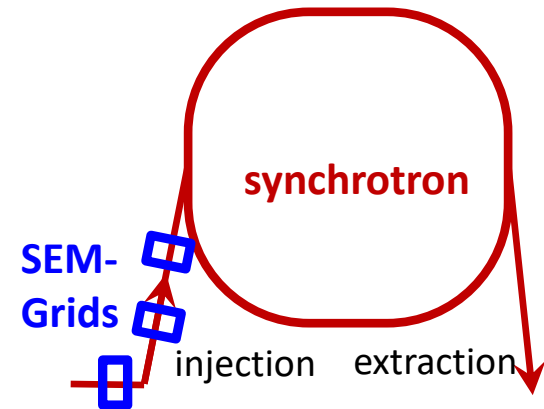
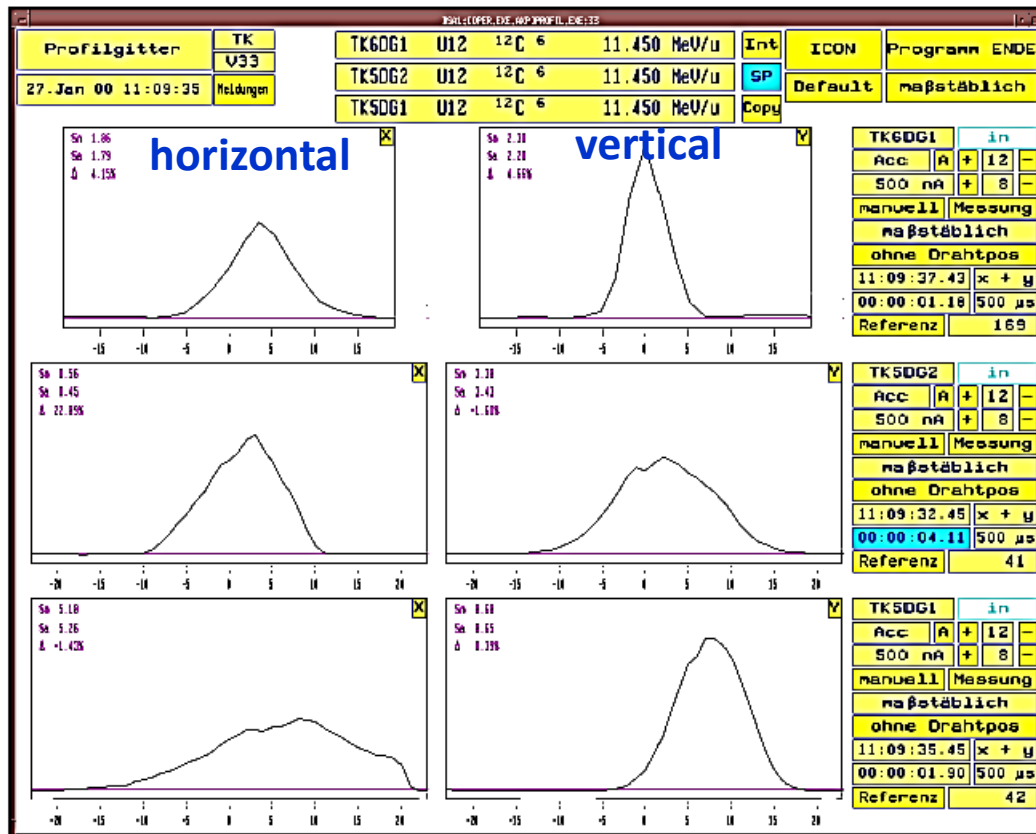
Each wire is equipped with one I/U converter
 different ranges settings by R_i
 \rightarrow very large dynamic range up to 10^6 .



Example of Profile Measurement with SEM-Grids

Even for low energies, several SEM-Grid can be used due to the $\approx 80\%$ transmission
 \Rightarrow frequently used instrument beam optimization: setting of quadrupoles, energy....

Example: C^{6+} beam of 11.450 MeV/u at different locations at GSI-LINAC



Outline:

- Scintillation screens:
emission of light, universal usage, limited dynamic range
- Optical Transition Radiation:
light emission due to crossing material boundary, mainly for relativistic beams
- SEM-Grid:
emission of electrons, workhorse, limited resolution
- **Wire scanner:**
emission of electrons, workhorse, scanning method
- **Ionization Profile Monitor**
- **Synchrotron Light Monitors**
- **Summary**

Slow, linear Wire Scanner

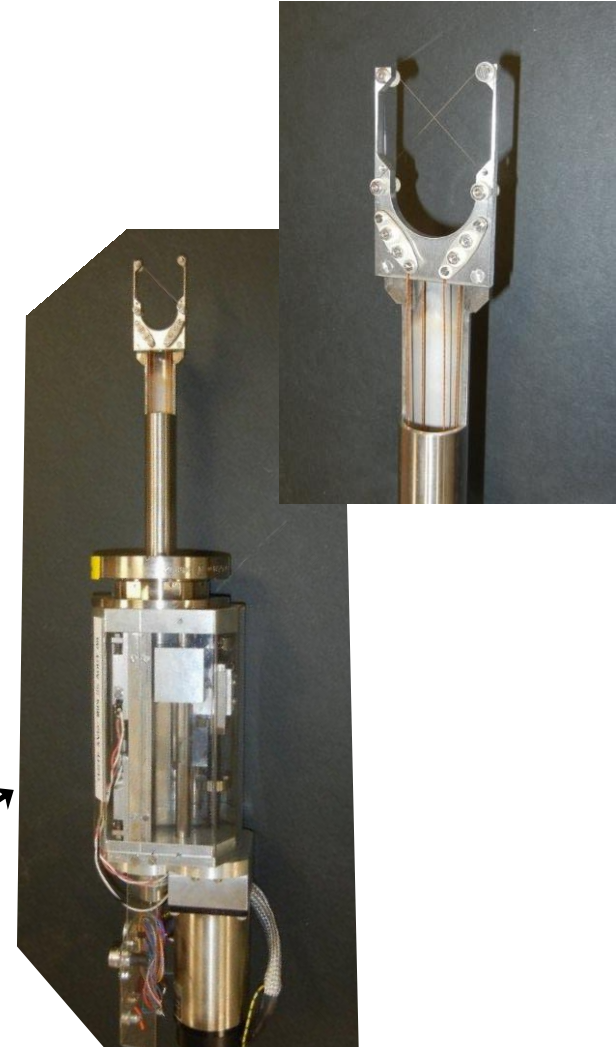
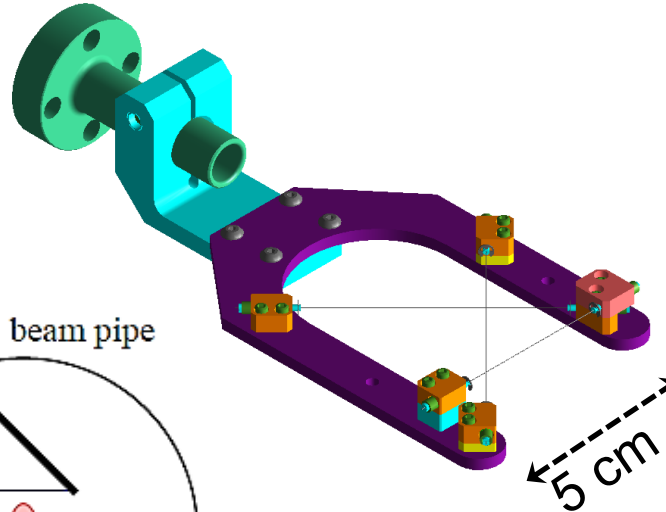
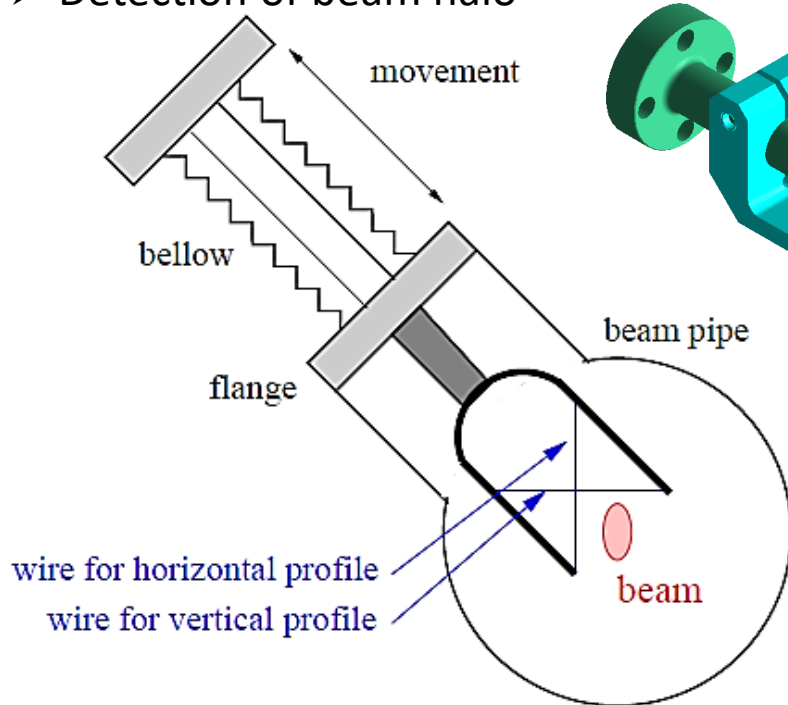
Idea: One wire is scanned through the beam!

Wire diameter $100 \mu\text{m} < d_{\text{wire}} < 10 \mu\text{m}$

Slow, linear scanner are used for:

- Low energy protons
- High resolution measurements for e^- beam
 by de-convolution $\sigma^2_{\text{beam}} = \sigma^2_{\text{meas}} - d^2_{\text{wire}}$
 \Rightarrow resolution down to $1 \mu\text{m}$ range can be reached
- Detection of beam halo

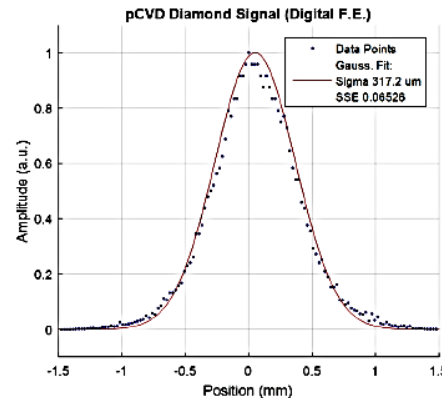
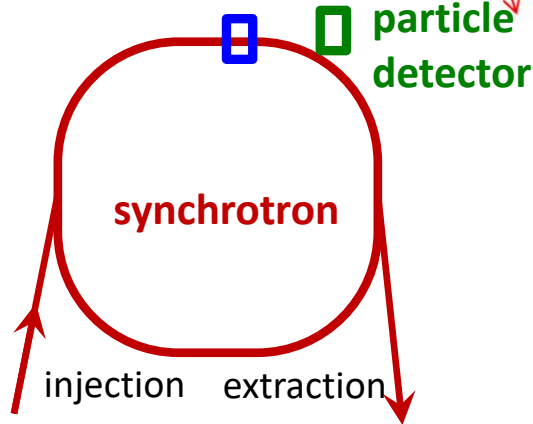
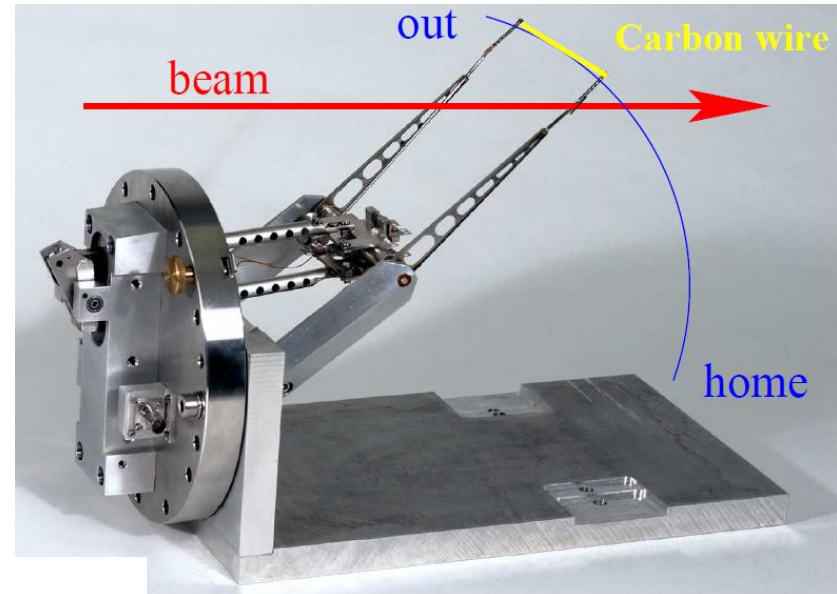
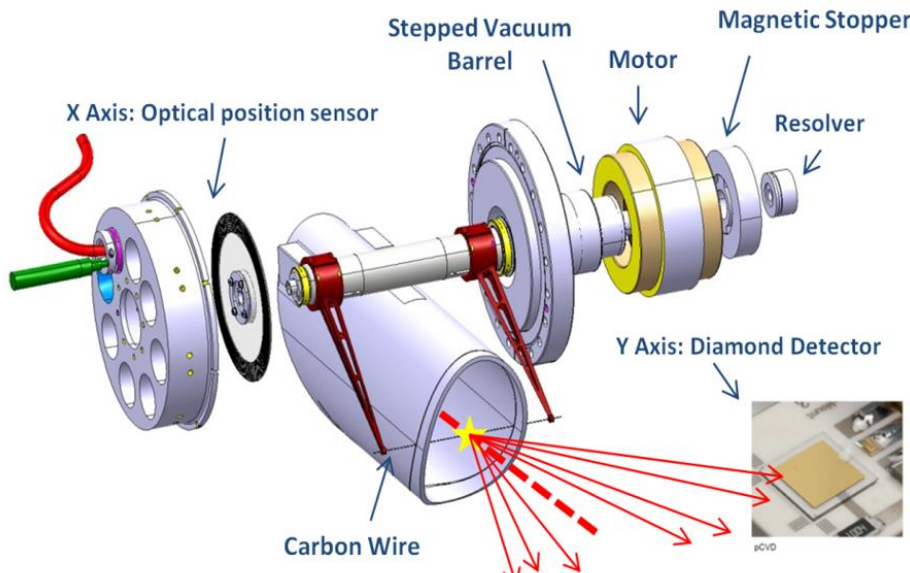
Example: Wires scanner at CERB LINAC4



Fast, Flying Wire Scanner

In a synchrotron one wire is scanned through the beam as fast as possible.

Fast pendulum scanner for synchrotrons; sometimes it is called '*flying wire*':



From <https://twiki.cern.ch/twiki/bin/viewauth/BWSUpgrade/>

Usage of Flying Wire Scanners

Material: Carbon or SiC → low Z-material for low energy loss and high temperature.

Thickness: Down to 10 μm → high resolution.

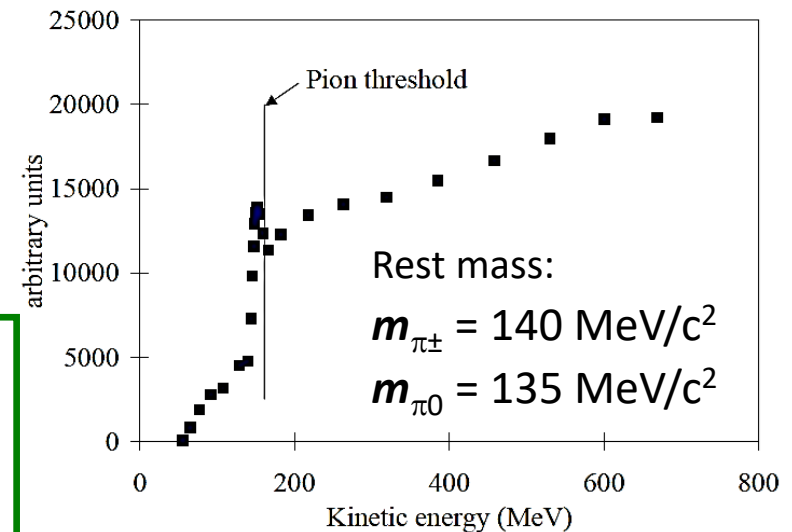
Detection: High energy **secondary particles** with a detector like a beam loss monitor

Secondary particles:

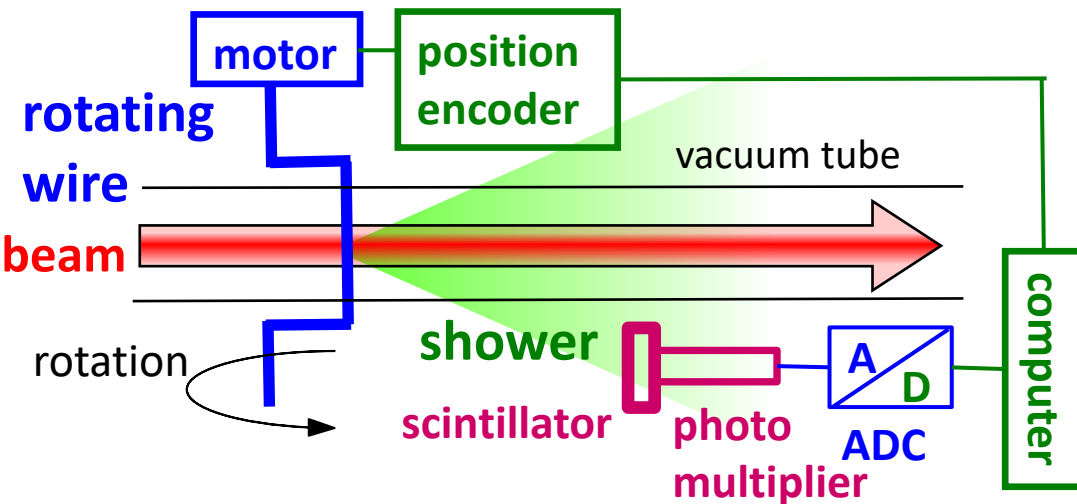
Proton beam → hadrons shower (π, n, p...)

Electron beam → Bremsstrahlung photons.

Proton impact on scanner at CERN-PS Booster:



U. Raich et al., DIPAC 2005



Kinematics of flying wire:

Velocity during passage typi. 10 m/s = 36 km/h & typical beam size \varnothing 10 mm

⇒ time for traversing the beam $t \approx 1 \text{ ms}$

Challenges: Wire stability for fast movement with high acceleration

Grid: Measurement at a single moment in time

Scanner: Scanning through beam \Rightarrow fast variations can not be monitored

\rightarrow for pulsed LINACs precise synchronization is needed

Grid: Resolution of a grid is fixed by the wire distance (typically 1 mm)

Scanner: For slow scanners the resolution is about the wire thickness (down to 10 μm)

\rightarrow used for e $^-$ -beams having small sizes (down to 10 μm)

Grid: Needs one electronics channel per wire

\rightarrow expensive electronics and data acquisition

Scanner: Needs a precise movable feed-through \rightarrow expensive mechanics.

Flying wire:

Grid: **Not** adequate at synchrotrons for stored beam parameters

Scanner: **At high energy synchrotrons:** flying wire scanners are nearly non-destructive

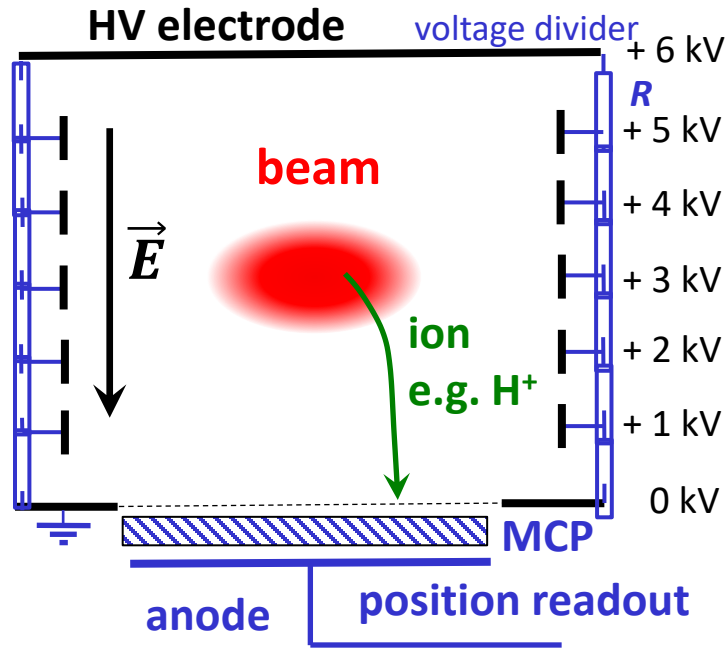
Outline:

- Scintillation screens:
emission of light, universal usage, limited dynamic range
- Optical Transition Radiation:
light emission due to crossing material boundary, mainly for relativistic beams
- SEM-Grid:
emission of electrons, workhorse, limited resolution
- Wire scanner:
emission of electrons, workhorse, scanning method
- **Ionization Profile Monitor:**
secondary particle detection from interaction beam-residual gas
- **Synchrotron Light Monitors**
- **Summary**

Ionization Profile Monitor at GSI Synchrotron

Non-destructive device for proton synchrotron:

- Beam ionizes the residual gas by electronic stopping
- Gas ions or e^- accelerated by E -field ≈ 1 kV/cm
- Spatial resolved single particle detection

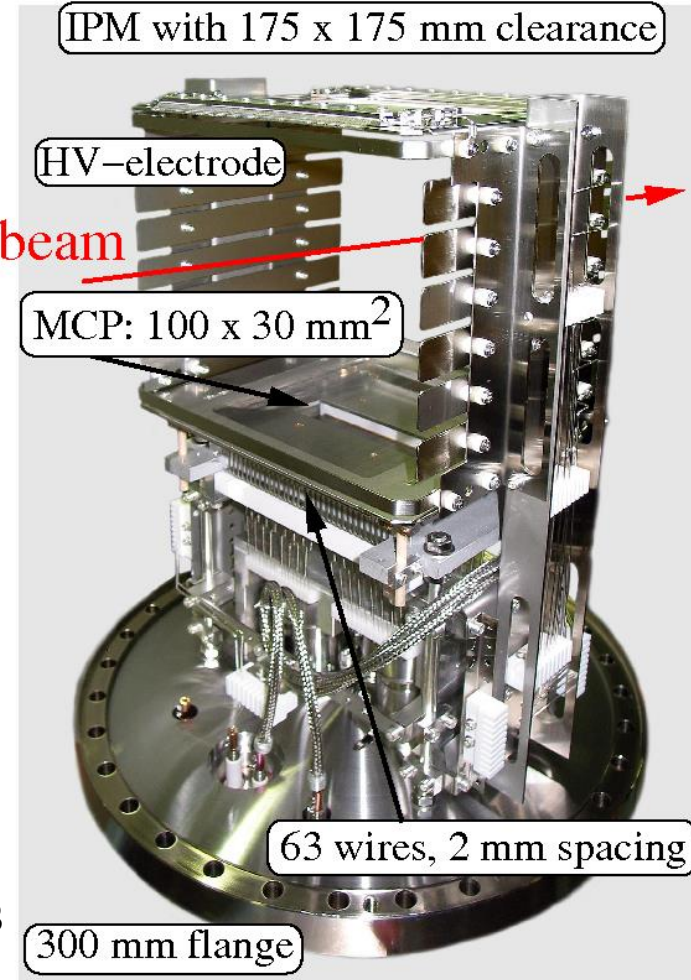


Typical vacuum pressure:

Transfer line: $p = 10^{-8} \dots 10^{-6}$ mbar $\Leftrightarrow n = 3 \cdot 10^8 \dots 3 \cdot 10^{10} \text{ cm}^{-3}$

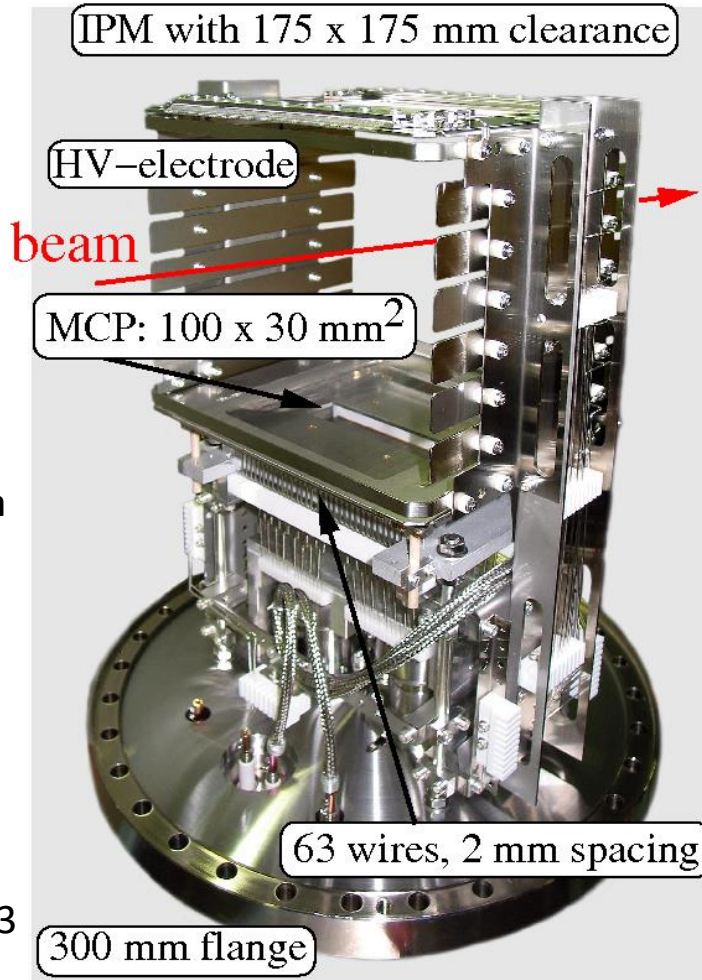
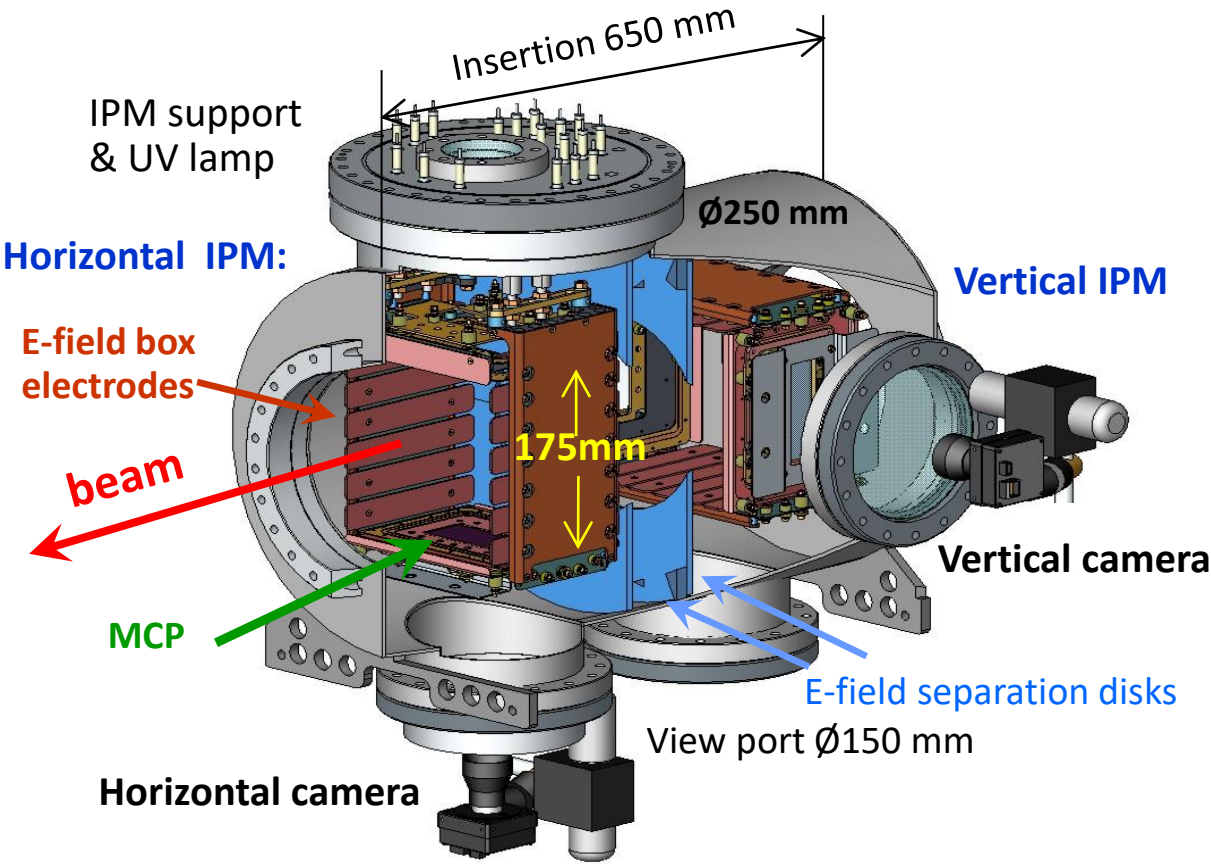
Synchrotron: $p = 10^{-11} \dots 10^{-9}$ mbar $\Leftrightarrow n = 3 \cdot 10^5 \dots 3 \cdot 10^7 \text{ cm}^{-3}$

Realization at GSI synchrotron:
One monitor per plane



Ionization Profile Monitor Realization

The realization for the heavy ion storage ring ESR at GSI: *Realization at GSI synchrotron: One monitor per plane*



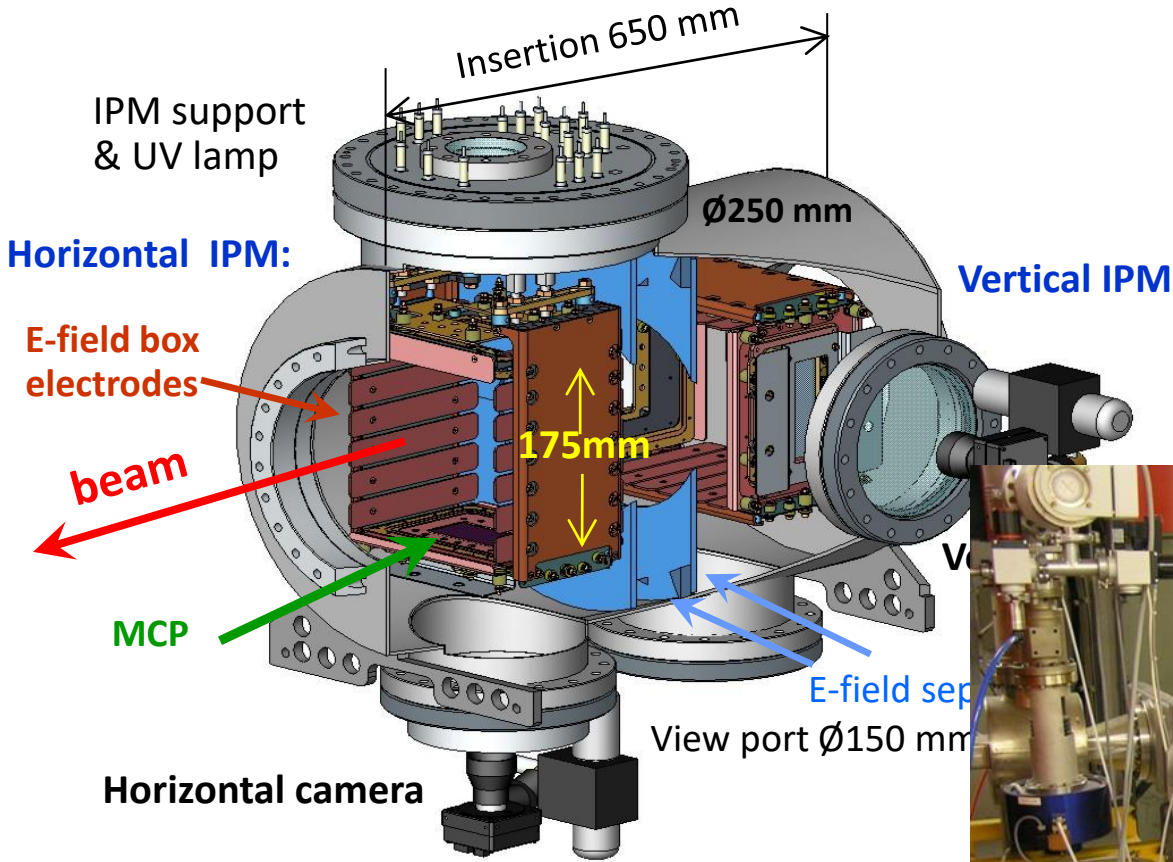
Typical vacuum pressure:

Transfer line: $p = 10^{-8} \dots 10^{-6}$ mbar $\Leftrightarrow n = 3 \cdot 10^8 \dots 3 \cdot 10^{10} \text{ cm}^{-3}$

Synchrotron: $p = 10^{-11} \dots 10^{-9}$ mbar $\Leftrightarrow n = 3 \cdot 10^5 \dots 3 \cdot 10^7 \text{ cm}^{-3}$

Ionization Profile Monitor Realization

The realization for the heavy ion storage ring ESR at GSI:



Realization at COSY synchrotron for one plane:



Outline:

- Scintillation screens:
emission of light, universal usage, limited dynamic range
- Optical Transition Radiation:
light emission due to crossing material boundary, mainly for relativistic beams
- SEM-Grid:
emission of electrons, workhorse, limited resolution
- Wire scanner:
emission of electrons, workhorse, scanning method
- Ionization Profile Monitor:
secondary particle detection from interaction beam-residual gas
- **Synchrotron Light Monitors:**
photon detection of emitted synchrotron light in optical and X-ray range
- **Summary**

Synchrotron Radiation Monitor

An electron bent (i.e. accelerated) by a dipole magnet emit synchrotron light
 see lecture 'Electron Beam Dynamics' by Lenny Rivkin

This light is emitted into a cone of opening $2/\gamma$ in lab-frame.

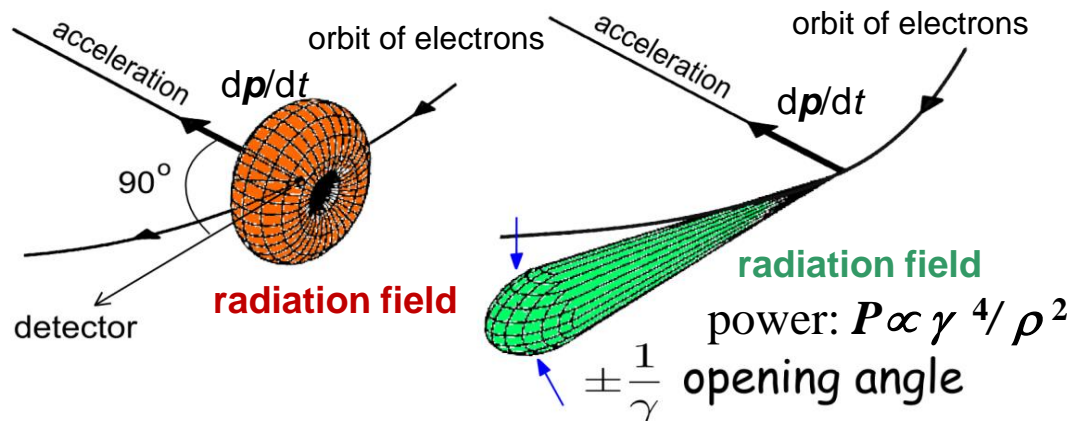
⇒ Well suited for rel. e^-

For protons:

Only for energies $E_{kin} > 100$ GeV

Rest frame of electron:

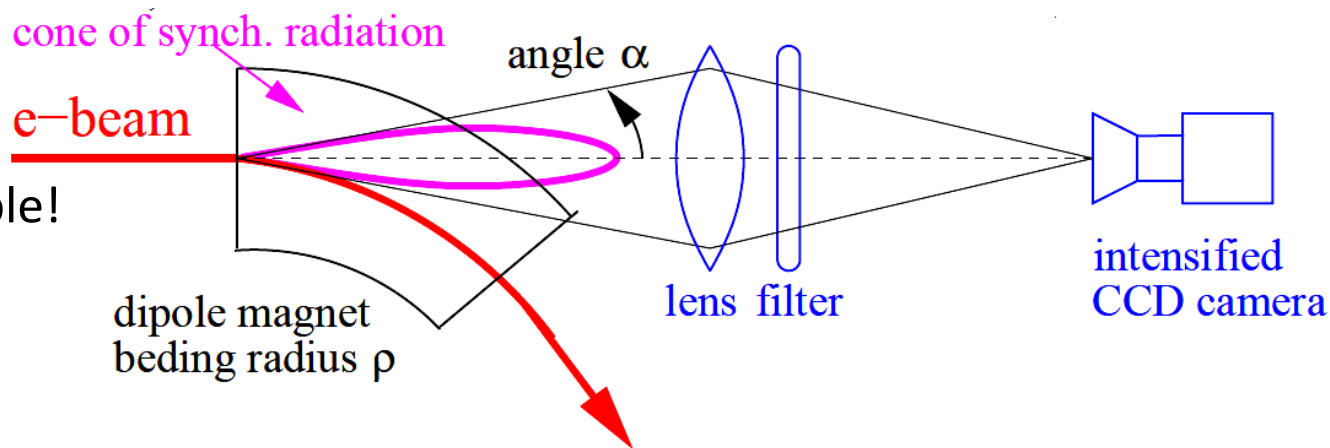
Laboratory frame:



The light is focused to a intensified CCD.

Advantage:

Signal anyhow available!



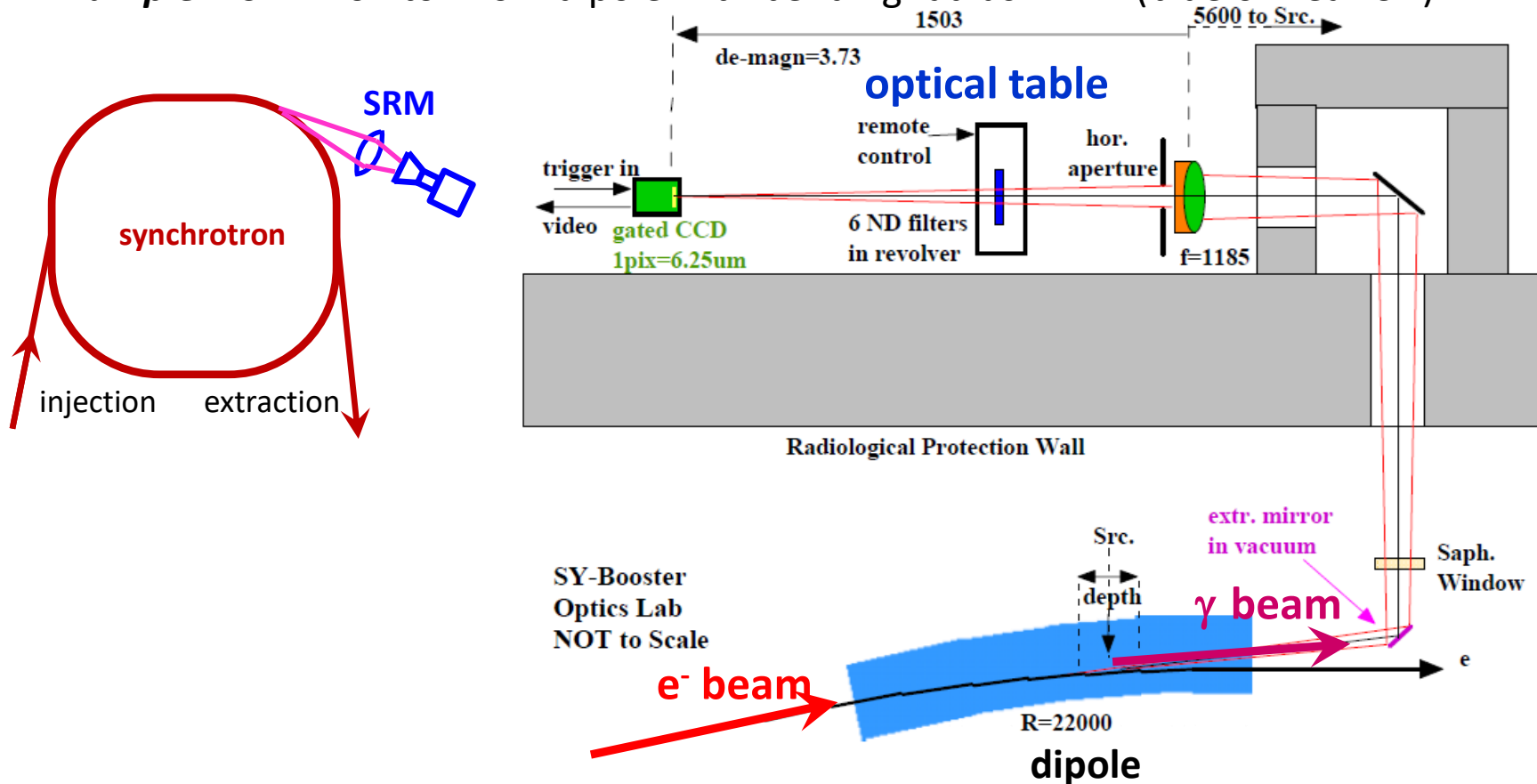
Realization of a Synchrotron Radiation Monitor

Extracting out of the beam's plane by a (cooled) mirror

→ Focus to a slit + wavelength filter for optical wavelength

→ Image intensified CCD camera

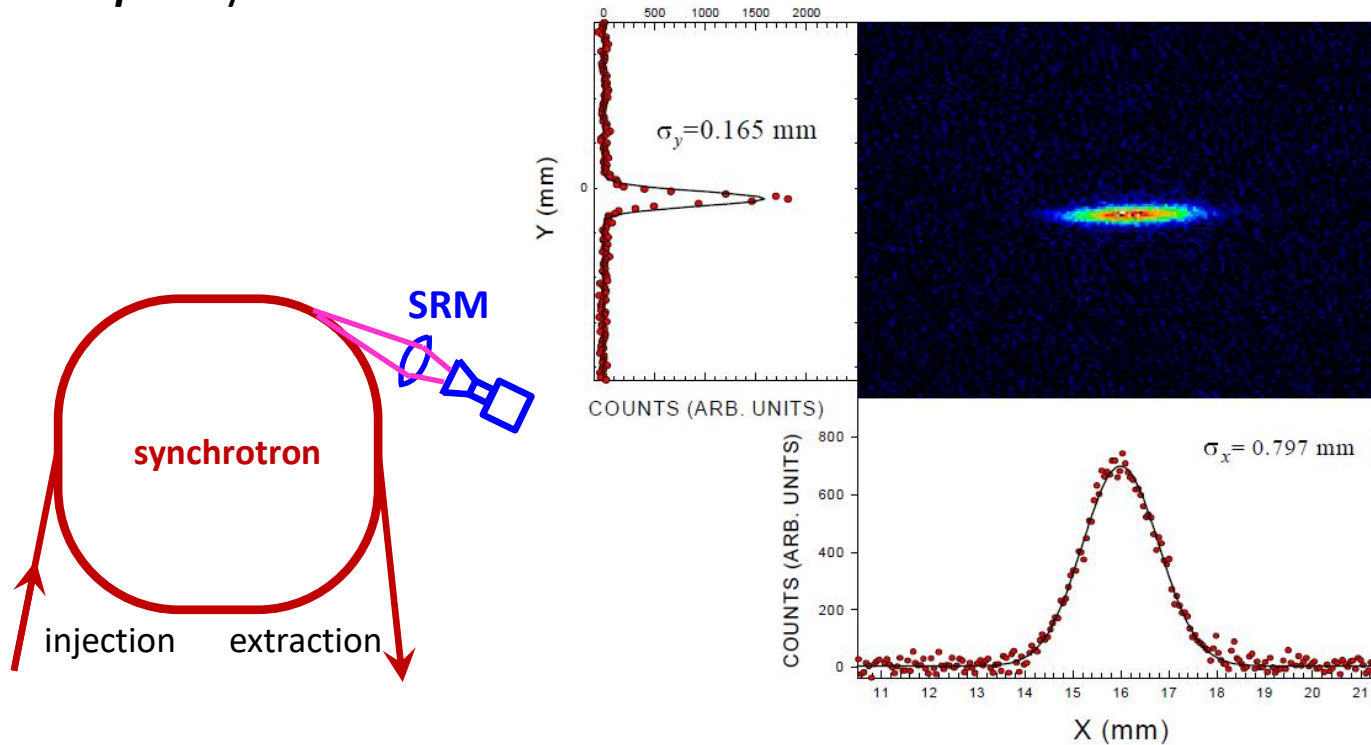
Example: ESRF monitor from dipole with bending radius 22 m (blue or near UV)



Courtesy K. Scheidt et al., DIPAC 2005

Result from a Synchrotron Light Monitor

Example: Synchrotron radiation facilityv APS accumulator ring and blue wavelength:



B.X. Yang (ANL) et al. PAC'97

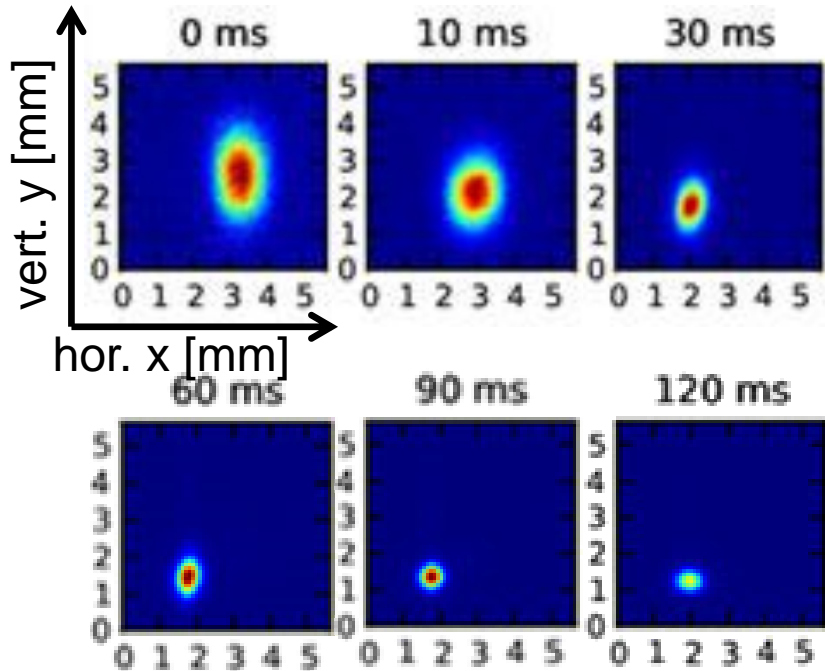
Advantage: Direct measurement of 2-dim distribution, good optics for visible light

Realization: Optics outside of vacuum pipe

Disadvantage: Resolution limited by the diffraction due to finite apertures in the optics.

'Adiabatic Damping' for an Electron Beam

Example: Booster at the light source ALBA acceleration from 0.1 → 3 GeV within 130 ms
 Profiles from synchrotron radiation monitor:



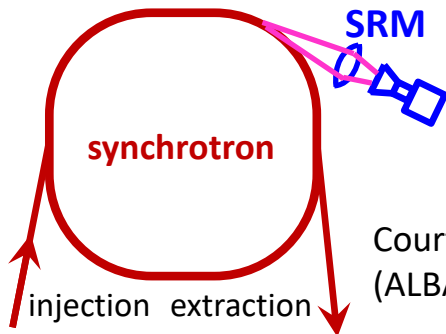
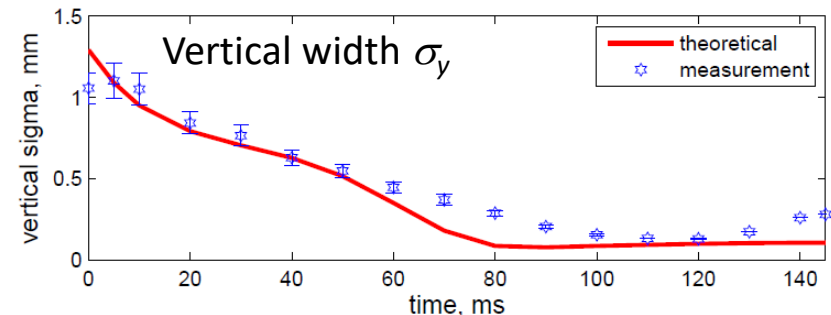
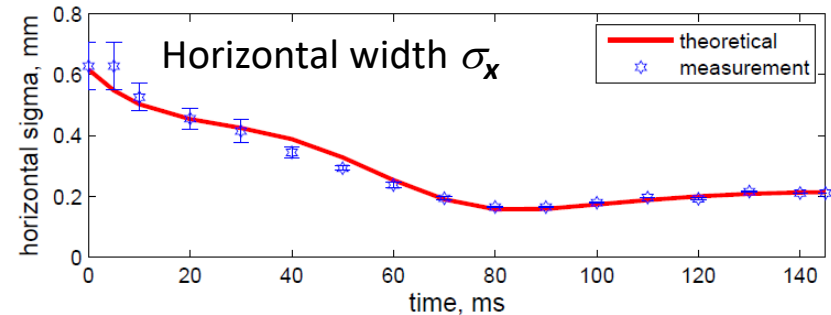
The beam emittance is influenced by:

- Adiabatic damping
- Longitudinal momentum contribution

$$\text{via dispersion } D(s) \Rightarrow \Delta x_D(s) = D(s) \cdot \frac{\Delta p}{p}$$

$$\Rightarrow \text{total width } \sigma_{tot}(s) = \sqrt{\varepsilon\beta(s) + \left(D(s) \cdot \frac{\Delta p}{p}\right)^2}$$

- Quantum fluctuation due to light emission



Courtesy U. Iriso & M. Pont (ALBA) et al. IPAC 2011

Diffraction Limit of Synchrotron Light Monitor

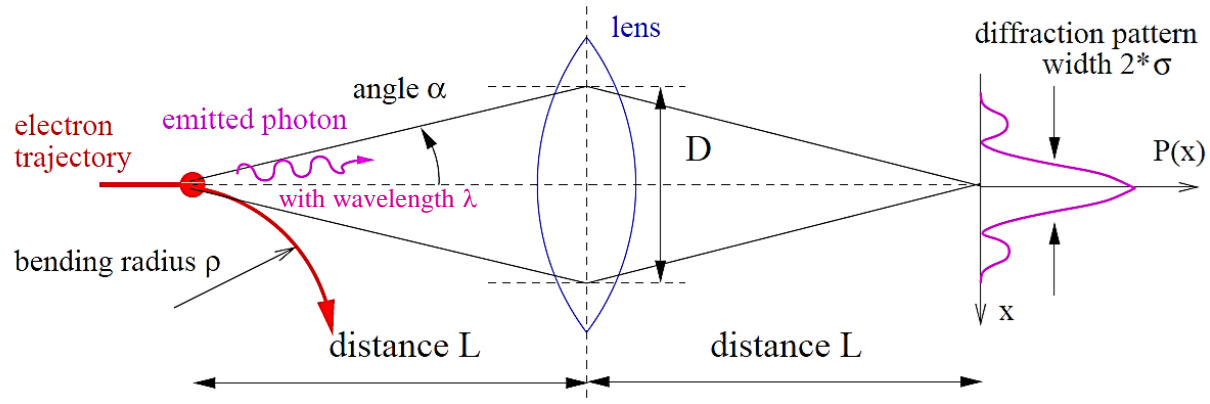
Limitations:

Diffraction limits the resolution due to Fraunhofer diffraction

Pattern width for 1:1 image:

$$\sigma \approx \frac{\lambda}{2D/L} \approx 0.6 \cdot \left(\frac{\lambda^2}{\rho}\right)^{1/3}$$

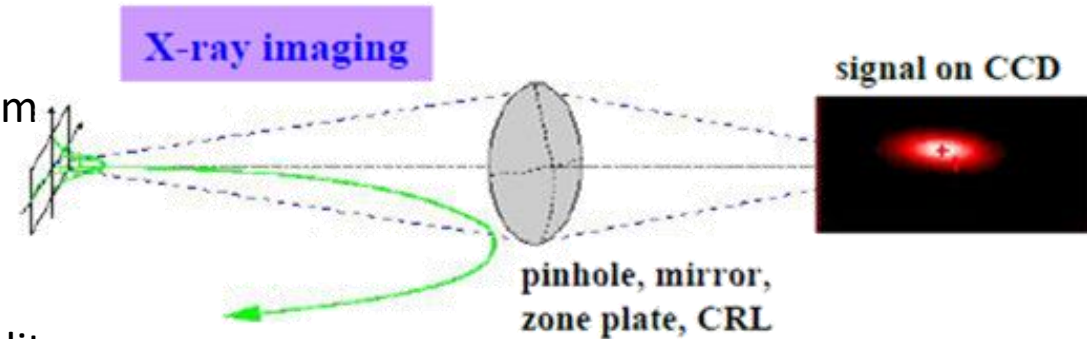
$\Rightarrow \sigma \approx 100 \mu\text{m}$ for typical cases



Improvements:

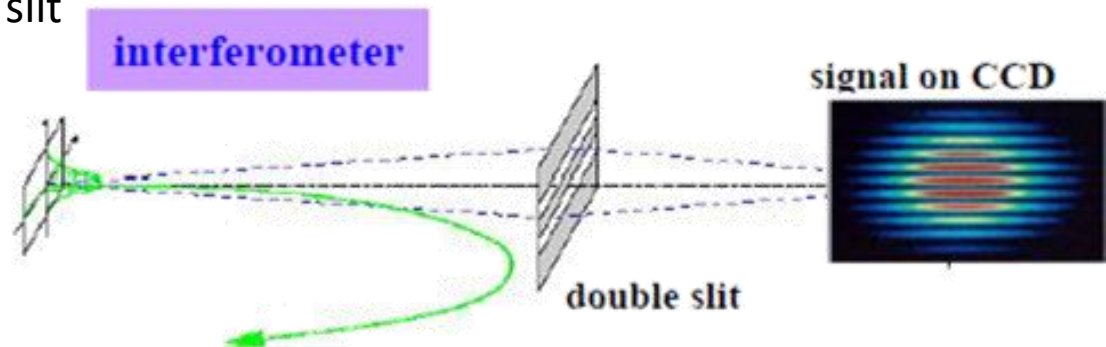
➤ Shorter wavelength:

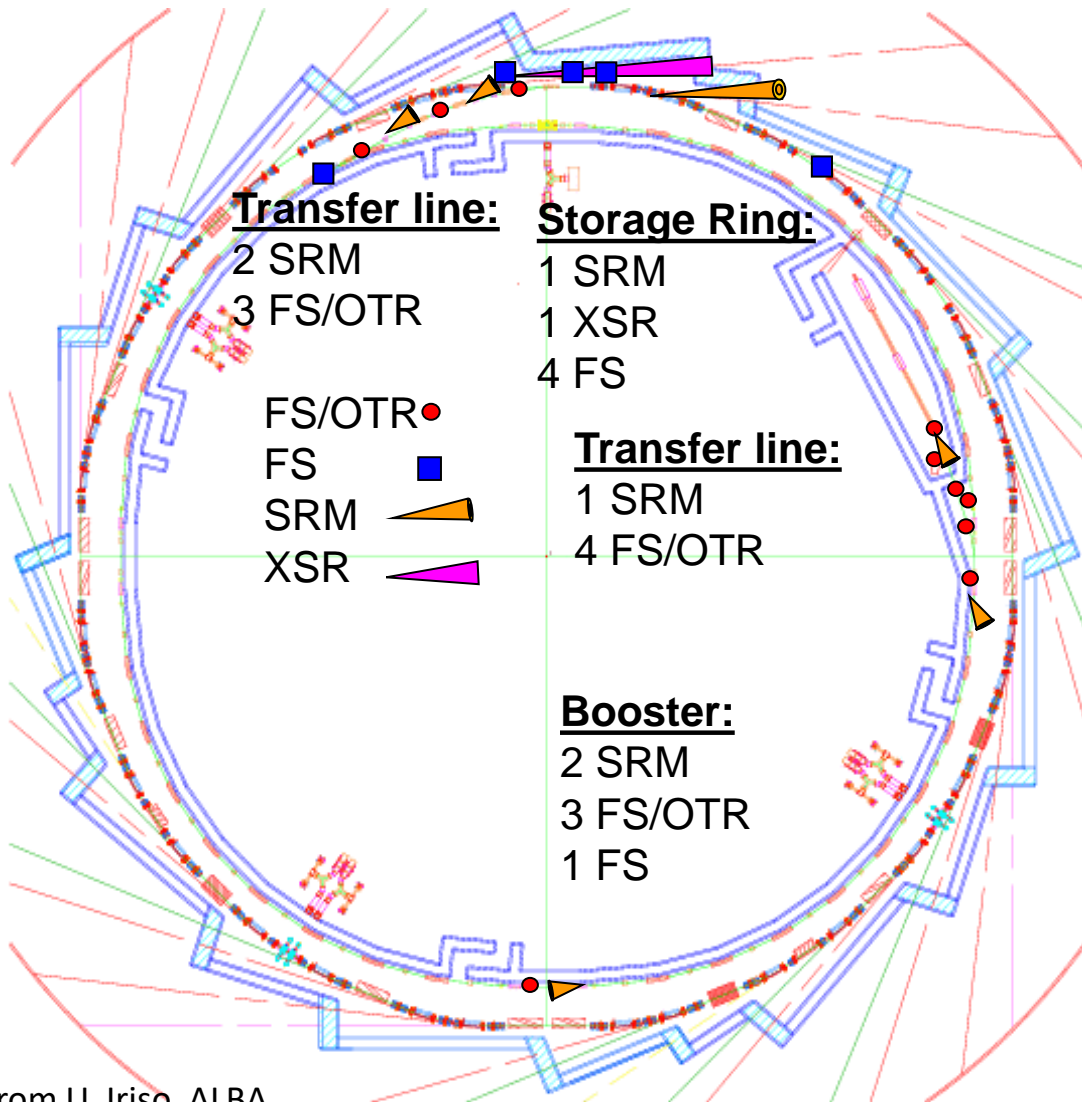
Using X-rays and an aperture of $\varnothing 1\text{mm}$
 → 'X-ray pin hole camera',
 achievable resolution $\sigma \approx 10 \mu\text{m}$



➤ Interference technique:

At optical wavelength using a double slit
 → interference fringe blurring
 compared to point source
 achievable resolution $\sigma \approx 1 \mu\text{m}$.





Transverse profile:

- Many location in transport line
- Single location in ring
- Different devices used

Abbreviation:

FS: Fluorescence Screen

OTR: Optical Trans. Rad. Screen

FS & OTR are destructive

SRM: Synchr. Radiation Monitor

XSR: X-ray pin hole camera

both **non-destructive**

From U. Iriso, ALBA

Different techniques are suited for different beam parameters:

e⁻-beam: typically \emptyset 0.01 to 3 mm, **protons:** typically \emptyset 1 to 30 mm

Intercepting \leftrightarrow non-intercepting methods

Direct observation of electrodynamics processes:

- Optical synchrotron radiation monitor: non-destructive, for e⁻-beams, complex, limited res.
- X-ray synchrotron radiation monitor: non-destructive, for e⁻-beams, very complex
- OTR screen: nearly non-destructive, large relativistic γ needed, e⁻-beams mainly

Detection of secondary photons, electrons or ions:

- Scintillation screen: destructive, large signal, simple setup, all beams
- Ionization profile monitor: non-destructive, expensive, limited resolution, for protons

Wire based electronic methods:

- SEM-grid: partly destructive, large signal and dynamic range, limited resolution
- Wire scanner: partly destructive, large signal and dynamics, high resolution, slow scan.

Measurement of transverse Emittance

The emittance characterizes the whole beam quality, assuming linear behavior as described by second order differential equation.

It is defined within the phase space as: $\varepsilon_x = \frac{1}{\pi} \int_A dx dx'$

The measurement is based on determination of:

- Either** profile width σ_x and angular width σ_x' at one location
- Or** profile width σ_x at different locations and linear transformations.

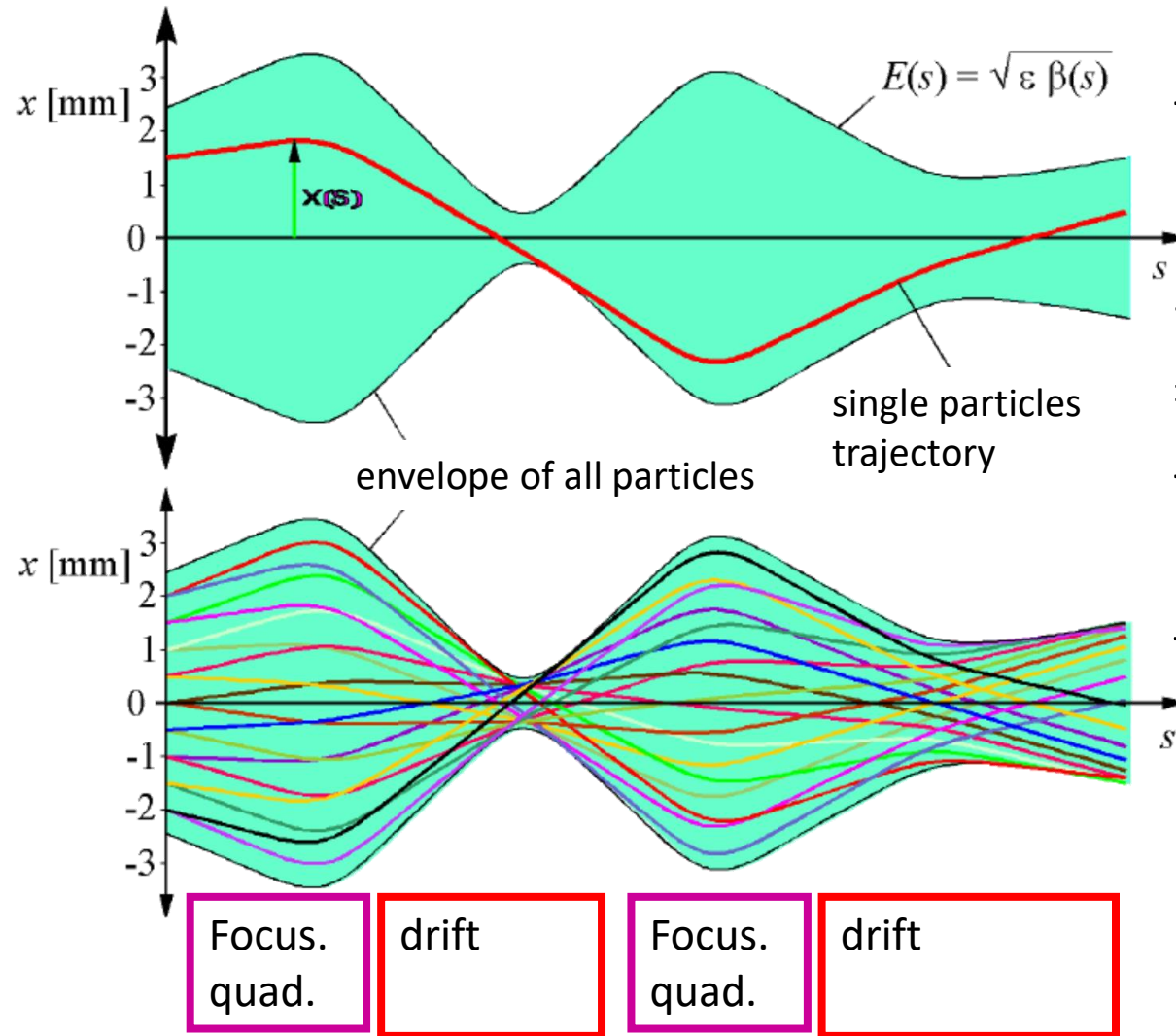
Different devices are used at transfer lines:

- Lower energies $E_{kin} < 100$ MeV/u: slit-grid device, pepper-pot (suited in case of non-linear forces).
- All beams: Quadrupole variation method using linear transformations (**not** well suited in the presence of non-linear forces)

Synchrotron: lattice functions results in stability criterion

⇒ beam width delivers emittance:
$$\varepsilon_x = \frac{1}{\beta_x(s)} \left[\sigma_x^2 - \left(D(s) \frac{\Delta p}{p} \right)^2 \right] \text{ and } \varepsilon_y = \frac{\sigma_y^2}{\beta_y(s)}$$

Trajectory and Characterization of many Particles



➤ Single particle trajectories are forming a beam

➤ They have a distribution of start positions and angles

⇒ Characteristic quantity is the **beam envelope**

➤ **Goal:**

Transformation of envelope

$s \leftrightarrow$ behavior of whole ensemble

see lecture

'Transverse linear Beam Dynamics'
by Wolfgang Hillert

Courtesy K.Wille

Definition of Coordinates and basic Equations

The basic vector is 6 dimensional:

$$\vec{x} = \begin{pmatrix} x \\ x' \\ y \\ y' \\ l \\ \delta \end{pmatrix} = \begin{pmatrix} \text{hori. spatial deviation} \\ \text{horizontal divergence} \\ \text{vert. spatial deviation} \\ \text{vertical divergence} \\ \text{long. deviation} \\ \text{momentum deviation} \end{pmatrix} = \begin{pmatrix} [\text{mm}] \\ [\text{mrad}] \\ [\text{mm}] \\ [\text{mrad}] \\ [\text{mm}] \\ [10^{-3}] \end{pmatrix}$$

The transformation of a single particle from a location s_0 to s_1 is given by the Transfer Matrix R : $\vec{x}(s_1) = R(s) \cdot \vec{x}(s_0)$

The transformation of a the envelope from a location s_0 to s_1 is given by the Beam Matrix σ : $\sigma(s_1) = R(s) \cdot \sigma(s_0) \cdot R^T(s)$

6-dim Beam Matrix with decoupled hor., vert. and long. plane:

$$\sigma = \begin{pmatrix} \sigma_{11} & \sigma_{12} & 0 & 0 & 0 & 0 \\ \sigma_{12} & \sigma_{22} & 0 & 0 & 0 & 0 \\ 0 & 0 & \sigma_{33} & \sigma_{34} & 0 & 0 \\ 0 & 0 & \sigma_{34} & \sigma_{44} & 0 & 0 \\ 0 & 0 & 0 & 0 & \sigma_{55} & \sigma_{56} \\ 0 & 0 & 0 & 0 & \sigma_{56} & \sigma_{66} \end{pmatrix}$$

horizontal
vertical
longitudinal
hor.-long. coupling
→ 9 values

Beam width for the three coordinates:

$$x_{rms} = \sqrt{\sigma_{11}}$$

$$y_{rms} = \sqrt{\sigma_{33}}$$

$$l_{rms} = \sqrt{\sigma_{55}}$$

Horizontal beam matrix:

$$\sigma_{11} = \langle x^2 \rangle$$

$$\sigma_{12} = \langle x x' \rangle$$

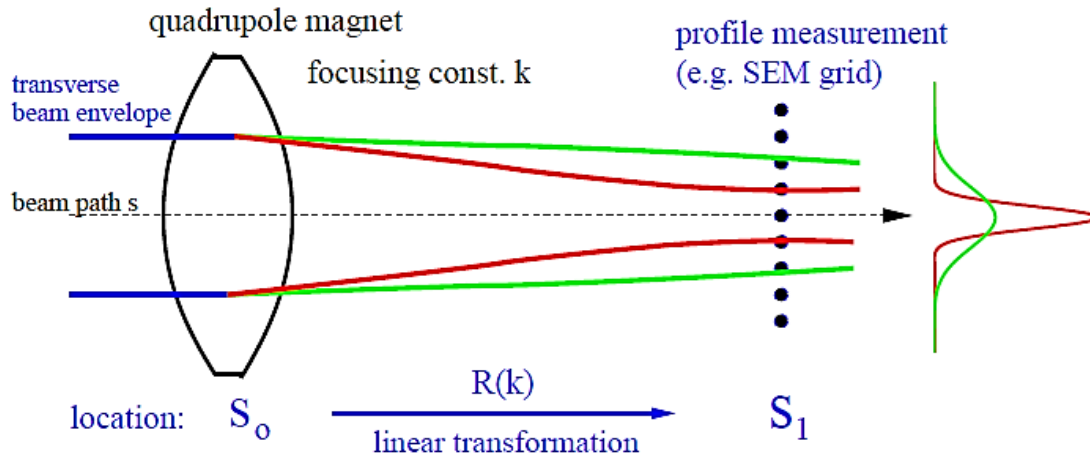
$$\sigma_{22} = \langle x'^2 \rangle$$

Outline:

- Definition and some properties of transverse emittance
- **Quadrupole strength variation and position measurement**
emittance from several profile measurement and beam optical calculation
- Slit-Grid device: scanning method

Emittance Measurement by Quadrupole Variation

From a profile determination, the emittance can be calculated via linear transformation, if a well known and constant distribution (e.g. Gaussian) is assumed.



- Measurement of beam width

$$x^2_{max} = \sigma_{11}(s_1, k)$$

matrix $R(k)$ describes the focusing.

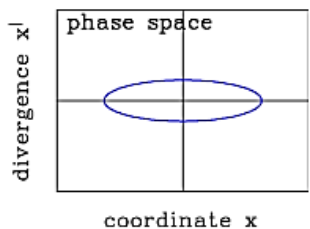
- With the drift matrix the transfer is

$$R(k_i) = R_{drift} \cdot R_{focus}(k_i)$$

- Transformation of the beam matrix

$$\sigma(s_1, k_i) = R(k_i) \cdot \sigma(s_0) \cdot R^T(k_i)$$

Task: Calculation of matrix $\sigma(s_0)$ at entrance s_0 , i.e. three elements

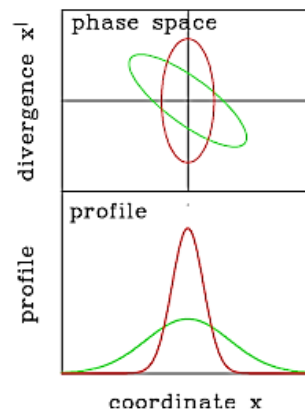


beam matrix:

(Twiss parameters)

$$\sigma_{11}(0), \sigma_{12}(0), \sigma_{22}(0)$$

to be determined



measurement:

$$x^2(k) = \sigma_{11}(1, k)$$

see lecture 'Linear Imperfections' by Volker Ziemann

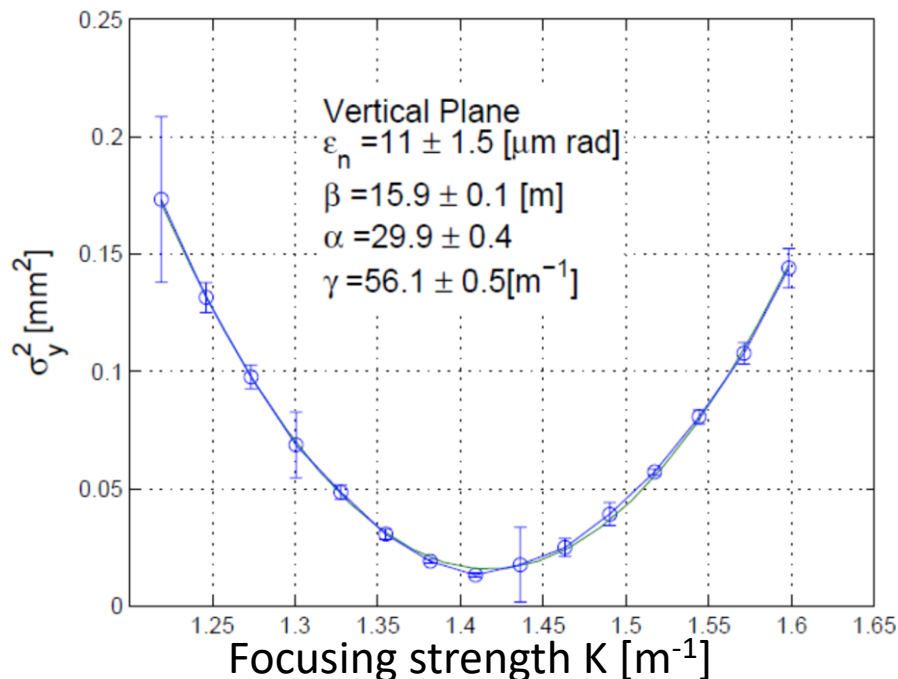
Measurement of transverse Emittance

Using the 'thin lens approximation' i.e. the quadrupole has a focal length of f :

$$\mathbf{R}_{focus}(\mathbf{K}) = \begin{pmatrix} 1 & 0 \\ -1/f & 1 \end{pmatrix} \equiv \begin{pmatrix} 1 & 0 \\ \mathbf{K} & 1 \end{pmatrix} \Rightarrow \mathbf{R}(L, \mathbf{K}) = \mathbf{R}_{drift}(L) \cdot \mathbf{R}_{focus}(\mathbf{K}) = \begin{pmatrix} 1 + L\mathbf{K} & L \\ \mathbf{K} & 1 \end{pmatrix}$$

Measurement of matrix-element $\sigma_{11}(s_1, K)$ from matrices $\sigma(s_1, K_i) = \mathbf{R}(K_i) \cdot \sigma(s_0) \cdot \mathbf{R}^T(K_i)$

Example: Square of the beam width at ELETTRA 100 MeV e^- Linac, YAG:Ce:



G. Penco (ELETTRA) et al., EPAC'08

For completeness: The relevant formulas

$$\begin{aligned} \sigma_{11}(\mathbf{1}, \mathbf{K}) &= L^2 \sigma_{11}(\mathbf{0}) \cdot \mathbf{K}^2 \\ &+ 2 \cdot (L \sigma_{11}(\mathbf{0}) + L^2 \sigma_{12}(\mathbf{0})) \cdot \mathbf{K} \\ &+ L^2 \sigma_{22}(\mathbf{0}) + \sigma_{11}(\mathbf{0}) \\ &\equiv a \cdot \mathbf{K}^2 - 2ab \cdot \mathbf{K} + ab^2 + c \\ &= a \cdot (\mathbf{K} - b)^2 + c \end{aligned}$$

A fit delivers the beam matrix elements $\sigma_{ij}(s_0)$

Assumptions:

- 'Regular' phase space distribution
- Well aligned beam, no steering
- No emittance blow-up due to space charge

Improved methods:

Based on e.g. tomographic reconstruction

Outline:

- Definition and some properties of transverse emittance
- Quadrupole strength variation and position measurement
emittance from several profile measurement and beam optical calculation
- **Slit-Grid device: scanning method**
scanning slit → beam position & grid → angular distribution

The Emittance for Gaussian and non-Gaussian Beams

The beam distribution can be non-Gaussian, e.g. at:

- Beams behind ion source
- Space charged dominated beams at LINAC & synchrotron
- Cooled beams in storage rings

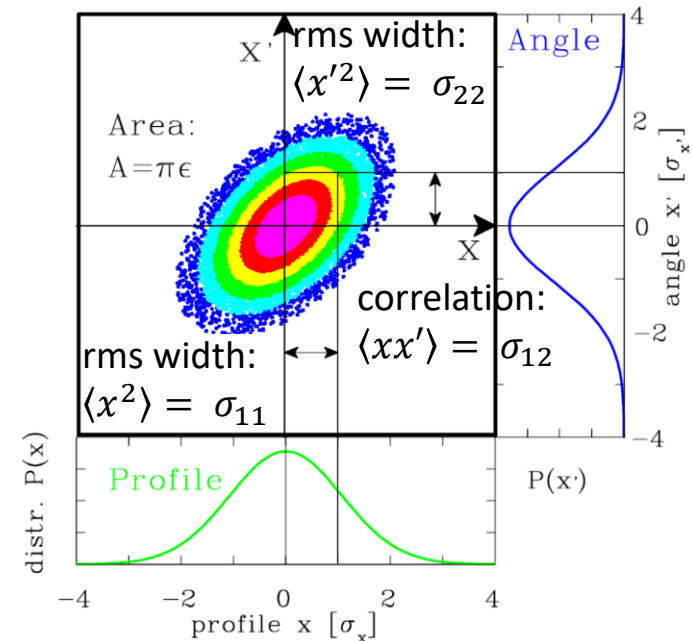
Generally: Emittance by 2nd statistical moments of 2-dim distribution:

Beam matrix:
$$\sigma = \begin{pmatrix} \langle x^2 \rangle & \langle xx' \rangle \\ \langle xx' \rangle & \langle x'^2 \rangle \end{pmatrix}$$

Emittance:
$$\epsilon_{rms} = \sqrt{\det \sigma}$$

$$= \sqrt{\underbrace{\langle x^2 \rangle \langle x'^2 \rangle}_{\text{Variances}} - \underbrace{\langle xx' \rangle^2}_{\text{Covariance i.e. correlation}}}$$

It describes the value for 1 standard derivation.

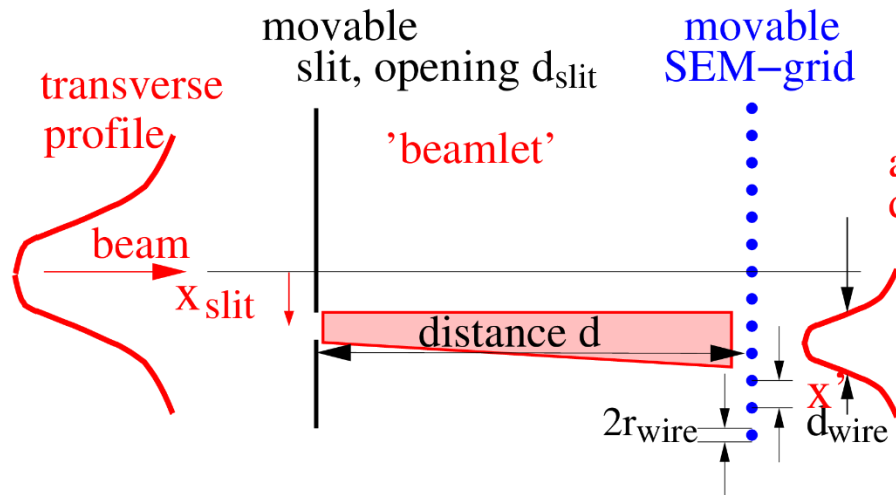


The Slit-Grid Measurement Device

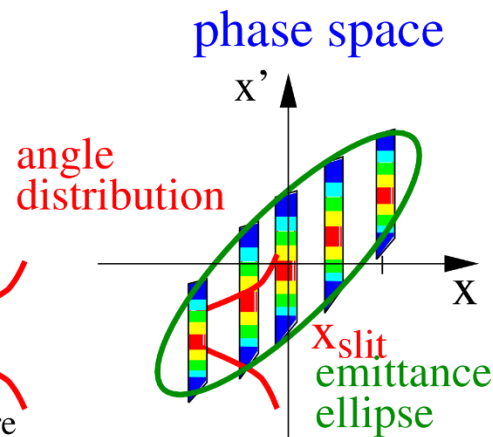
Slit-Grid: Direct determination of position and angle distribution.

Used for protons with $E_{kin} < 100 \text{ MeV/u} \Rightarrow \text{range } R < 1 \text{ cm}$.

Hardware



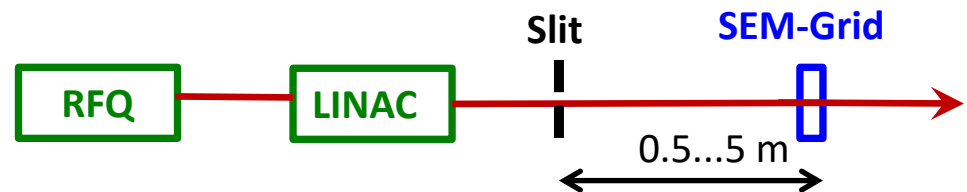
Analysis



Slit: position $P(x)$ with typical width: 0.1 to 0.5 mm

Distance: typ. 0.5 to 5 m (depending on beam energy 0.1 ... 100 MeV)

SEM-Grid: angle distribution $P(x')$



Display of Measurement Results

The distribution is depicted as a function of position [mm] & angle [mrad]

The distribution can be visualized by

- Mountain plot
- Contour plot

Calc. of 2nd moments $\langle x^2 \rangle$, $\langle x'^2 \rangle$ & $\langle xx' \rangle$

Emittance value ϵ_{rms} from

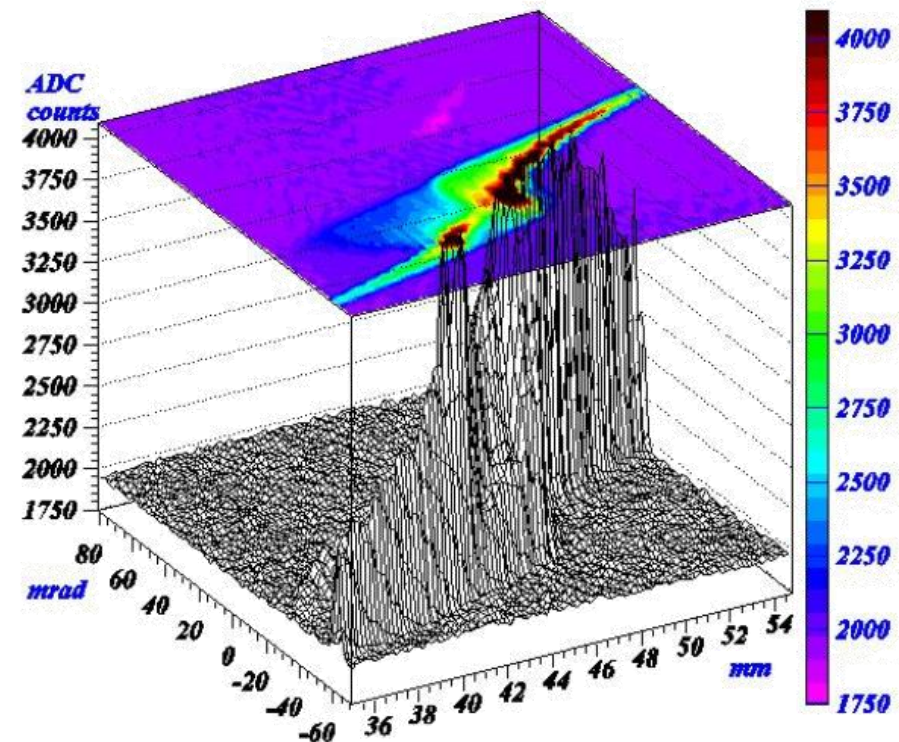
$$\epsilon_{rms} = \sqrt{\langle x^2 \rangle \cdot \langle x'^2 \rangle - \langle xx' \rangle^2}$$

Problems:

- Finite **binning** results in limited resolution
- **Background** → large influence on $\langle x^2 \rangle$, $\langle x'^2 \rangle$ & $\langle xx' \rangle$
- **Or fit of distribution with an ellipse**

⇒ **Effective emittance only**

Remark: Behind a ion source the beam might be non-Gaussian due to plasma density and aberration at quadrupoles



Beam: Ar⁴⁺, 60 keV, 15 μ A
at Spiral2 Phoenix ECR source.

P. Ausset, DIPAC 2009

See lecture 'Sources' by Klaus Knie

Summary for transverse Emittance Measurement

Emittance is the important quantity for comparison to theory.

It includes absolute value (value of ϵ) & orientation in phase space (σ_{ij} or α , β and γ)

three independent values $\epsilon_{rms} = \sqrt{\sigma_{11} \cdot \sigma_{22} - \sigma_{12}^2} \equiv \sqrt{\langle x^2 \rangle \langle x'^2 \rangle - \langle xx' \rangle^2}$

assuming no coupling between horizontal, vertical and longitudinal planes

Transfer line, all beams → profile measurement + linear transformation:

➤ **Quadrupole variation:** one location, different setting of a quadrupole

Assumptions: ➤ well aligned beam, no steering

➤ no emittance blow-up due to space charge

Transfer line, low energy beams → direct measurement of x- and x'-distribution:

➤ **Slit-grid:** movable slit → x -profile, grid → x' -profile

➤ Requirement: Beam is stopped in $\approx 1\text{cm} \Leftrightarrow$ protons $E_{kin} \lesssim 100\text{ MeV}$

Remark: Non-linear transformation possible via tomographic reconstruction

Important remark: For a synchrotron with a *stable beam storage*,

width measurement is sufficient using $x_{rms} = \sqrt{\epsilon_{rms} \cdot \beta}$

Measurement of longitudinal Parameters

Measurement of longitudinal parameter:

Bunch length measurement at

- Synchrotron light sources: Streak camera
- Linear light sources: Electro-optical modulator
- Summary

Longitudinal ↔ transverse correspondences:

- position relative to rf ↔ transverse center-of-mass
- bunch structure in time ↔ transverse profile
- momentum or energy spread ↔ transverse divergence
- longitudinal emittance ↔ transverse emittance.

The Bunch Position measured by a Pick-Up

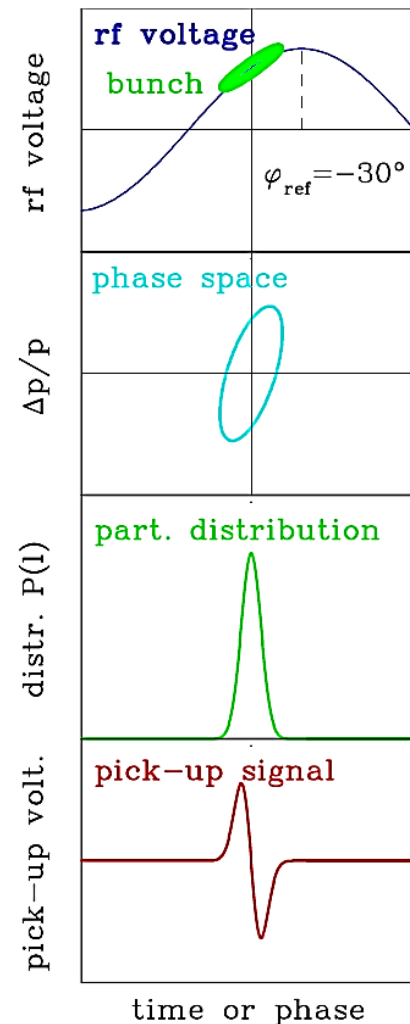
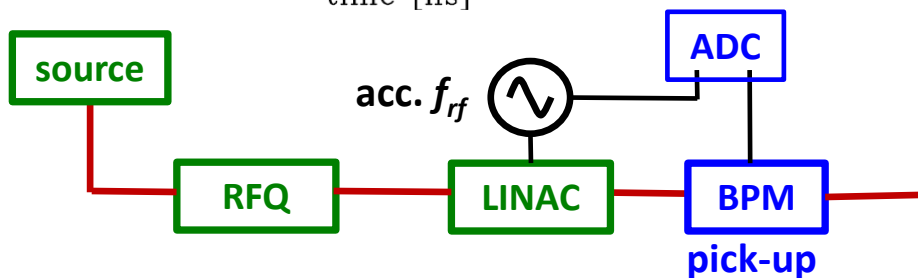
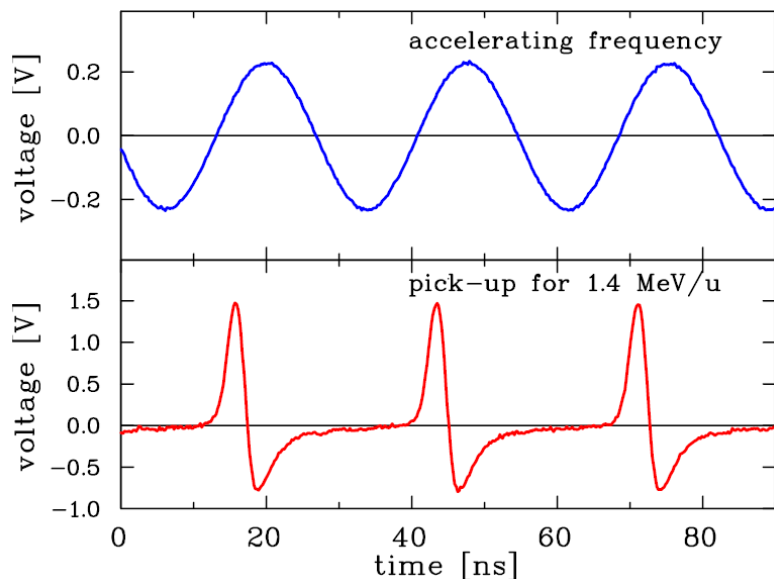
The **bunch position** is given relative to the accelerating rf.

e.g. $\varphi_{ref} = -30^\circ$ inside a rf cavity

must be well aligned for optimal acceleration

Transverse correspondence: Beam position

Example: Pick-up signal for $f_{rf} = 36$ MHz rf at GSI-LINAC:

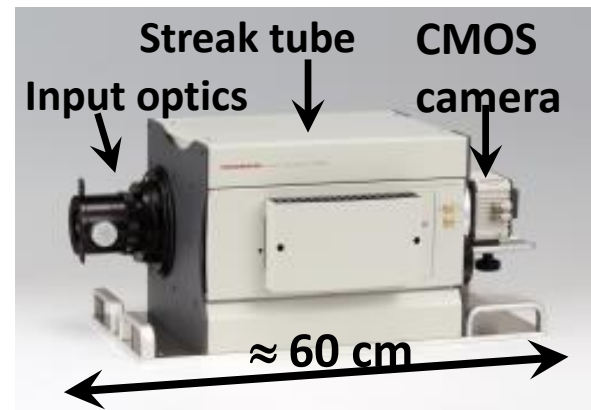
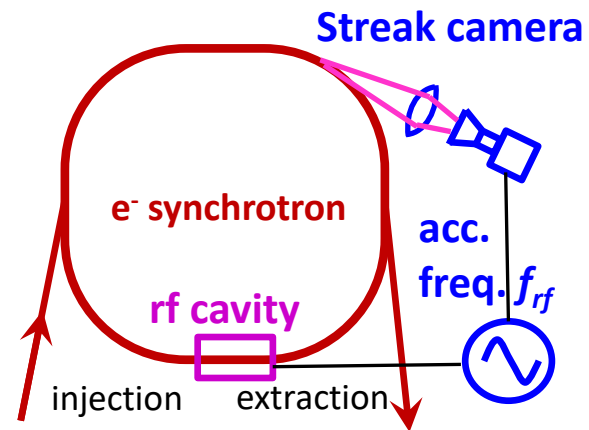
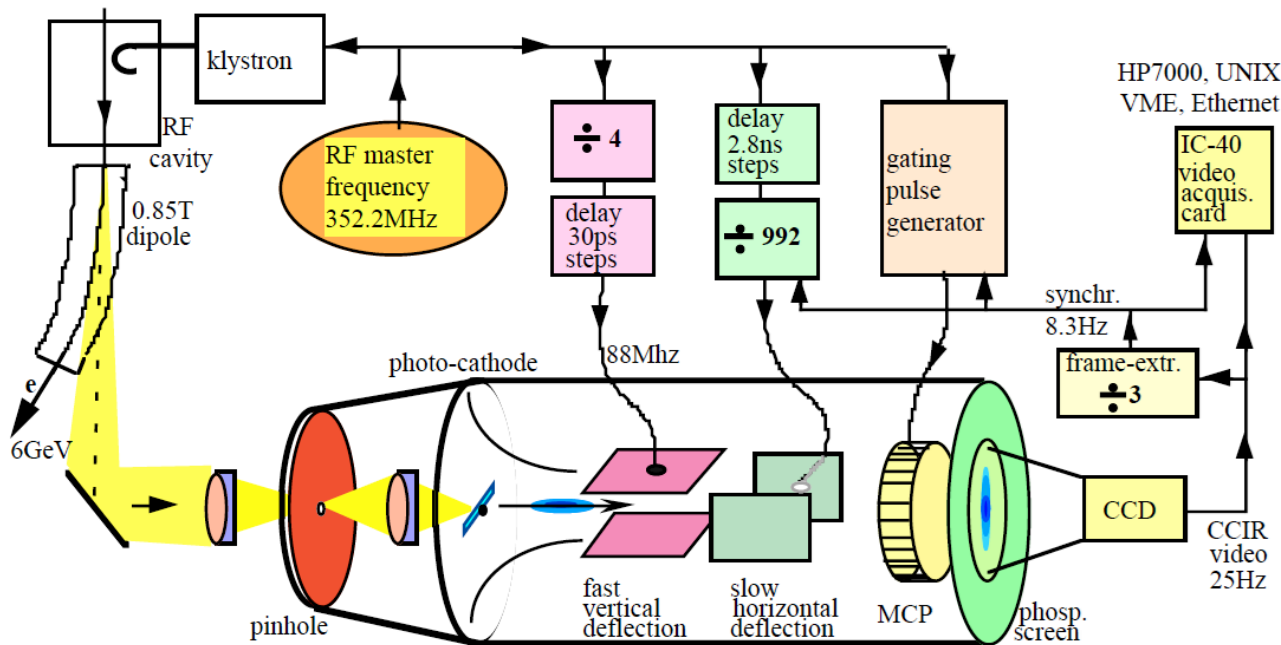


Bunch Length Measurement for relativistic Electrons

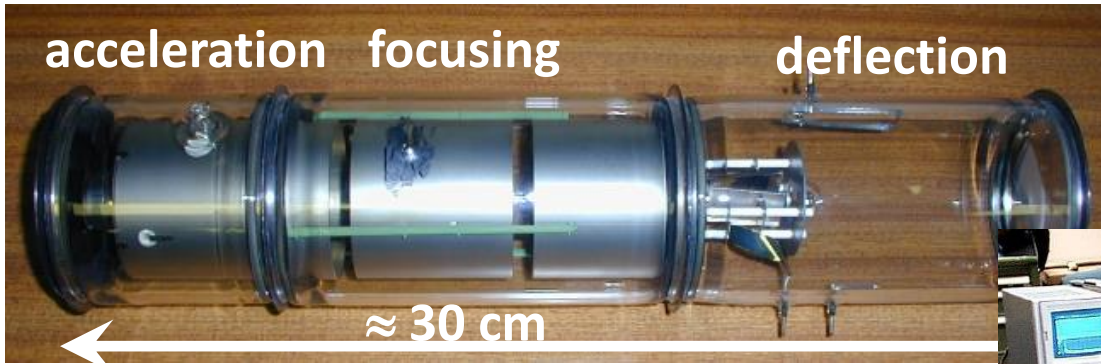
Electron bunches are too short ($\sigma_t < 100$ ps) to be covered by the bandwidth of pick-ups ($f < 3$ GHz $\Leftrightarrow t_{rise} > 100$ ps) for structure determination.

→ Time resolved observation of synchr. light with a streak camera: Resolution ≈ 1 ps.

Scheme of a streak camera

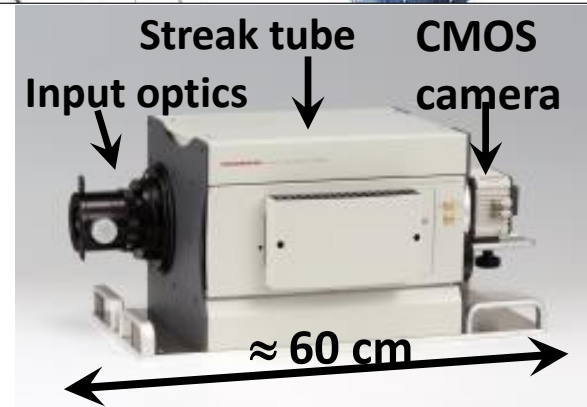
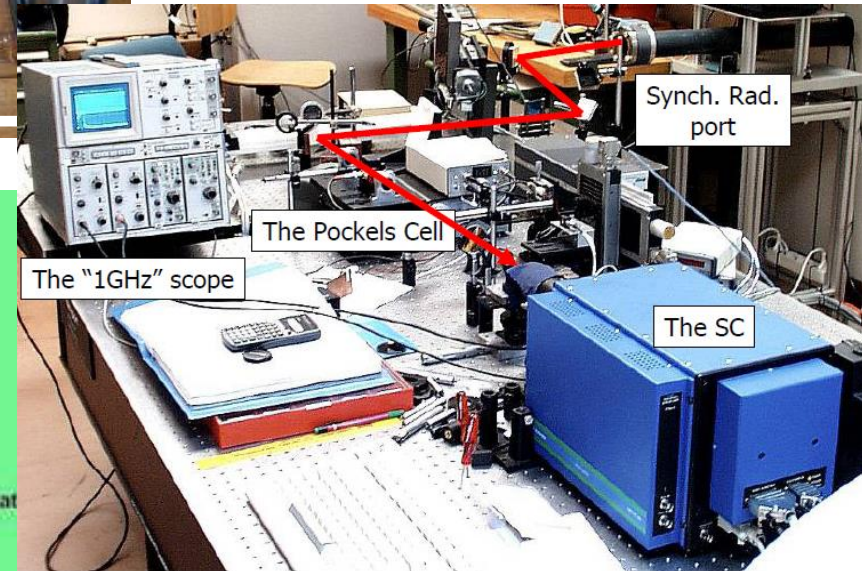
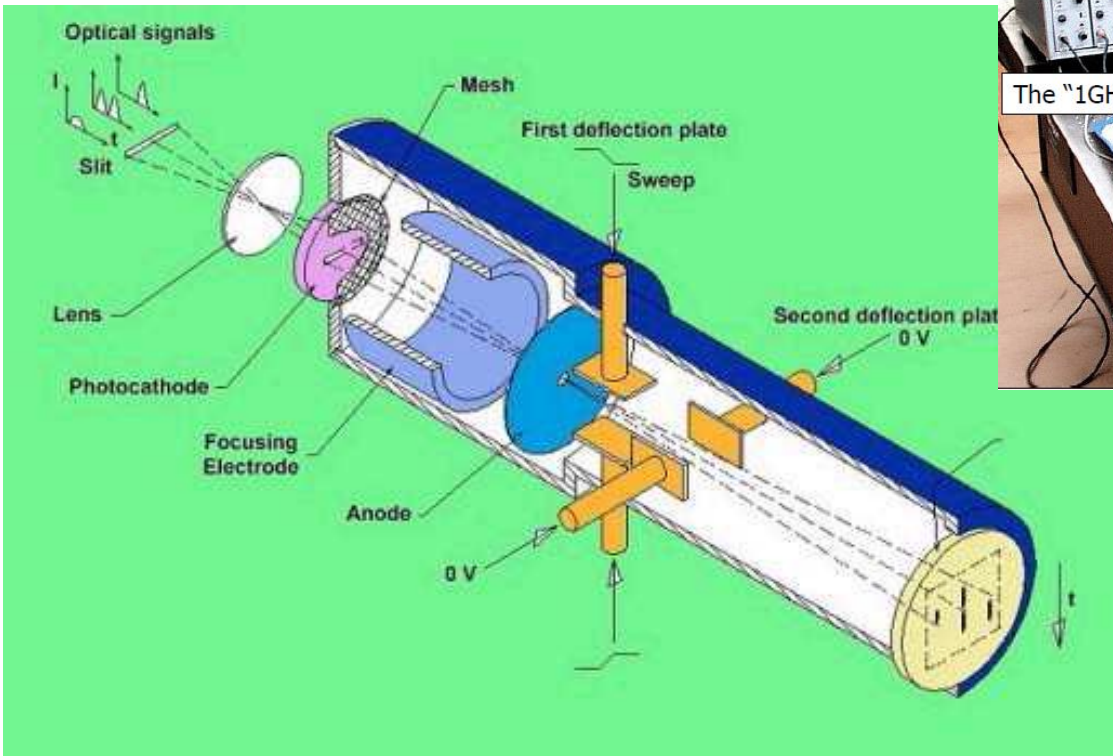


Technical Realization of a Streak Camera



Hardware of a streak camera

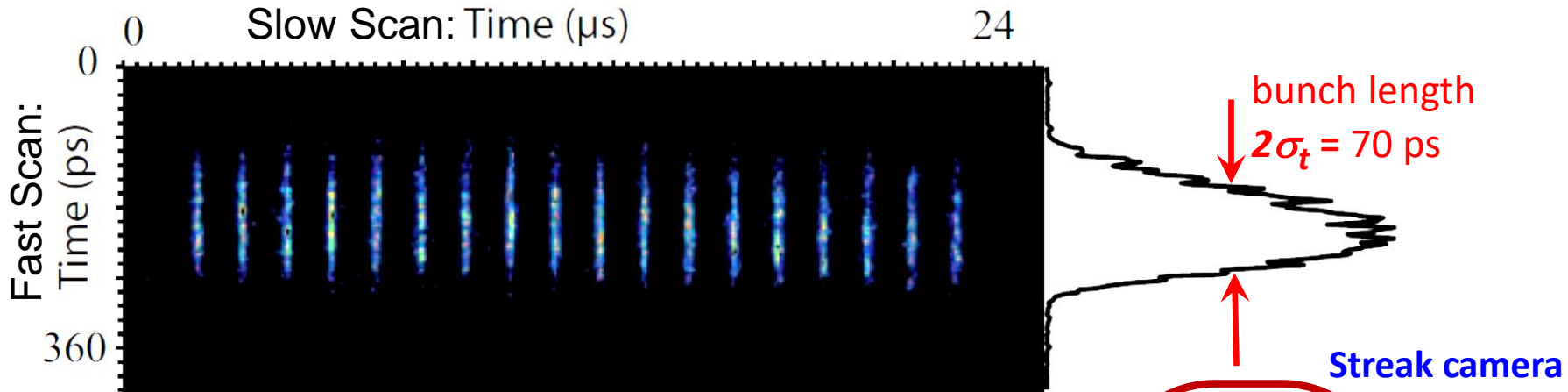
Time resolution down to 0.5 ps



Results of Bunch Length Measurement by a Streak Camera

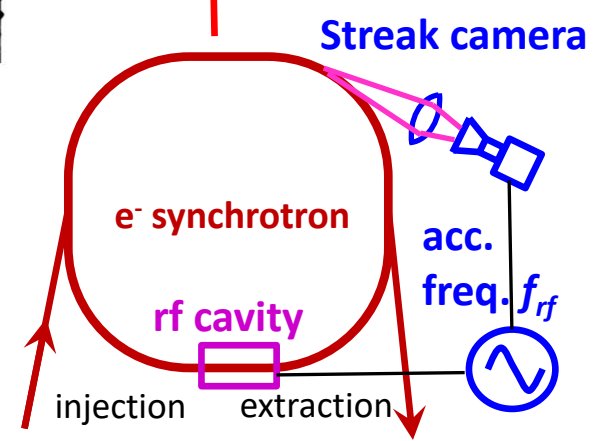
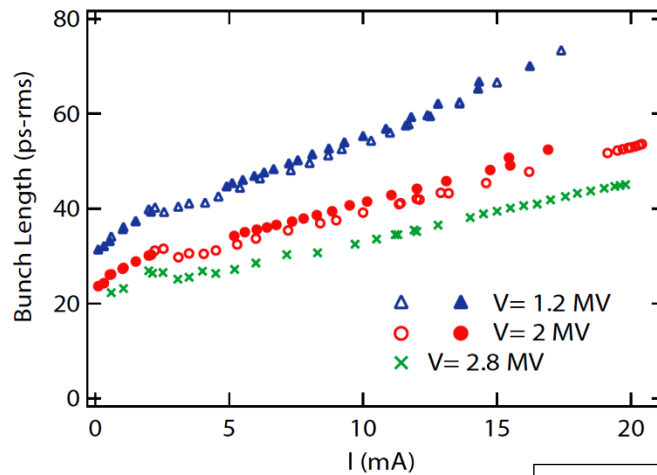
The streak camera delivers a fast scan in vertical direction (here 360 ps full scale) and a slower scan in horizontal direction (24 μ s).

Example: Bunch length at the synchrotron light source SOLEIL for $U_{rf} = 2$ MV for slow direction 24 μ s and scaling for fast scan 360 ps: measure $\sigma_t = 35$ ps.



Short bunches are desired by the users

Example: Bunch length σ_t as a function of stored current (i.e. space charge de-focusing) at SOLEIL



Courtesy of M. Labat et al., DIPAC'07

See lecture 'Electron Beam Dynamics' by Lenny Rivkin

Measurement of longitudinal Parameters

Measurement of longitudinal parameter:

Bunch length measurement at

- Synchrotron light sources: Streak camera
- Linear light sources: Electro-optical modulators
- Summary

Bunch Length Measurement by electro-optical Method

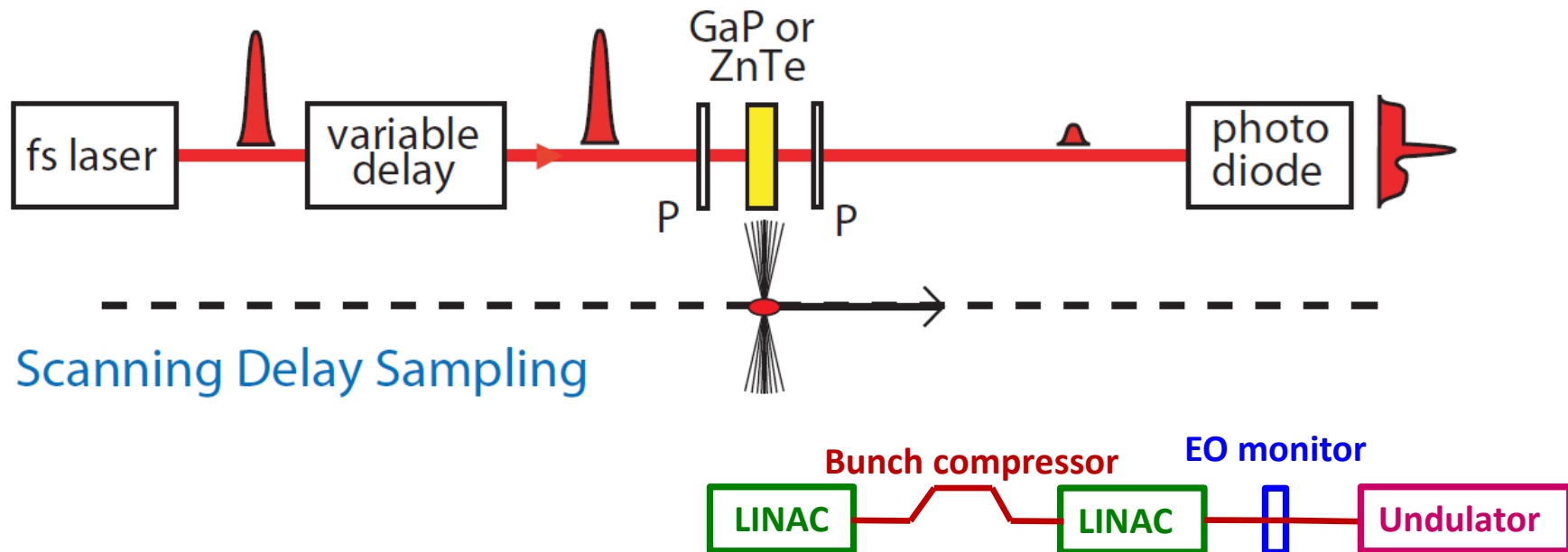
For Free Electron Lasers → bunch length below 1 ps is achieved

- Below the resolution of streak camera
- Short laser pulses with $t \approx 10$ fs and electro-optical modulator

Electro optical modulator: Birefringent, rotation angle depends on external electric field

Relativistic electron bunch: transverse ele. field $E_{\perp,lab} = \gamma E_{\perp,rest}$ carries the time information

Scanning of delay between bunch and laser → time profile after several pulses.



Courtesy S.P.Jamison et al., EPAC 2006

See lecture 'Synchrotron light circular machines & FELs' by Eduard Prat

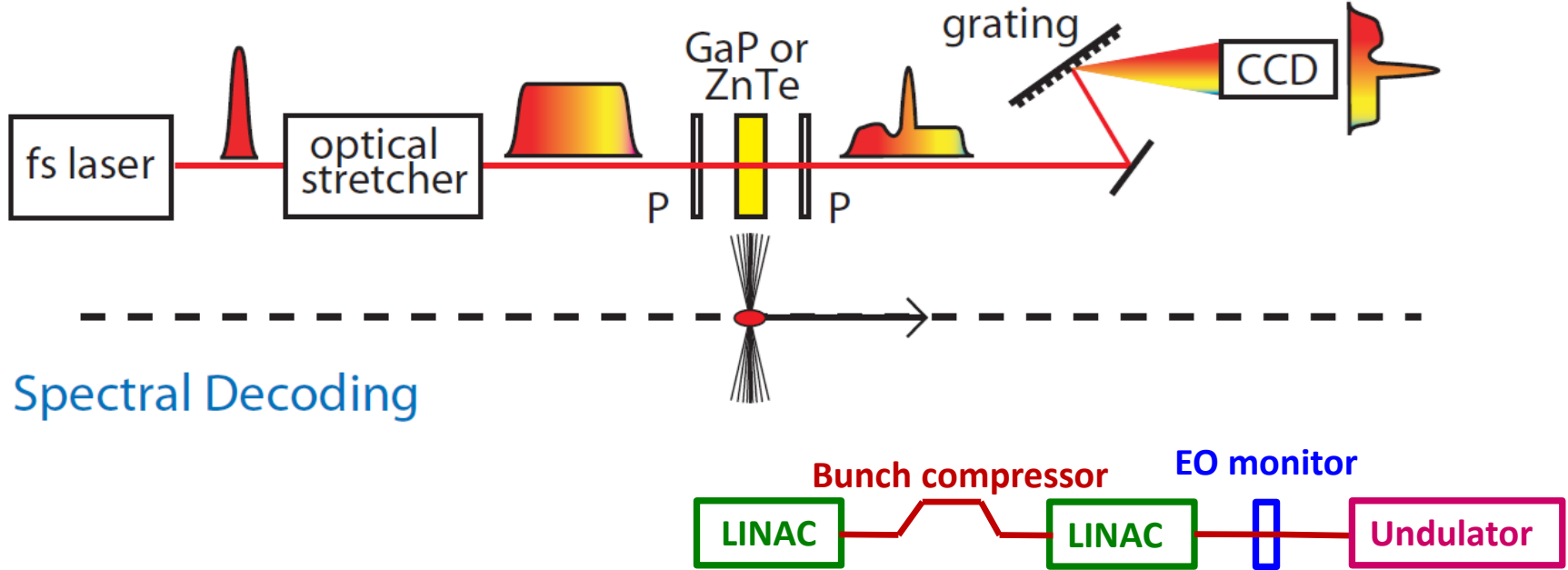
Bunch Length Measurement by electro-optical Method

For Free Electron Lasers → bunch length below 1 ps is achieved

Short laser pulse \Leftrightarrow broad frequency spectrum (property of Fourier Transformation)

Optical stretcher: Separation of colors by different path length

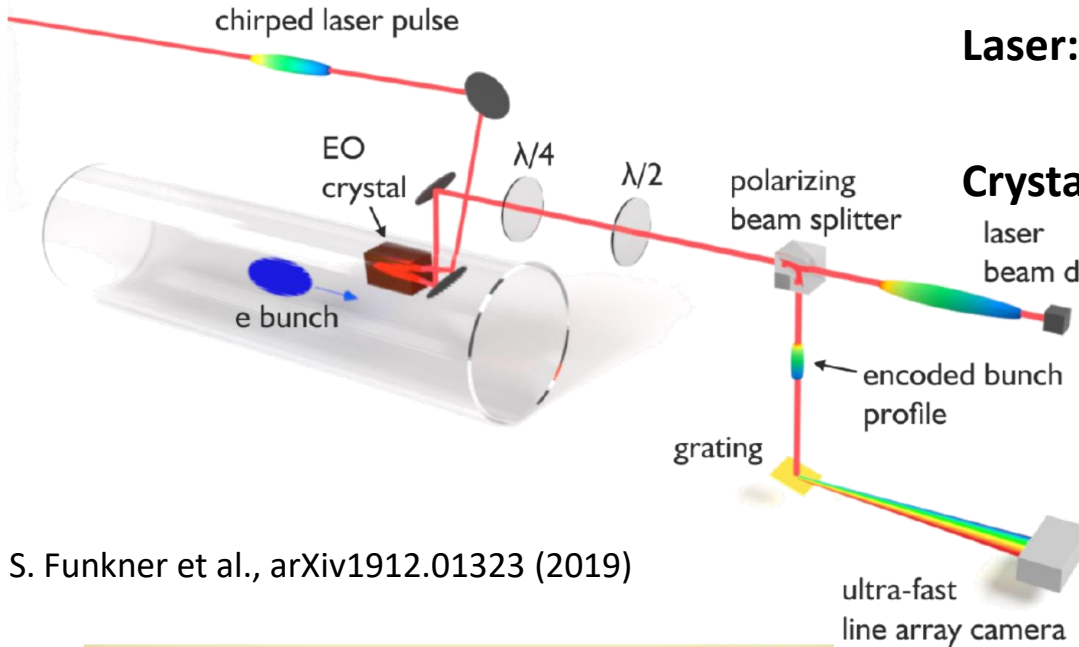
\Rightarrow different colors at different time \Rightarrow **single-shot observation**



Spectral Decoding

Courtesy S.P.Jamison et al., EPAC 2006

Hardware of a spectral-decoded EOSD Scanning Setup

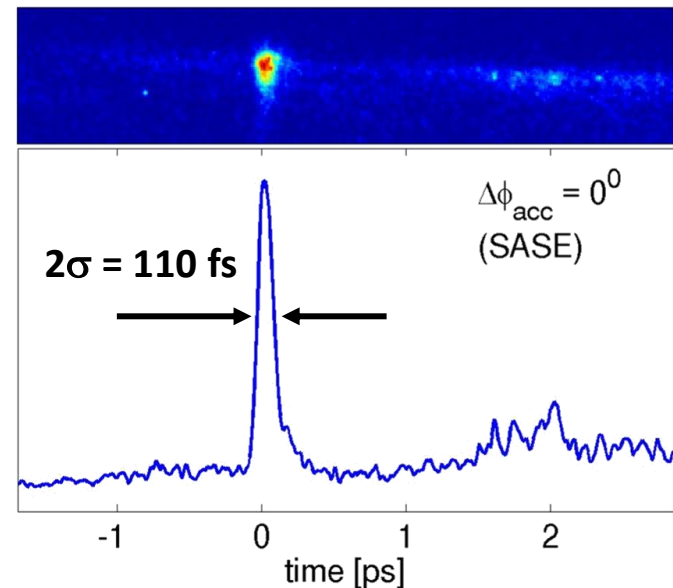


Laser: Commercial Ti:Sa or Yb-fibre,
10 fs duration, near IR,

Crystal: GaP or ZnTe, 100 μm thickness

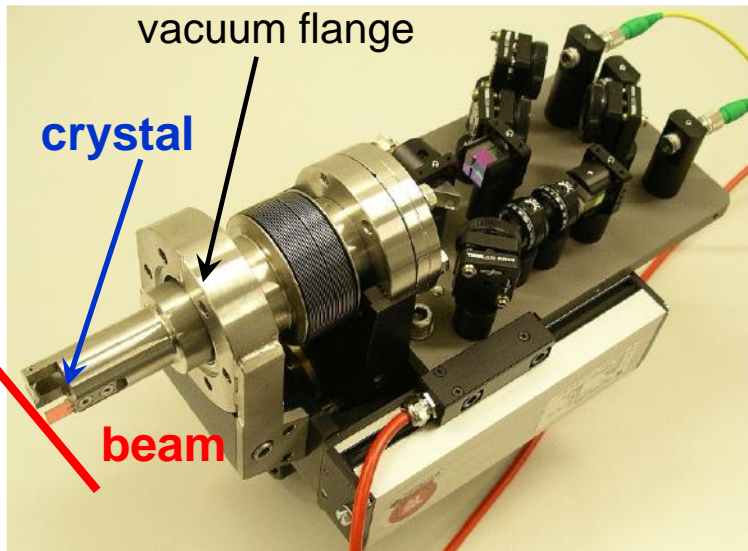
Example: Bunch length at FLASH
100 fs bunch duration = 30 μm length !

S. Funkner et al., arXiv1912.01323 (2019)



B. Steffen et al, DIPAC 2009

B. Steffen et al., Phys. Rev. AB 12, 032802 (2009)



Devices for bunch length at light sources:

Streak cameras:

- Time resolved monitoring of synchrotron radiation
 - for relativistic e^- -beams, $10 \text{ ps} < t_{\text{bunch}} < 1 \text{ ns}$
- Time resolution limit of streak camera $\approx 1 \text{ ps}$

Laser-based electro-optical modulation:

- Electro-optical modulation of short laser pulse
 - very high time resolution down to some fs time resolution
- Technical complex installation

Diagnostics is the 'sensory organ' for the beam.

It required for operation and development of accelerators

Several categories of demands leads to different installations:

- Quick, non-destructive measurements leading to a single number or simple plots
- Complex instrumentation used for hard malfunction and accelerator development
- Automated measurement and control of beam parameters i.e. feedback

The goal and a clear interpretation of the results is a important design criterion.

General comments:

- Quite different technologies are used, based on various physics processes
- Accelerator development goes parallel to diagnostics development
(\Rightarrow it makes fun as many skills are required).

Thank you for your attention!

- H. Schmickler (Ed.) *Beam Instrumentation*, Proc. CERN Accelerator School, Tuusula 2018.
- D. Brandt (Ed.), *Beam Diagnostics for Accelerators*, Proc. CERN Accelerator School, Dourdan, CERN-2009-005, 2009.
- Proceedings of several CERN Acc. Schools (introduction & advanced level, special topics).
- V. Smaluk, *Particle Beam Diagnostics for Accelerators: Instruments and Methods*, VDM Verlag Dr. Müller, Saarbrücken 2009.
- P. Strehl, *Beam Instrumentation and Diagnostics*, Springer-Verlag, Berlin 2006.
- M.G. Minty and F. Zimmermann, *Measurement and Control of Charged Particle Beams*, Springer-Verlag, Berlin 2003.
- S-I. Kurokawa, S.Y. Lee, E. Perevedentev, S. Turner (Eds.), *Proceeding of the School on Beam Measurement*, Proceedings Montreux, World Scientific Singapore (1999).
- P. Forck, *Lecture Notes on Beam Instrumentation and Diagnostics*, JUAS School, JUAS Indico web-site.
- Contributions to conferences, in particular to **International Beam Instrumentation Conference IBIC**.

Backup slides

Broadening due to the Beam's Space Charge: Ion Detection

Influence of the residual gas ion trajectory by :

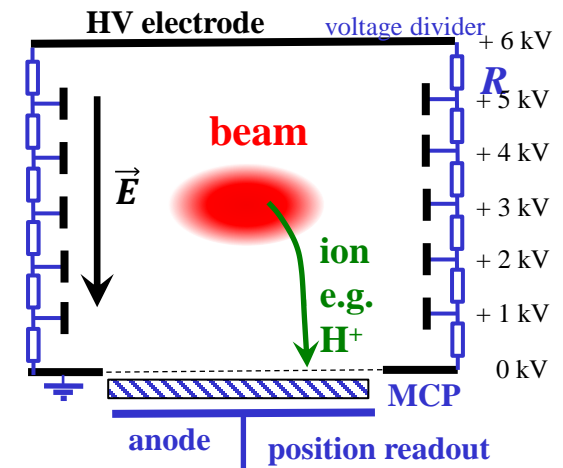
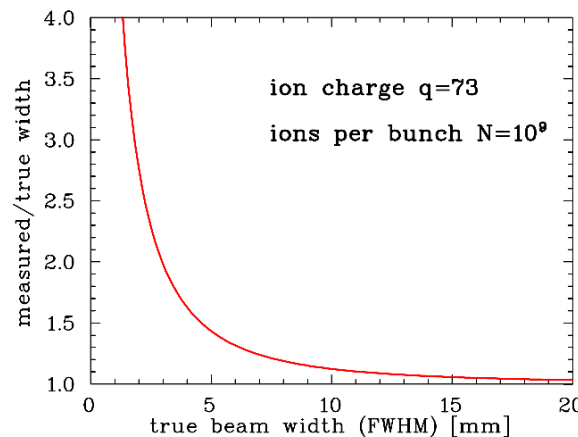
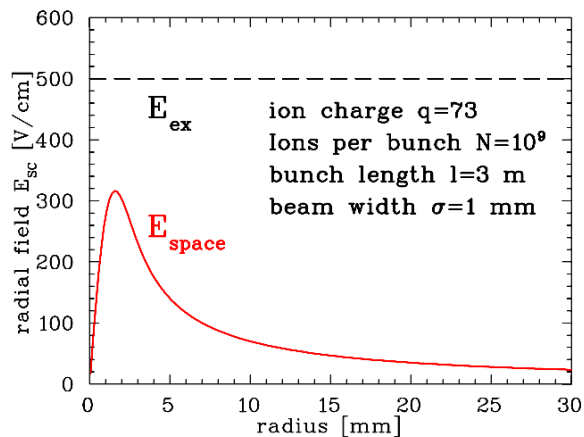
- External electric field E_{ex}
- Electric field of the beam's space charge E_{space}

e.g. Gaussian density distribution for round beam: $E_{space}(r) = \frac{1}{2\pi\epsilon_0} \cdot \frac{qeN}{l} \cdot \frac{1}{r} \cdot \left[1 - \exp\left(-\frac{r^2}{2\sigma^2}\right) \right]$

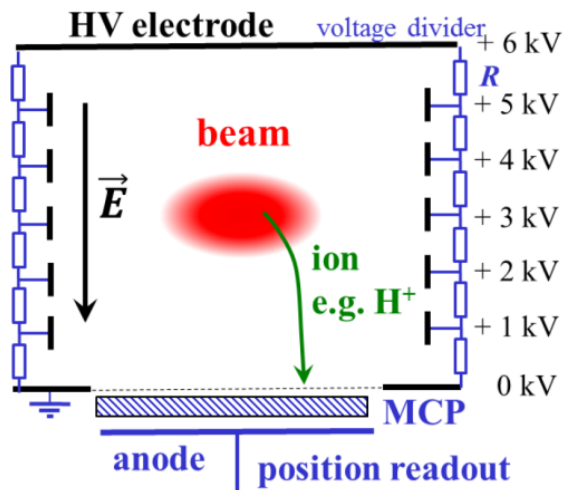
Estimation of correction: $\sigma_{corr}^2 \approx \frac{e^2 \ln 2}{4\pi\epsilon_0 \sqrt{m_p c^2}} \cdot \frac{qN}{l} \cdot d_{gap} \cdot \sqrt{\frac{1}{eU_{ex}}} \propto N \cdot d_{gap} \cdot \sqrt{\frac{1}{U_{ex}}}$

With the measured beam width is given by convolution: $\sigma_{meas}^2 = \sigma_{true}^2 + \sigma_{corr}^2$

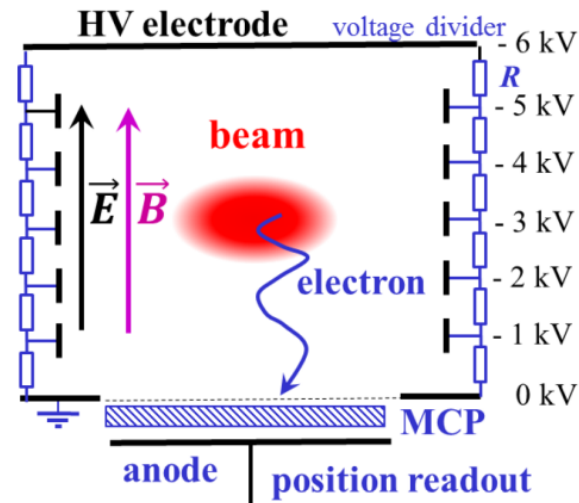
Example: U^{73+} , 10^9 particles per 3 m bunch length, cooled beam with $\sigma_{true} = 1$ mm FWHM.



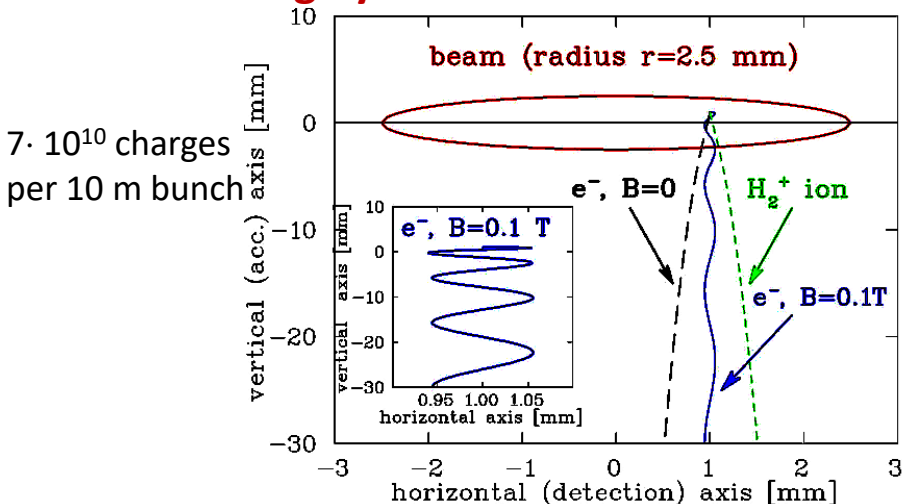
Ion detection mode:



Electron detection mode:



⇒ broadening by beam's electric field



e^- detection in an external magnetic field

$$\rightarrow \text{cyclotron radius } r_c = \frac{mv_{\perp}}{eB}$$

for $E_{kin,\perp} = 10 \text{ eV}$ & $B = 0.1 \text{ T} \Rightarrow r_c \approx 100 \mu\text{m}$

E_{kin} from atomic physics, $\approx 100 \mu\text{m}$ resolution of MCP

Time-of-flight: $\approx 1 - 2 \text{ ns} \Rightarrow 2 - 3 \text{ cycles}$.

B-field: Dipole with large aperture

\rightarrow IPM is expensive & large device!

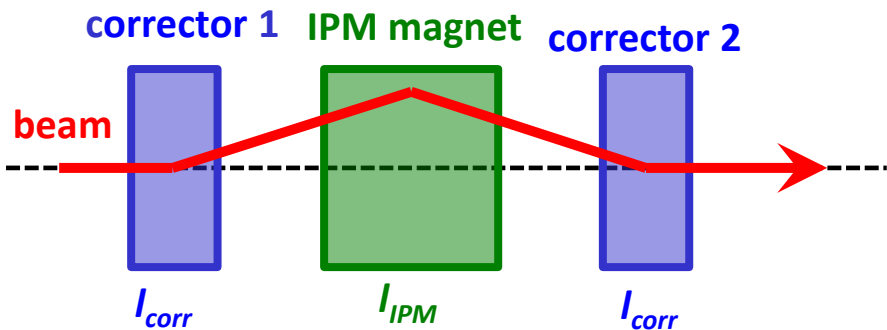
Magnetic field for electron guidance:

Maximum image distortion:

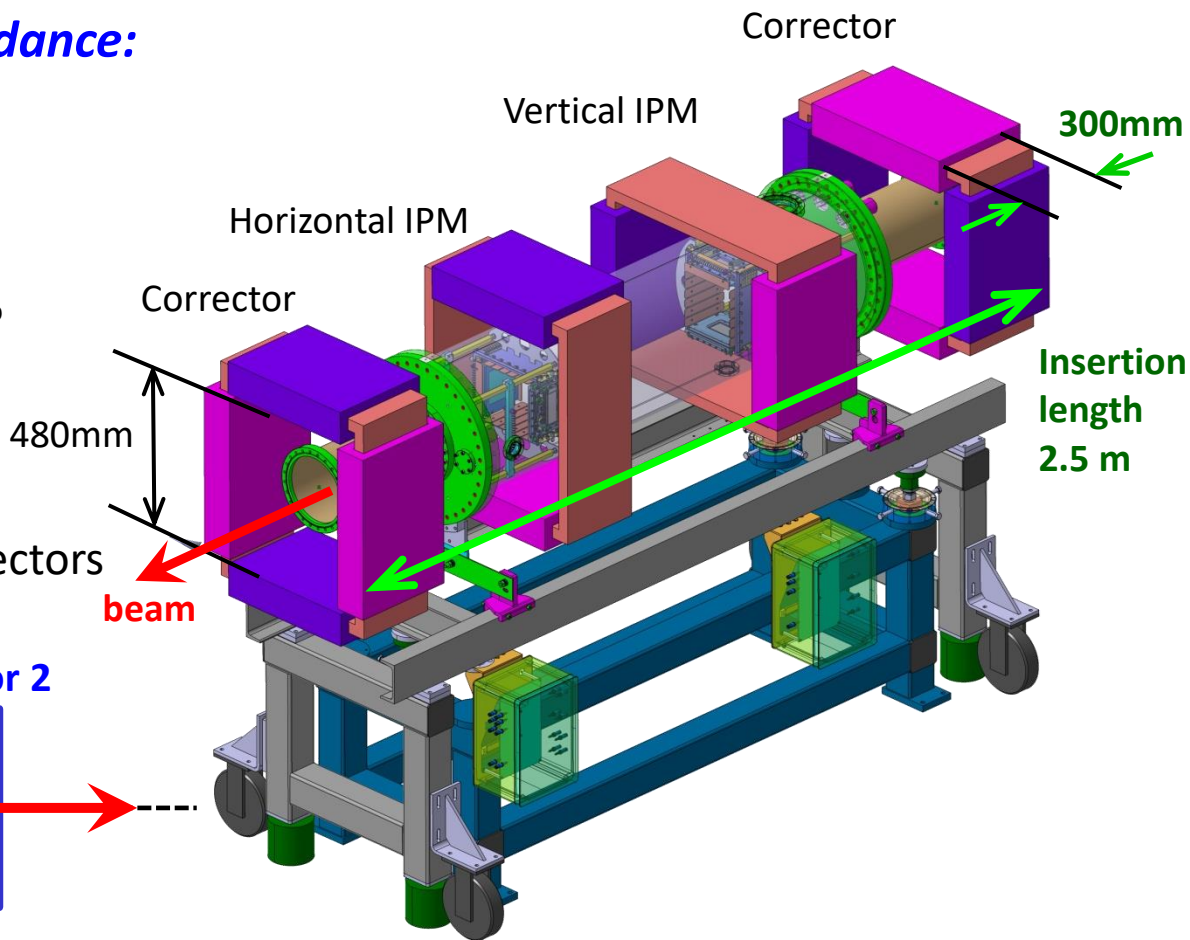
5% of beam width $\Rightarrow \Delta B/B < 1\%$

Challenges:

- High B -field homogeneity of 1%
- Clearance up to 500 mm
- Correctors required to compensate beam steering
- Insertion length 2.5 m incl. correctors



$$B_{cor} \cdot I_{corr} = -\frac{1}{2} B_{IPM} \cdot I_{IPM}$$



Remark: For MCP wire-array readout lower clearance required

IPM: Magnet Design

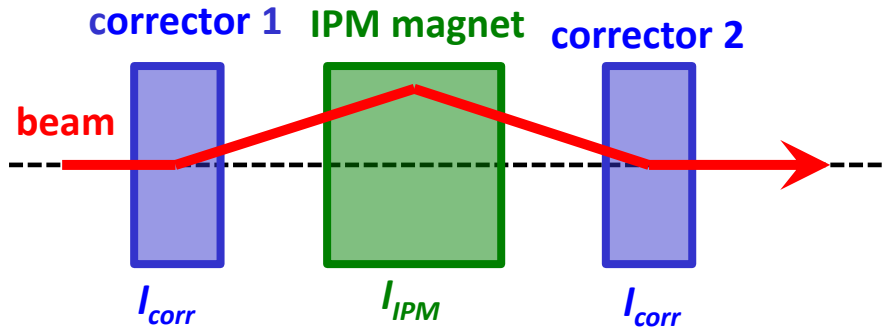
Magnetic field for electron guidance:

Maximum image distortion:

5% of beam width $\Rightarrow \Delta B/B < 1\%$

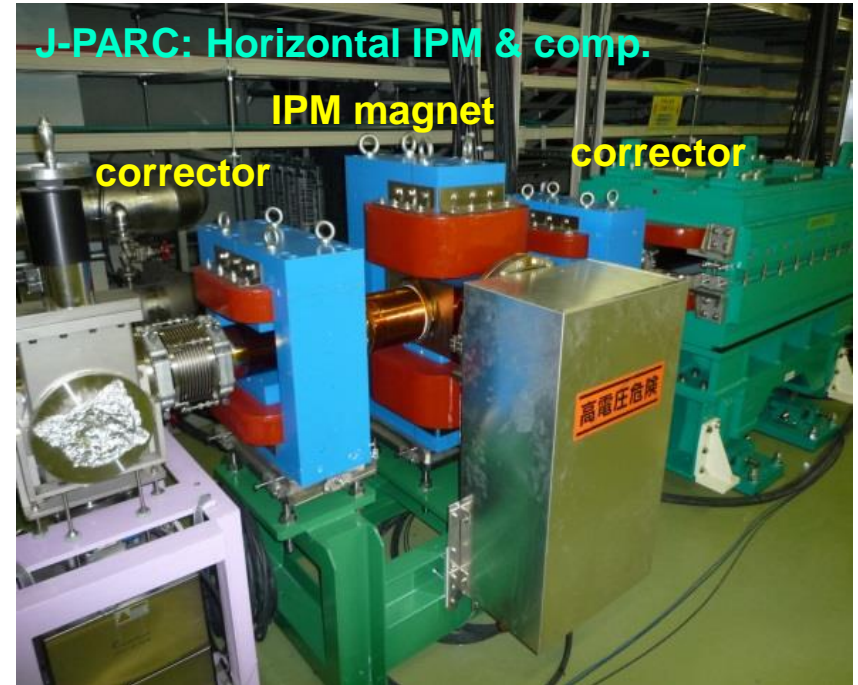
Challenges:

- High B -field homogeneity of 1%
- Clearance up to 500 mm
- Correctors required to compensate beam steering
- Insertion length 2.5 m incl. correctors



$$B_{cor} \cdot I_{corr} = -\frac{1}{2} B_{IPM} \cdot I_{IPM}$$

Remark: For MCP wire-array readout lower clearance required



Magnet: $B = 250$ mT, Gap 220 mm
IPM: Profile 32 strips, 2.5 mm width

Remark for electron beams:

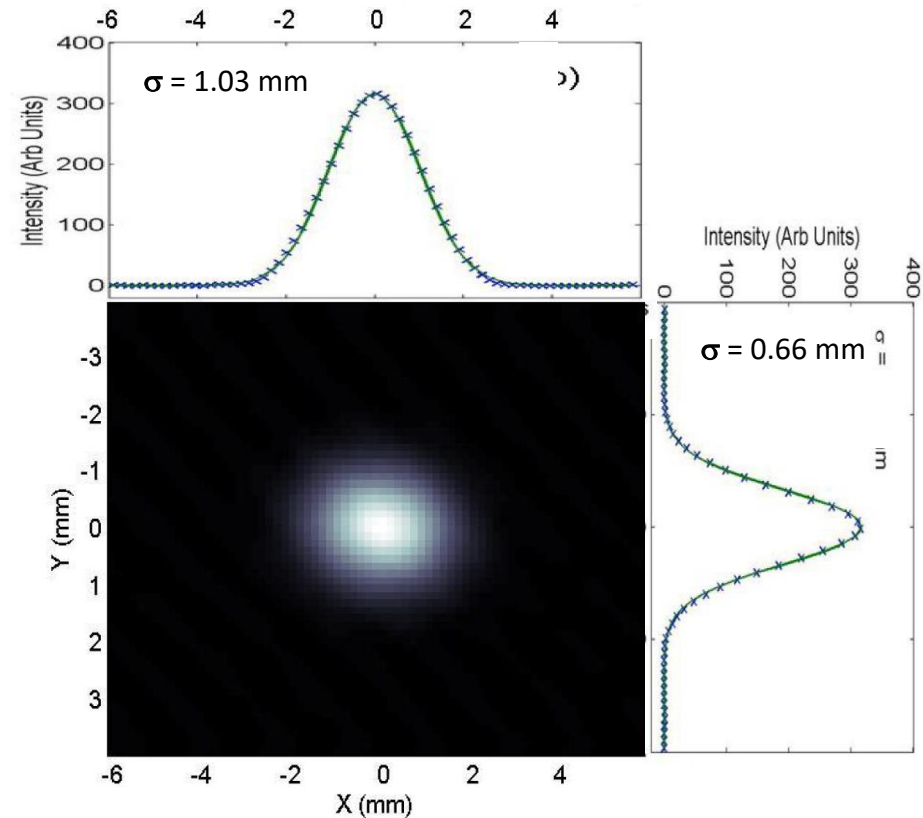
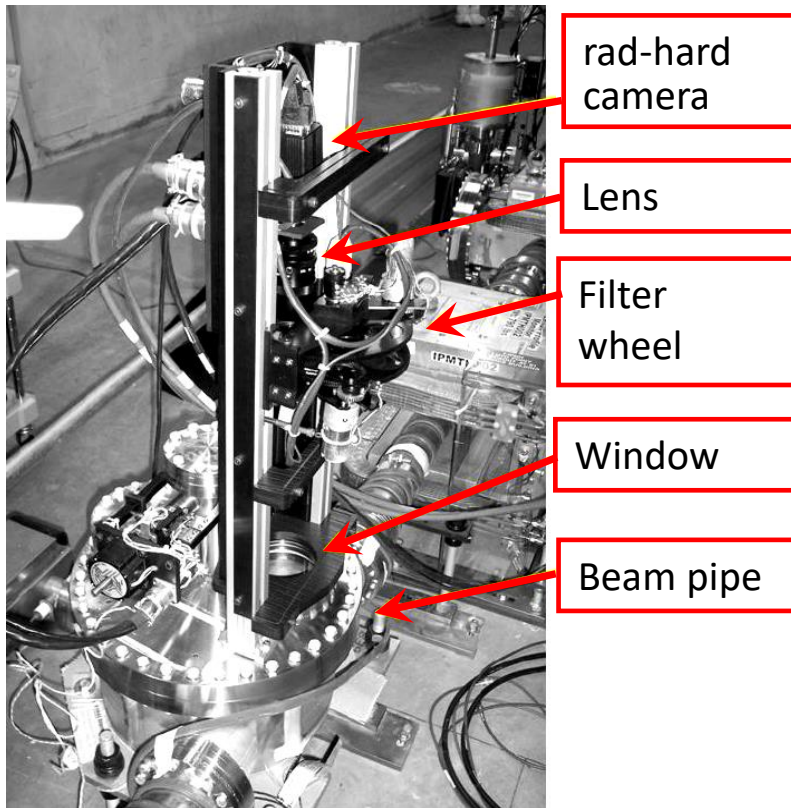
Resolution of 50 μm is insufficient, but sometimes used for photon beams

OTR-Monitor: Technical Realization and Results

Example of realization at TERATRON:

- Insertion of foil
e.g. 5 μm Kapton coated with 0.1 μm Al
- Advantage:** thin foil \Rightarrow low heating & straggling
2-dim image visible

Results at FNAL-TEVATRON synchrotron
with 150 GeV proton
Using fast camera: Turn-by-turn measurement



Courtesy V.E. Scarpine (FNAL) et al., BIW'06

Coherent Optical Transition Radiation

Observation of coherent OTR for **compressed** bunches at LINAC based light sources

Reason: Coherent emission **if** bunch length \approx wavelength ($t_{bunch} = 2 \text{ fs} \Leftrightarrow l_{bunch} = 600 \text{ nm}$)

or bunch fluctuations \approx wavelength

Parameter reach

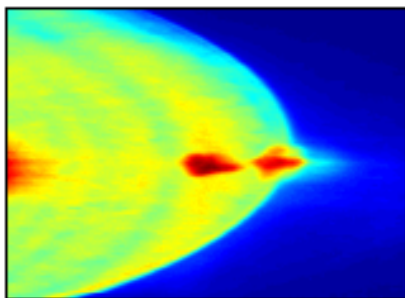
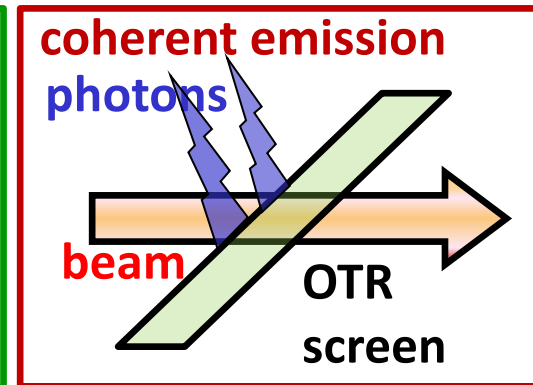
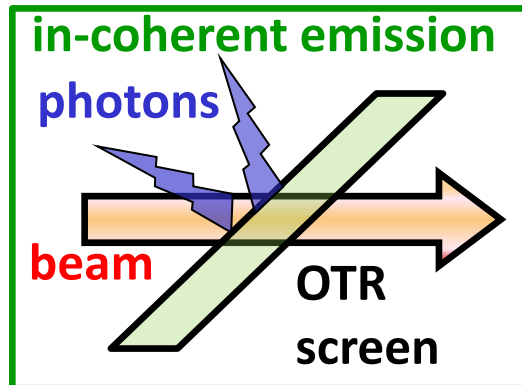
for most LINAC-based FELs!

Beam parameter: FLASH, 700 MeV,

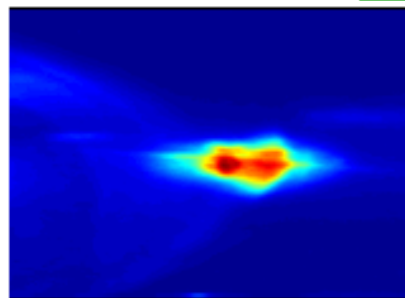
0.5 nC, with bunch compression

OTR screen

scint. screen



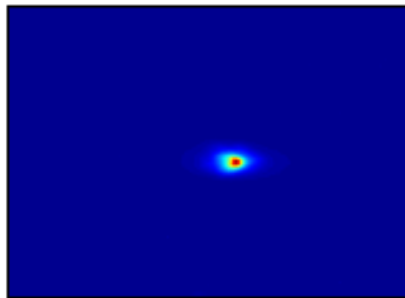
(a) OTR screen



(c) LuAG screen



(b) OTR screen, +100ns delay



(d) LuAG screen, +100ns delay

prompt emission for OTR and scint. screen

→ **coherent and in-coherent OTR**

100 ns delayed emission

→ no OTR as expected (classical process)

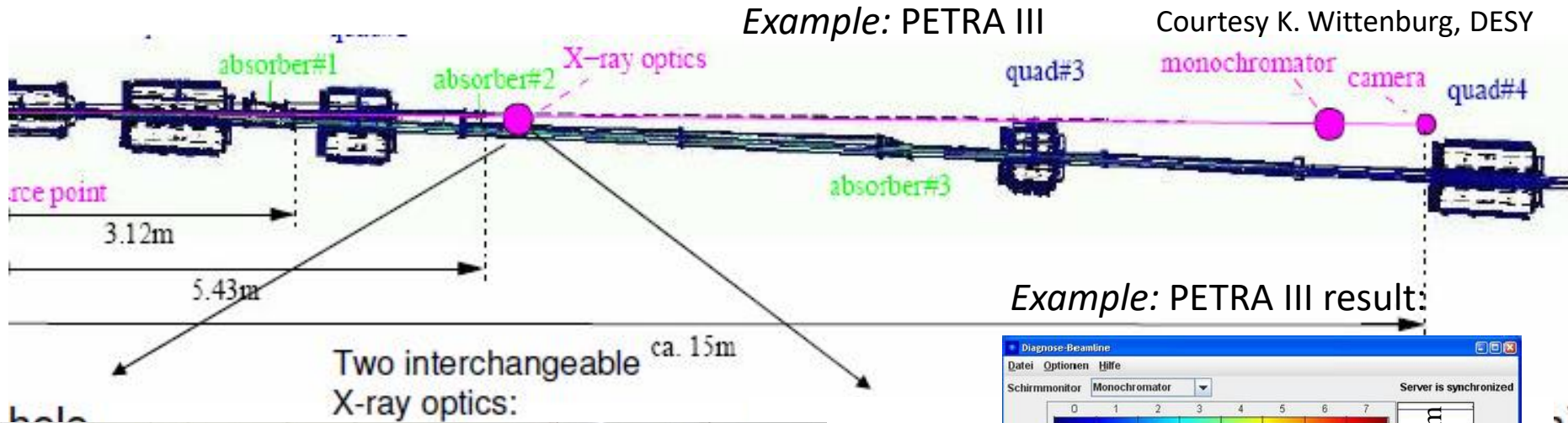
→ emission by scint. screen due to lifetime

⇔ correct profile image!

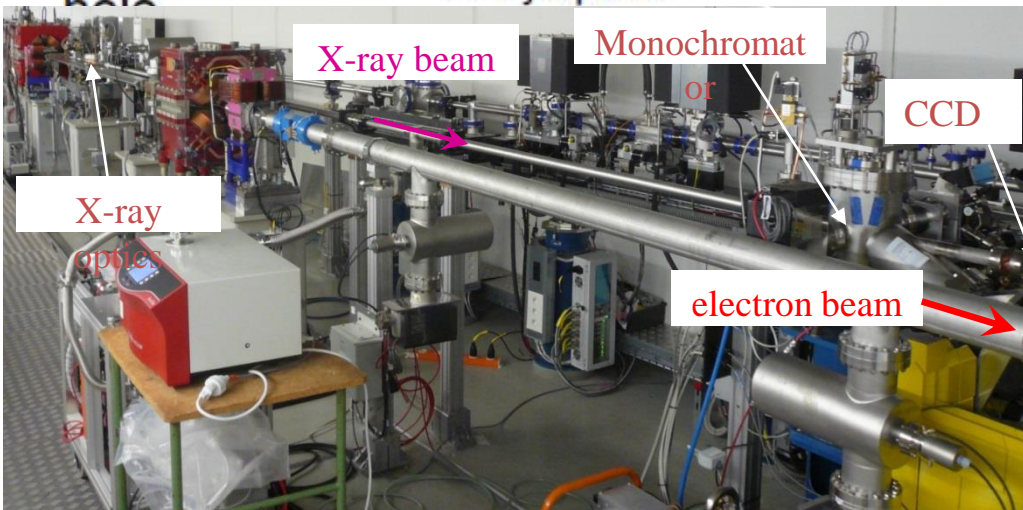
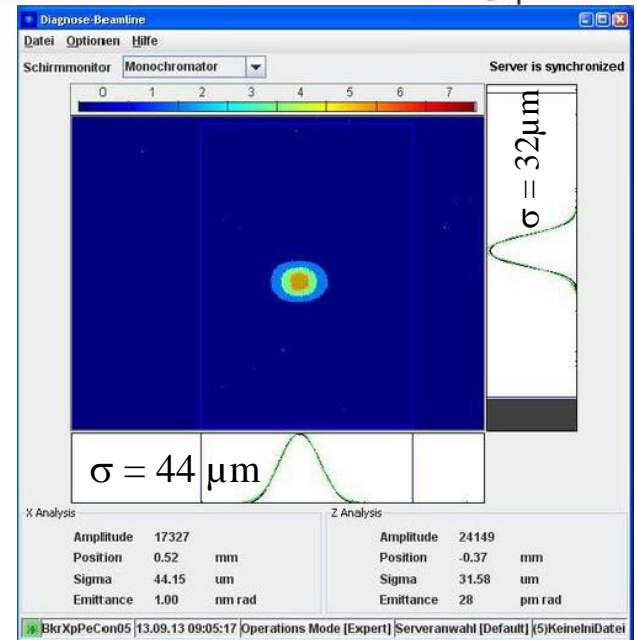
Contrary of M. Yan et al., DIPAC'11 & S. Wesch, DIPAC'11

X-ray Pin-Hole Camera

The diffraction limit is $\Rightarrow \sigma \cong 0.6 \cdot (\lambda^2 / \rho)^{1/3} \Rightarrow$ *shorter wavelength by X-rays.*



Example: PETRA III result:



Double Slit Interference for Radiation Monitors

The **blurring of interference pattern** due to finite size of the sources

⇒ spatial coherence parameter γ delivers **rms** beam size

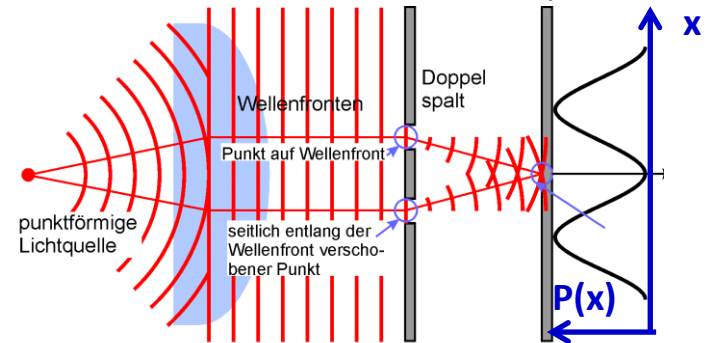
i.e. ‘de-convolution’ of blurred image!

→ highest resolution, but complex method

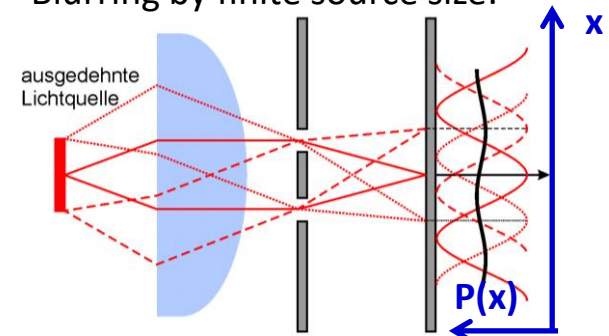
Typical resolution for three methods:

- Direct optical observation: $\sigma \approx 100 \mu\text{m}$
- Direct x-ray observation : $\sigma \approx 10 \mu\text{m}$
- Interference optical obser: $\sigma \approx 1 \mu\text{m}$

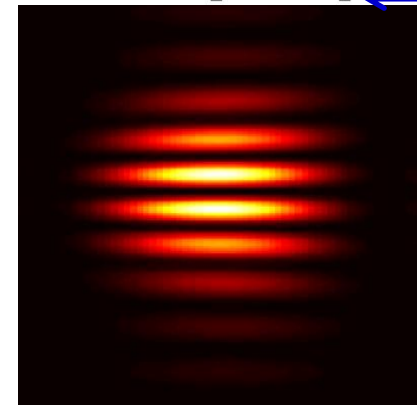
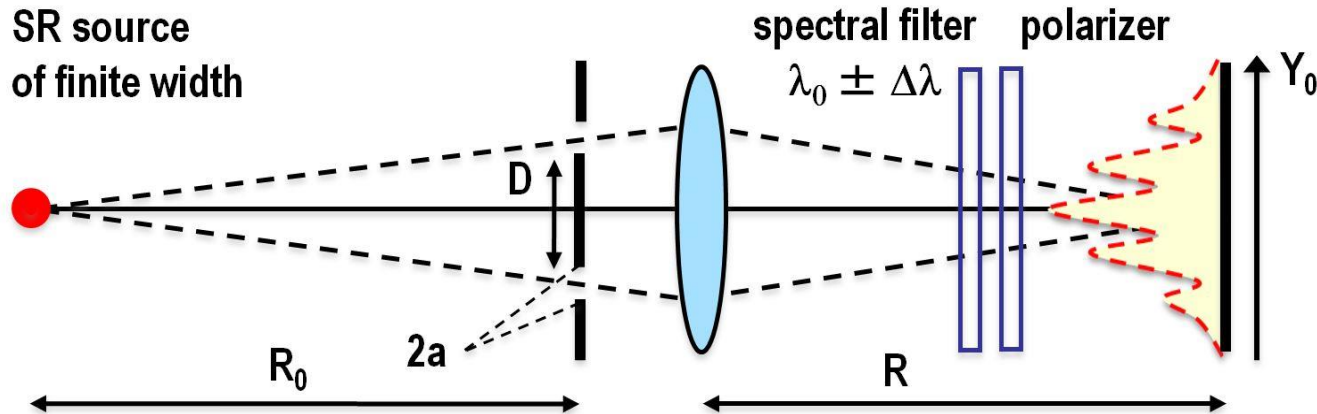
Ideal double slit interference pattern:



Blurring by finite source size:



SR source of finite width



Courtesy of V. Schlott PSI

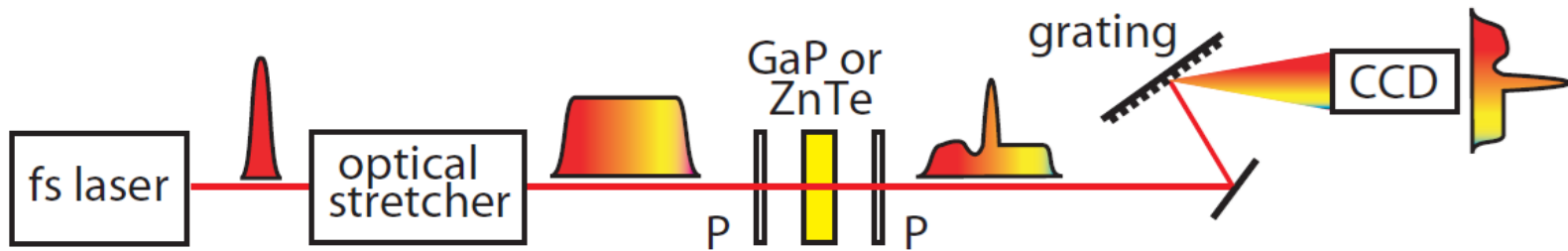
Optical Strecher for electro-optical Method

For Free Electron Lasers → bunch length below 1 ps is achieved

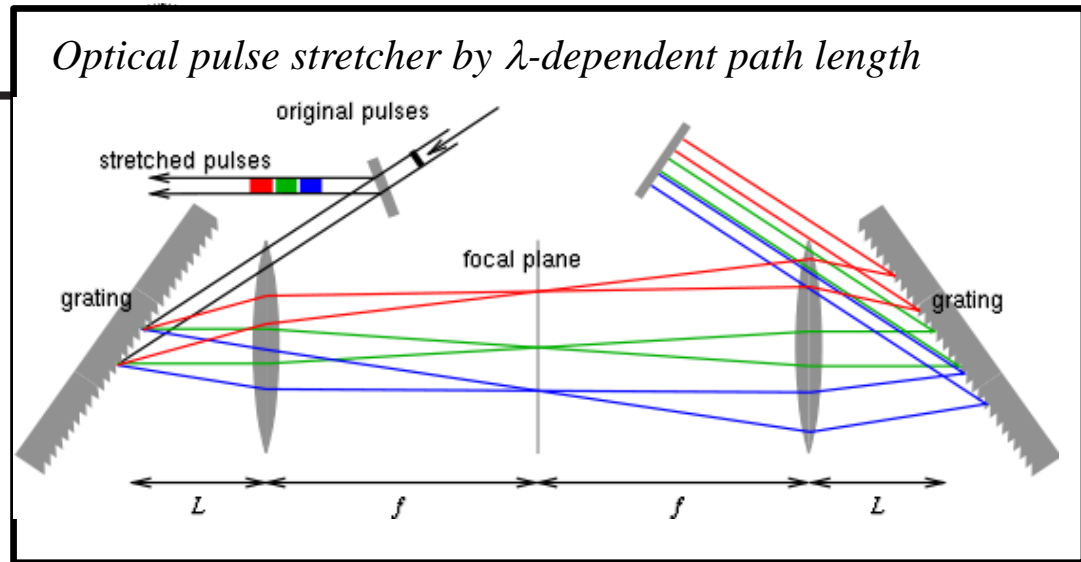
Short laser pulse \Leftrightarrow broad frequency spectrum (property of Fourier Transformation)

Optical stretcher: Separation of colors by different path length

\Rightarrow different colors at different time \Rightarrow **single-shot observation**



Spectral Decoding



Courtesy S.P.Jamison et al., EPAC 2006

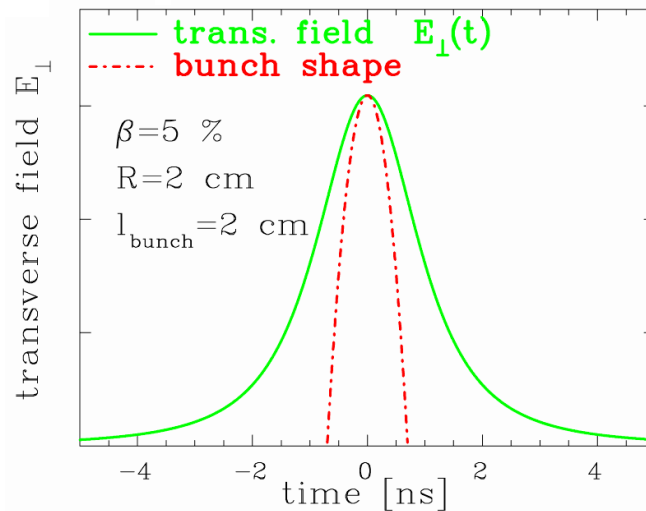
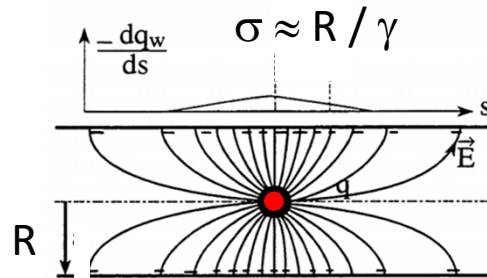
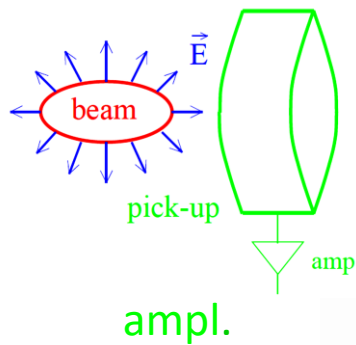
Bunch Structure at low E_{kin} : Not possible with Pick-Ups

Pick-ups are used for:

- precise for bunch-center relative to rf
- course image of bunch shape

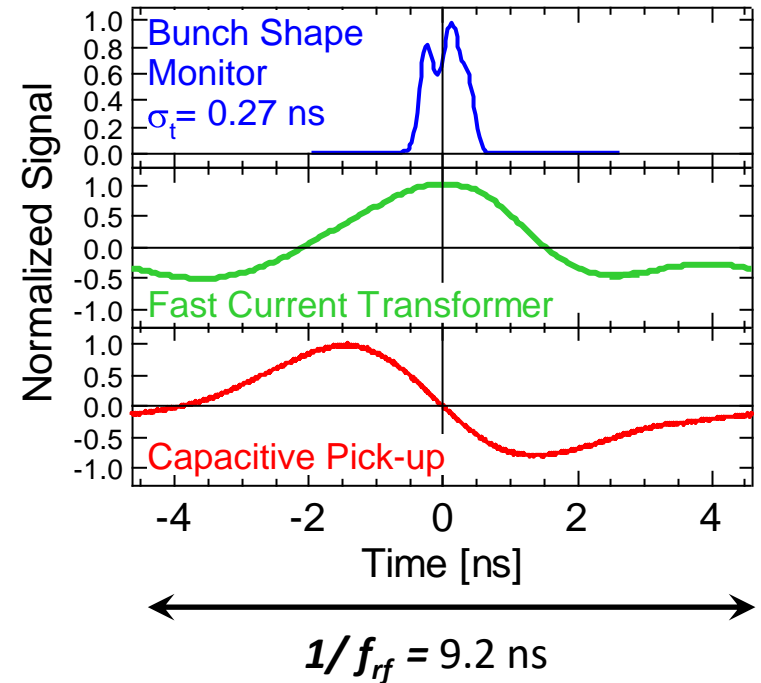
But:

For $\beta \ll 1 \rightarrow$ long. E -field significantly modified:



Example: Comparison pick-up – particle counter:

Ar beam of 1.4 MeV/u ($\beta = 5.5\%$), $f_{rf} = 108 \text{ MHz}$



\Rightarrow the pick-up signal is insensitive to bunch 'fine-structure'

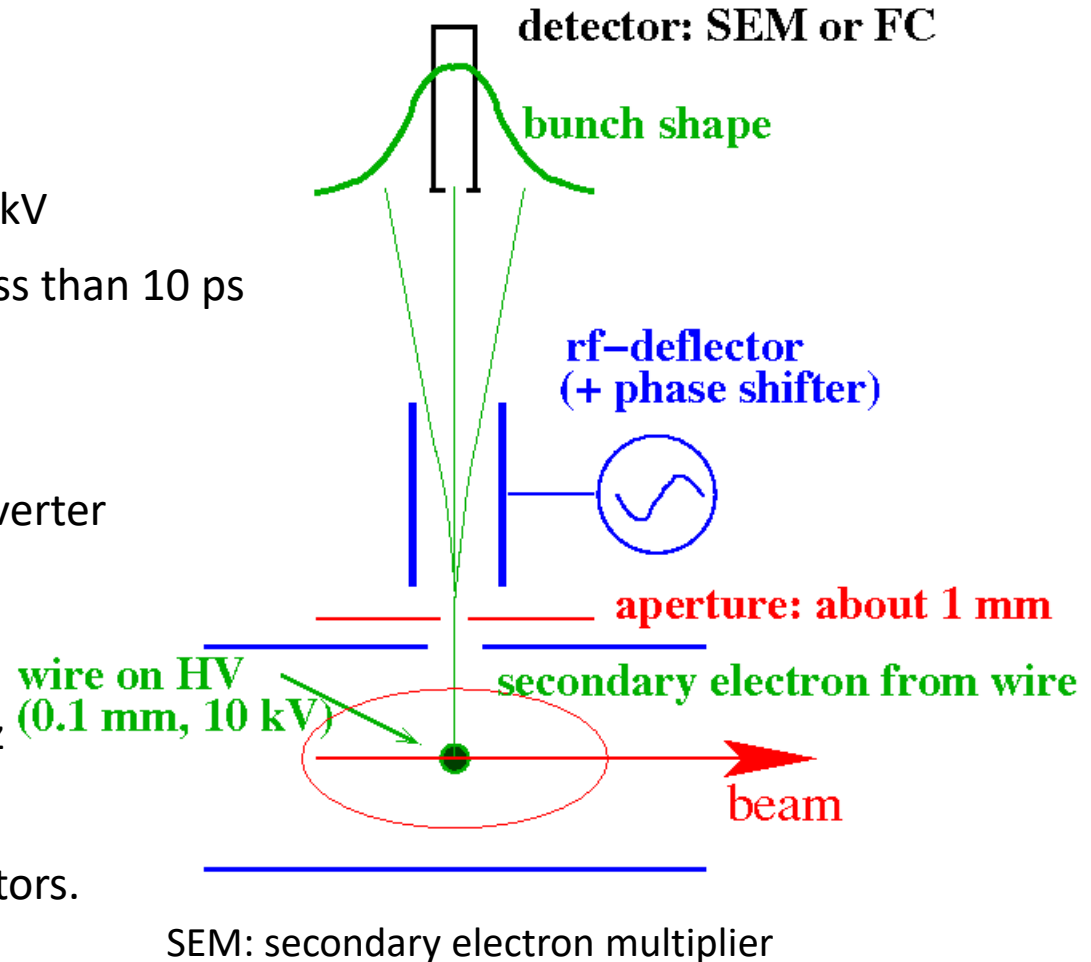
Secondary e^- liberated from a wire carrying the time information.

→ Bunch Shape Monitor (BSM)

Working principle:

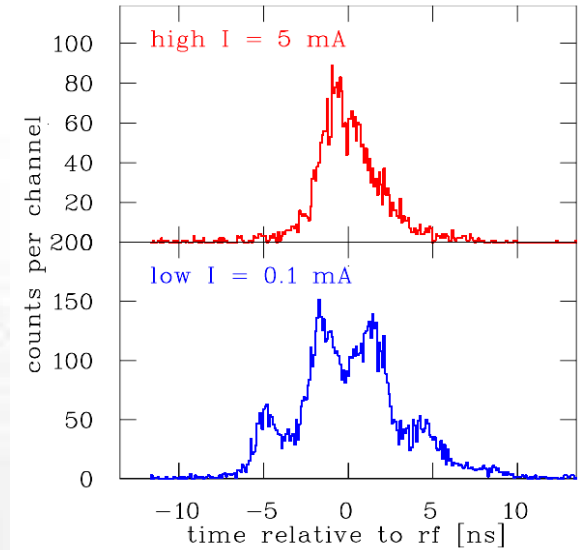
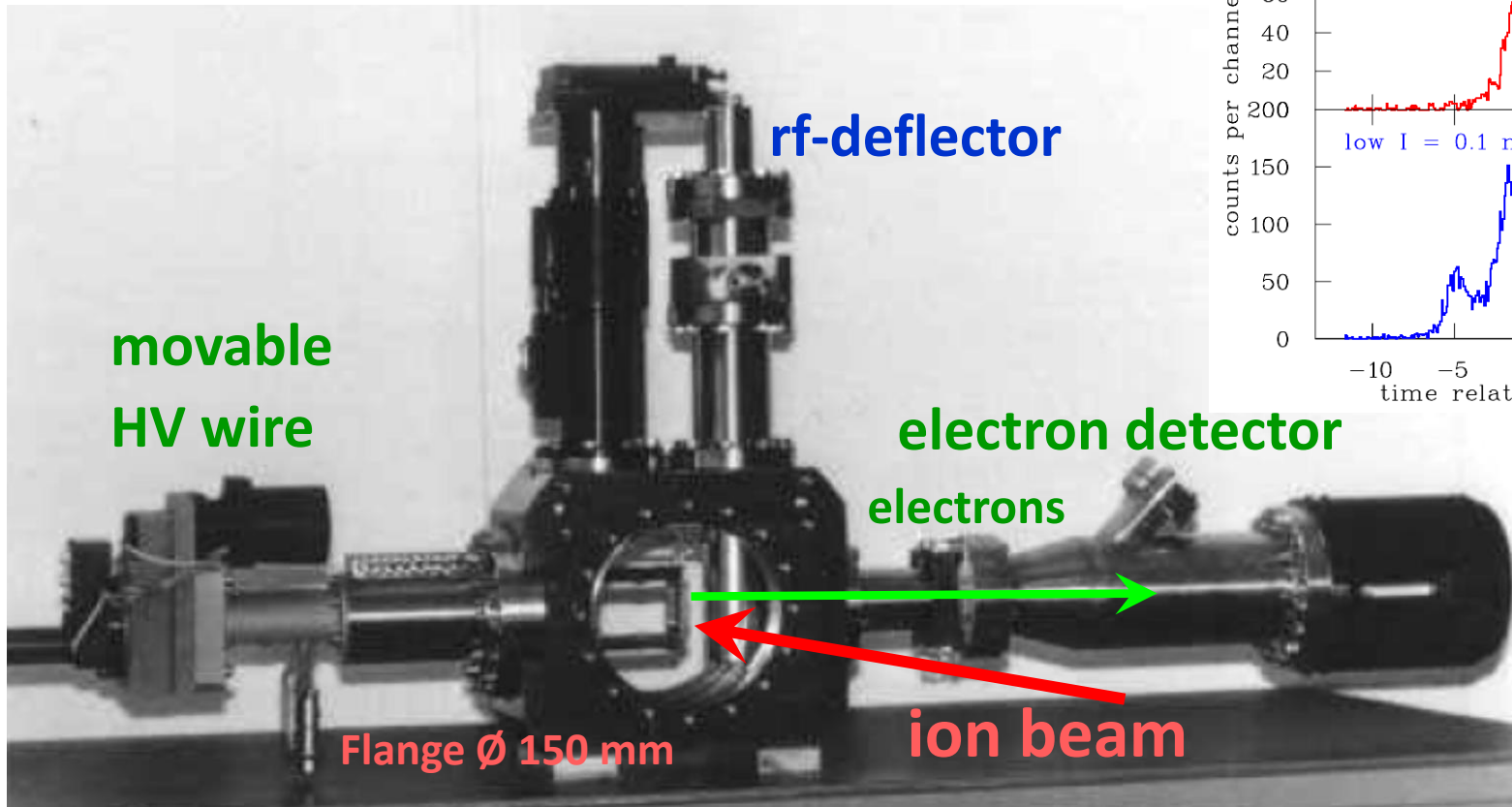
- insertion of a 0.1 mm wire at ≈ 10 kV
- emission of secondary e^- within less than 10 ps
- secondary e^- are accelerated
- toward an rf-deflector
- rf-deflector as 'time-to-space' converter
- detector with a thin slit
- slow shift of the phase
- resolution ≈ 10 ps $\approx 1^\circ$ @ 280 MHz
- Measurements are comparable

to that obtained with particle detectors.



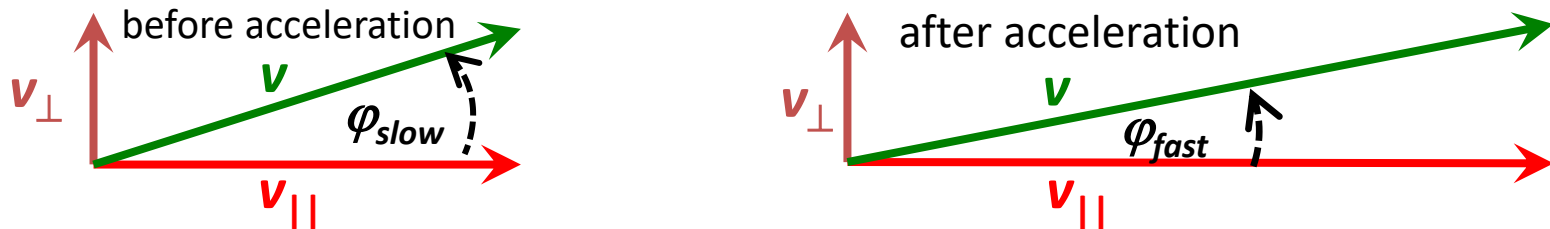
Realization of Bunch Shape Monitor at CERN LINAC2

Example: The bunch shape behind RFQ with 120 keV/u:



'Adiabatic' Damping during Acceleration

The emittance $\varepsilon = \int dx dx'$ is defined via the position deviation and angle in **lab-frame**



After acceleration the longitudinal velocity is increased \Rightarrow angle φ is smaller

The angle is expressed in momenta: $x' = p_{\perp} / p_{\parallel}$ the emittance is $\langle xx' \rangle = 0$: $\varepsilon = x \cdot x' = x \cdot p_{\perp} / p_{\parallel}$

\Rightarrow under ideal conditions the emittance can be normalized to the momentum $p_{\parallel} = \gamma \cdot m \cdot \beta c$

\Rightarrow normalized emittance $\varepsilon_{norm} = \beta \gamma \cdot \varepsilon$ is preserved with the Lorentz factor γ and velocity $\beta = v/c$

Example: Acceleration in GSI-synchrotron for C^{6+} from 6.7 \rightarrow 600 MeV/u ($\beta = 12 \rightarrow 79\%$) observed by IPM

$$\text{theoretical width: } \langle x \rangle_f = \sqrt{\frac{\beta_i \cdot \gamma_i}{\beta_f \cdot \gamma_f}} \cdot \langle x \rangle_i$$

$$= 0.33 \cdot \langle x \rangle_i$$

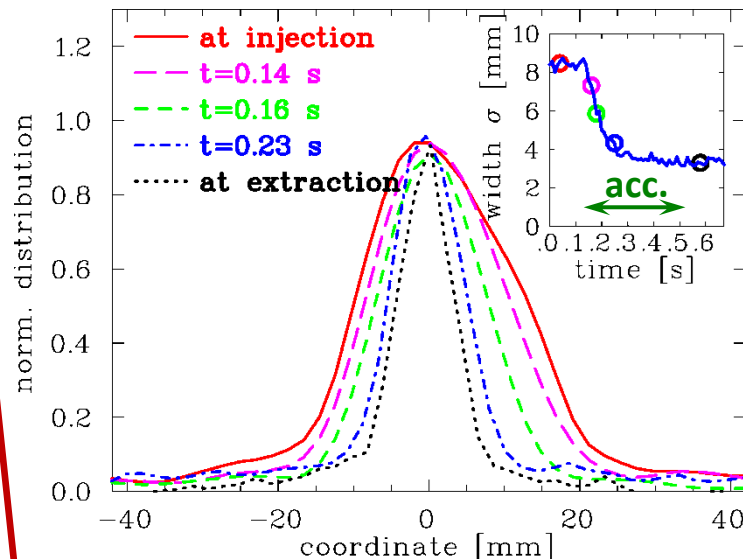
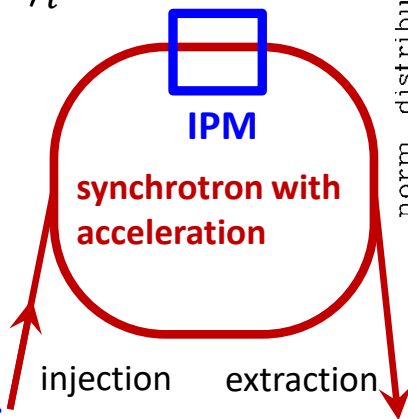
$$\text{measured width: } \langle x \rangle_f \approx 0.37 \cdot \langle x \rangle_i$$

IPM is well suited

for long time observations

without beam disturbance

\rightarrow mainly used at proton synchrotrons.



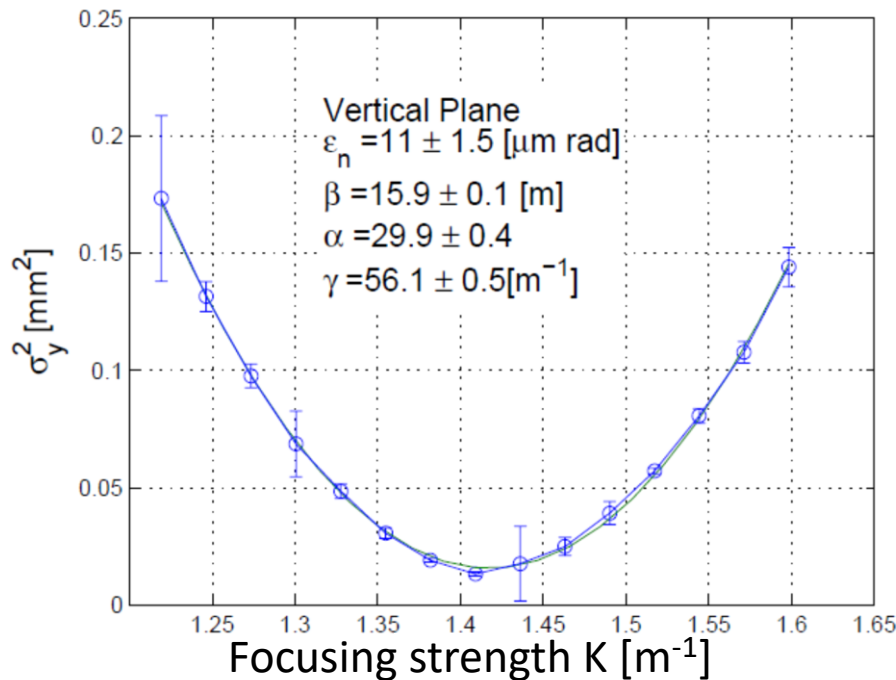
Measurement of transverse Emittance

Using the 'thin lens approximation' i.e. the quadrupole has a focal length of f :

$$\mathbf{R}_{focus}(\mathbf{K}) = \begin{pmatrix} \mathbf{1} & \mathbf{0} \\ -\mathbf{1}/f & \mathbf{1} \end{pmatrix} \equiv \begin{pmatrix} \mathbf{1} & \mathbf{0} \\ \mathbf{K} & \mathbf{1} \end{pmatrix} \Rightarrow \mathbf{R}(L, \mathbf{K}) = \mathbf{R}_{drift}(L) \cdot \mathbf{R}_{focus}(\mathbf{K}) = \begin{pmatrix} \mathbf{1} + L\mathbf{K} & L \\ \mathbf{K} & \mathbf{1} \end{pmatrix}$$

Measurement of matrix-element $\sigma_{11}(s_1, K)$ from matrices $\sigma(s_1, K_i) = \mathbf{R}(K_i) \cdot \sigma(s_0) \cdot \mathbf{R}^T(K_i)$

Example: Square of the beam width at ELETTRA 100 MeV e^- Linac, YAG:Ce:



G. Penco (ELETTRA) et al., EPAC'08

For completeness: The relevant formulas

$$\begin{aligned} \sigma_{11}(\mathbf{1}, \mathbf{K}) &= L^2 \sigma_{11}(\mathbf{0}) \cdot \mathbf{K}^2 \\ &+ 2 \cdot (L \sigma_{11}(\mathbf{0}) + L^2 \sigma_{12}(\mathbf{0})) \cdot \mathbf{K} \\ &+ L^2 \sigma_{22}(\mathbf{0}) + \sigma_{11}(\mathbf{0}) \\ &\equiv a \cdot \mathbf{K}^2 - 2ab \cdot \mathbf{K} + ab^2 + c \\ &= a \cdot (\mathbf{K} - b)^2 + c \end{aligned}$$

The three matrix elements at the quadrupole:

$$\sigma_{11}(\mathbf{0}) = \frac{a}{L^2}$$

$$\sigma_{12}(\mathbf{0}) = -\frac{a}{L^2} \left(\frac{1}{L} + b \right)$$

$$\sigma_{22}(\mathbf{0}) = \frac{1}{L^2} \left(ab^2 + c + \frac{2ab}{L} + \frac{a}{L^2} \right)$$

$$\epsilon_{rms} \equiv \sqrt{\det \sigma(\mathbf{0})} = \sqrt{\sigma_{11}(\mathbf{0}) \cdot \sigma_{22}(\mathbf{0}) - \sigma_{12}^2(\mathbf{0})} = \sqrt{ac} / L^2$$

The Emittance for Gaussian and non-Gaussian Beams

The beam distribution can be non-Gaussian, e.g. at:

- Beams behind ion source
- Space charged dominated beams at LINAC & synchrotron
- Cooled beams in storage rings

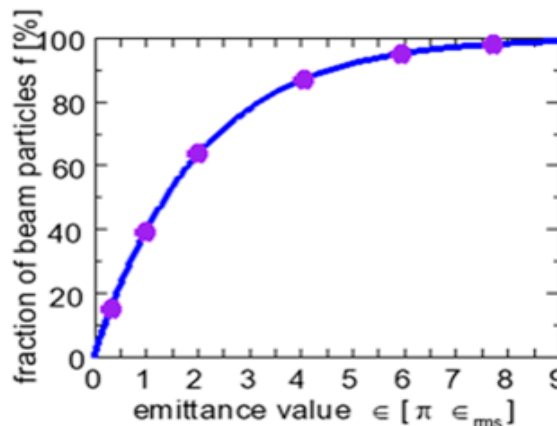
General description of emittance by statistical moments of 2-dim distribution:

$$\epsilon_{rms} = \sqrt{\underbrace{\langle x^2 \rangle \langle x'^2 \rangle}_{\text{Variances}} - \underbrace{\langle xx' \rangle^2}_{\text{Covariance i.e. correlation}}}$$

It describes the value for 1 standard derivation

For Gaussian beams only: $\epsilon_{rms} \leftrightarrow$ interpreted as area containing a fraction f of ions:

$$\epsilon(f) = -2\pi\epsilon_{rms} \cdot \ln(1-f)$$



Emittance $\epsilon(f)$	Fraction f
$1 \cdot \epsilon_{rms}$	15 %
$\pi \cdot \epsilon_{rms}$	39 %
$2\pi \cdot \epsilon_{rms}$	63 %
$4\pi \cdot \epsilon_{rms}$	86 %
$8\pi \cdot \epsilon_{rms}$	98 %

Care:
No common definition of emittance concerning the fraction f